



**NTNU – Trondheim**  
Norwegian University of  
Science and Technology

# Effect of Heat Flux and External System Configuration on Pressure Drop Oscillations in a Horizontal Pipe

**Tina Louise Langeland**

Master of Energy and Environmental Engineering

Submission date: June 2015

Supervisor: Maria Fernandino, EPT

Co-supervisor: Carlos Alberto Dorao, EPT

Norwegian University of Science and Technology  
Department of Energy and Process Engineering



EPT-M-2015-48

**MASTER THESIS**

for

Tina Louise Langeland

Spring 2015

Effect of heat flux and external system configuration on pressure drop oscillations in a horizontal pipe

*Effekten av varmeflukt og det eksterne systemet på trykkfalls oscillasjoner i et horisonalt rør*

**Background and objective**

Boiling flow instabilities are present in several heat exchanging systems, such as nuclear reactors, cryogenic and chemical processes and high-density power electronic devices. These oscillations are undesirable since they can cause mechanical and thermal fatigue of components by mechanical vibrations and thermal oscillations, working conditions outside the original design specifications and, in more extreme cases, components failure and rupture. Pressure drop oscillations (PDOs) are one of the most common dynamic two-phase flow instabilities. Although PDOs have been studied in the past, its complex dynamics and how the whole external system influences their characteristics is still not well understood.

In this work, PDOs will be studied experimentally, with focus on the effect of heat flux, inlet and outlet restrictions and compressible volume on the PDOs occurrence and their physical characteristics.

**The following tasks are to be considered:**

1. Literature review on pressure drop oscillations (PDOs), with focus on the physical phenomena involved, its main characteristics (such as frequency and amplitude) and how they are affected by different operating parameters (system pressure, heat flux, mass flux and inlet temperature).
2. Perform experiments in the Two Phase Flow Instabilities rig at EPT lab, setting the appropriate conditions for the occurrence of PDOs.
3. Validation of the experimental facility and instrumentation for single-phase flow.
4. Study the effect of heat flux, inlet and outlet restriction, compressible volume and pump bypass on PDO occurrence and their physical characteristics.

Within 14 days of receiving the written text on the master thesis, the candidate shall submit a research plan for his project to the department.

When the thesis is evaluated, emphasis is put on processing of the results, and that they are presented in tabular and/or graphic form in a clear manner, and that they are analyzed carefully.

The thesis should be formulated as a research report with summary both in English and Norwegian, conclusion, literature references, table of contents etc. During the preparation of the text, the candidate should make an effort to produce a well-structured and easily readable report. In order to ease the evaluation of the thesis, it is important that the cross-references are correct. In the making of the report, strong emphasis should be placed on both a thorough discussion of the results and an orderly presentation.

The candidate is requested to initiate and keep close contact with his/her academic supervisor(s) throughout the working period. The candidate must follow the rules and regulations of NTNU as well as passive directions given by the Department of Energy and Process Engineering.

Risk assessment of the candidate's work shall be carried out according to the department's procedures. The risk assessment must be documented and included as part of the final report. Events related to the candidate's work adversely affecting the health, safety or security, must be documented and included as part of the final report. If the documentation on risk assessment represents a large number of pages, the full version is to be submitted electronically to the supervisor and an excerpt is included in the report.

Pursuant to "Regulations concerning the supplementary provisions to the technology study program/Master of Science" at NTNU §20, the Department reserves the permission to utilize all the results and data for teaching and research purposes as well as in future publications.

The final report is to be submitted digitally in DAIM. An executive summary of the thesis including title, student's name, supervisor's name, year, department name, and NTNU's logo and name, shall be submitted to the department as a separate pdf file. Based on an agreement with the supervisor, the final report and other material and documents may be given to the supervisor in digital format.

- Work to be done in lab (Water power lab, Fluids engineering lab, Thermal engineering lab)  
 Field work

Department of Energy and Process Engineering, 14. January 2015



Olav Bolland  
Department Head



Maria Fernandino  
Academic Supervisor

Research Advisor: Carlos A. Dorao

## Abstract

Heat transfer processes can greatly benefit from the use of the boiling and condensation in two-phase flows. However, the use of two-phase flows may induce instabilities in the heat transfer system, causing control problems and possible damage to the equipment. Pressure Drop Oscillations (PDOs) are one of the instabilities prone to occur in convective heat transfer systems. The PDOs are characterized by oscillations of low frequency with interfering, high frequency signals known as Density Wave Oscillations (DWOs). In order to be able to control this kind of oscillations in a thermal system, a better understanding of the parameters affecting the PDOs is needed.

In this thesis, experimental work considering the effect of the external system and heat flux on the PDOs have been performed using the Two-Phase Flow Instability Facility located at the Varmeteknisk lab, EPT, NTNU. During the experiments, a single, horizontal channel of 5 mm inner diameter was used as the test section, R134a as the working fluid and a regulative surge tank containing nitrogen gas was used as the the compressible volume required for occurrence of PDOs.

For the external system, experimental analyses of the effect of the inlet and outlet restrictions of the heated test section, different compressible volumes and the pump bypass were conducted. It was shown that a restriction of either the inlet or outlet of the test section reduced the PDOs. Larger compressible volumes increased the PDOs, while they decreased for smaller volumes. With the use of a pump bypass, the system stabilized faster with regards to the PDOs.

Different heat fluxes applied to the test section showed that the PDOs could be regulated by both the amount and the distribution of the heat applied. For an uniform, decreasing heat flux the PDOs decreased, while for an uniform, increasing heat flux the PDOs first increased before decreasing in magnitude. Both a linear increasing and decreasing heat profile were applied to the test section. The results showed that the decreasing heat profile, generating larger amount of vapour in the test section, increased the PDOs and especially the interfering, high frequency signals. The increasing heat profile had a stabilizing effect on the system. A discussion concerning the interfering, high frequency signals that were observed to occur together with the PDOs was carried out along with experiments resulting in a conclusion that the signals may actually be another kind of oscillations than the DWOs.



## Sammendrag

Varmeoverføringsprosesser kan oppnå høyere utnyttelsesgrad ved bruk av koking og kondens i tofase-strømninger. Imidlertid kan bruken av tofase-strømmer forårsake ustabilitet i varmeoverføringssystemet, gi styringsproblemer og muligens skade utstyret. En trykkfalls-svingning (PDO) er en av de ustabilitetene som har en tendens til å oppstå i konvektive varmeoverføringssystemer. PDOer er preget av svingninger med lav frekvens og med forstyrrende, høyfrekvente signaler som kalles Tetthetsbølge-svingninger (DWOer). For å være i stand til å kontrollere denne type svingninger i et termisk system, er en bedre forståelse av de ulike parametrene som påvirker PDOer nødvendig.

I denne oppgaven har det blitt utført eksperimentelt arbeid for å vurdere effekten av det eksterne systemet og varmefluks på PDOer. Arbeidet er blitt utført ved hjelp av en tofase-strømnings lab, Two-Phase Flow Instability Facility, som ligger på Varmeteknisk lab, EPT, NTNU. Under forsøkene ble det brukt en enkel, horisontal kanal med indre diameter på 5 mm som testseksjon, R134a som testvæske og en regulerende tank delvis fylt med nitrogengass som det komprimerende volumet som er nødvendig for forekomst av PDO. For det eksterne systemet ble det utført eksperimentelle analyser av effekten av innløps- og utløps restriksjoner av den oppvarmede testseksjonen, forskjellige kompressible volum og en bypass for pumpen. Det ble vist at en begrensning av enten innløpet eller utløpet av testseksjonen reduserte PDOene. Et større, komprimert volum økte PDOene, mens de ble redusert for mindre volumer. Med bruk av en bypass for pumpen stabiliserte systemet seg raskere med hensyn til PDO.

Forskjellige varmeflukser påført testseksjonen viste at PDOene kan reguleres av både mengden og fordelingen av varmen som tilføres. For en avtagende, uniform varmefluks over testseksjonen ble PDOene redusert, mens for en uniform, økende varmefluks økte PDOene først før de ble redusert. Både en lineær økende og avtagende varmeprofil ble påført testseksjonen. Resultatene viste at den avtagende varmeprofilene, som genererer større mengde damp i testseksjonen, økte PDOene og særlig de forstyrrende, høyfrekvente signalene. Den økende varmeprofilen hadde en stabiliserende effekt på systemet. En diskusjon angående de forstyrrende, høyfrekvente signalene som ble observert å forekomme sammen med PDO ble utført i tillegg til eksperimenter. Dette resulterte i en konklusjon om at de forstyrrende, høyfrekvente signalene faktisk kan være en annen type oscillasjoner enn DWOer.





## Preface

This Master's thesis (TEP4900) is submitted for the fulfilment of the Master's program Energy and Environmental Engineering at the Norwegian University of Science and Technology.

I would like to thank my main supervisor, Professor Maria Fernandino for all help and guidance throughout the master thesis. I am also very grateful to my co-supervisor Professor Carlos A. Dorao for guidance and always taking time to discuss the achieved results.

Thanks are also expressed to Leonardo C. Ruspini and Ezequiel M. Chiapero for designing the two-phase flow facility and the laboratory staff, especially Reidar Tellebon, for always having solutions to problems occurring at the facility.

Finally, I would like to thank my parents and Audun for always supporting and believing in me.

Trondheim, 10. June, 2015

*Tina Louise Langeland*



# Table of Contents

<b>MSc Thesis Description Sheet</b>	<b>i</b>
<b>Abstract</b>	<b>iii</b>
<b>Sammendrag</b>	<b>v</b>
<b>Preface</b>	<b>vii</b>
<b>List of Figures</b>	<b>xiii</b>
<b>List of Tables</b>	<b>xvii</b>
<b>Nomenclature</b>	<b>xix</b>
<b>1 Introduction</b>	<b>1</b>
1.1 Background and Motivation . . . . .	1
1.2 Objectives . . . . .	2
1.3 Scope . . . . .	2
1.4 Orgainzation of This Thesis . . . . .	3
<b>2 Two-phase Flow Instabilities</b>	<b>5</b>
2.1 Two-phase Flow . . . . .	5
2.1.1 Parameters . . . . .	5
2.2 Pressure Drop Characteristic Curve . . . . .	7
2.3 Flow Instabilities . . . . .	9
2.3.1 Ledinegg Instabilities . . . . .	9
2.3.2 Density Wave Oscillations . . . . .	11
2.3.3 Thermal Oscillations . . . . .	12
2.4 Pressure Drop Oscillations . . . . .	13
2.4.1 Main Characteristics . . . . .	14
<b>3 Previous Work</b>	<b>17</b>
3.1 Two-Phase Flow Instabilities . . . . .	17

3.2	Pressure Drop Oscillations . . . . .	17
3.2.1	Effect of the External System and Heat Flux . . . . .	18
3.2.2	Experimental Work Done at the Two-Phase Flow Instabilities Facility at NTNU . . . . .	25
3.3	Other Studies . . . . .	26
3.4	Summary . . . . .	30
<b>4</b>	<b>Two-phase Flow Instabilities Facility</b>	<b>33</b>
4.1	Components . . . . .	33
4.1.1	Test Section . . . . .	34
4.1.2	Surge Tank . . . . .	36
4.1.3	Heat Exchangers . . . . .	36
4.1.4	Pump . . . . .	36
4.2	Operational Limits . . . . .	36
4.2.1	Heat Flux . . . . .	37
4.2.2	Vapour Quality . . . . .	37
4.3	Loss Coefficients . . . . .	38
4.4	Measurements . . . . .	38
4.4.1	Experimental Accuracy . . . . .	39
4.4.2	Error Estimation . . . . .	39
4.5	Software Interface - LabVIEW . . . . .	41
4.6	Experimental Procedure . . . . .	41
4.7	Risk Assesment . . . . .	43
<b>5</b>	<b>Validation and Characterization of the System</b>	<b>45</b>
5.1	Validation . . . . .	45
5.1.1	Single Phase Pressure Drop Validation . . . . .	45
5.1.2	Single Phase Heat Transfer Validation . . . . .	46
5.2	System Characterization . . . . .	47
5.2.1	Internal System . . . . .	48
5.2.2	External System . . . . .	48
5.3	Summary . . . . .	50
<b>6</b>	<b>Experimental Results - Effect of the External System</b>	<b>51</b>
6.1	Results . . . . .	51
6.1.1	Effect of Inlet Restriction . . . . .	54
6.1.2	Effect of Outlet Restriction . . . . .	54
6.1.3	Effect of the Pump Bypass . . . . .	57
6.1.4	Effect of the Compressible Volume . . . . .	59
6.2	Discussion . . . . .	60
<b>7</b>	<b>Experimental Results -Effect of Heat Flux</b>	<b>63</b>

7.1	Results . . . . .	63
7.1.1	Effect of Heating Power . . . . .	63
7.1.2	Effect of Different Heating Profiles . . . . .	65
7.1.3	DWO Interaction . . . . .	68
7.2	Discussion . . . . .	70
<b>8</b>	<b>Conclusion</b>	<b>75</b>
<b>9</b>	<b>Future Work</b>	<b>77</b>
	<b>Bibliography</b>	<b>79</b>
	<b>Appendix</b>	
<b>A</b>	<b>"Effect of external system in the characteristics of Pressure Drop Oscillations"</b>	<b>83</b>



# List of Figures

2.1	Flow pattern in two-phase flow in a horizontal pipe during evaporation [Collier & Thome, 1994]. . . . .	6
2.2	An example of the pressure drop characteristic curve for some given parameters ( $P_i=8.5$ bar, $T_{sub}=30$ °C, $q''=32$ kW/m <sup>2</sup> ) [Chiapero et al., 2013]. . . . .	7
2.3	Operating reference values: $T_{sub} = 30$ °C, $q'' = 32$ kW/m <sup>2</sup> and $P_{in} = 8.5$ bar. Results from Chiapero et al. [2013]. . . . .	8
2.4	Different supply curves for the static pipe behaviour [Chiapero, 2013]. . . . .	11
2.5	A simple system for DWO occurrence [Kakac & Bon, 2008]. . . . .	12
2.6	Set up for the Surge Tank [Chiapero et al., 2012]. . . . .	14
2.7	External and internal characteristics curves [Ruspini et al., 2014]. . . . .	14
2.8	Stability boundaries for DWOs and PDOs according to the pressure drop characteristic curve [Kakac & Bon, 2008]. . . . .	15
3.1	Experimental results from Dogan et al. [1983]. . . . .	18
3.2	PDOs superimposed by DWOs shown for the pressure, wall temperature and mass flow rate during operational conditions of $T_{in}=10$ °C, $P_W=800$ W, $G=0.05$ g/sec [Padki et al., 1991]. . . . .	20
3.3	Drawing of the limit cycle for PDOs with the superimposed DWOs [Liu & Kakaç, 1991]. . . . .	21
3.4	1 <sup>st</sup> PDO when the compressible volume was located before the pre-heater [Guo et al., 2001]. . . . .	24
3.5	2 <sup>nd</sup> PDO when the compressible volume was located at the inlet of the test section [Guo et al., 2001]. . . . .	24
3.6	The limiting cycles for the two parallel channels during equal heating [Chiapero et al., 2014b]. . . . .	25
3.7	Evolution of PDOs superimposed by DWOs while the mass flow rate is increased [Ruspini, 2013]. . . . .	27
3.8	The limit cycle of PDOs superimposed by DWOs over the pressure drop characteristic curve [Ruspini, 2013]. . . . .	27
3.9	The PDOs superimposed by DWOs as they occur in pressure and mass flow oscillations [Ruspini, 2013]. . . . .	28

3.10	An example of the DWOs occurring in the system with conditions of $P_{in}=8.4$ bar, $T_{in}=17$ °C and $P_W=870$ W [Ruspini, 2013]. . . . .	28
3.11	Pressure drop characteristic curves for distinct heat fluxes showing the different instabilities regions. The boiling onset oscillations occurred in region <i>A</i> , the PDOs in region <i>B</i> and the DWOs in region <i>C</i> . The parameters used were: $P_{in}=38$ bar and $T_{sub}=90$ °C [Wang et al., 1996].	29
3.12	The temperature and mass flux oscillations developing during boiling onset oscillations using parameters of $P_{in}=50$ bar, $G=1124$ kg/m <sup>2</sup> s, $q''=337$ kw/m <sup>2</sup> and $T_{sub}=60$ °C [Wang et al., 1996]. . . . .	29
4.1	Sketch of the facility. . . . .	34
4.2	Picture of the facility at the lab [Chiapero, 2013]. . . . .	35
4.3	Set up for the heaters in the test section, dimensions given in mm. Adopted from [Ruspini, 2013; Sørum, 2014]. . . . .	35
4.4	Overview of the user interface controlling the facility. . . . .	42
5.1	Measured single phase pressure drop compared to theoretical value. . .	46
5.2	Single phase heat transfer achieved compared to the theoretical value. .	48
5.3	Pressure drop characteristic curve for the heated test section ( $\Delta P_{TS}$ ). .	49
5.4	Pressure drop characteristic curve for the flow loop ( $\Delta P_{system}$ ). . . . .	49
5.5	The pump response with the pump bypass closed and opened 3 turns. .	50
6.1	PDO with no interfering, high frequency components. . . . .	53
6.2	PDO with interfering, high frequency components. . . . .	53
6.3	The limit cycle for the PDOs with no high frequency components while using a low compressible volume. . . . .	55
6.4	The limit cycle for the PDOs with high frequency components while using a high compressible volume. . . . .	56
6.5	Effect of increasing the inlet restriction on the PDOs where green corresponds to the mass flux before the surge tank and purple to the mass flux at the inlet of the test section. . . . .	57
6.6	Effect of the outlet restrictions, adiabatic or orifice, on the PDOs while using low ( $3.4 \times 10^{-3}$ m <sup>3</sup> ) and high ( $6.8 \times 10^{-3}$ m <sup>3</sup> ) compressible volumes where green corresponds to the mass flux before the surge tank and purple to the mass flux at the inlet of the test section. . . . .	58
6.7	The effect of opening the pump bypass BP 0, 1, 2 and 3 turns on the PDOs where green corresponds to the mass flux before the surge tank and purple to the mass flux at the inlet of the test section. . . . .	59
6.8	Effect of different compressible volumes on PDOs with the pump bypass valve closed where green corresponds to the mass flux before the surge tank and purple to the mass flux at the inlet of the test section. . . . .	60



6.9	Effect of different compressible volumes on PDOs for pump bypass valve opened three turns where green corresponds to the mass flux before the surge tank and purple to the mass flux at the inlet of the test section. .	61
7.1	Effect of decreasing heat flux on the PDOs characteristics for uniform heating. . . . .	64
7.2	Effect of increasing heat flux on the PDOs characteristics for uniform heating. . . . .	65
7.3	Effect of uniform, linearly increasing and decreasing heat profiles on PDOs for $q''_{tot}=35 \text{ kW/m}^2$ . . . . .	66
7.4	Effect of uniform, parabolic and triangle heat profiles on the PDOs while using $q''_{tot}=35 \text{ kW/m}^2$ . . . . .	67
7.5	Mass flow rate evolution during uniform heat distribution and two cases where the bulk of the heat was applied to the first and first two heaters. All three cases were performed while using $q''_{tot}=35 \text{ kW/m}^2$ and an adiabatic outlet. . . . .	68
7.6	Mass flow rate evolution during uniform, linearly increasing and decreasing heat profiles for $q''_{tot}=47.7 \text{ kW/m}^2$ and orifice outlet. . . . .	69
7.7	Pressure evolution during uniform, linearly increasing and decreasing heat profiles for $q''_{tot}=47.7 \text{ kW/m}^2$ and an orifice outlet. . . . .	69
7.8	Reference case for the PDO evolution in mass flux compared to a low flow rate test case with $G=550 \text{ kg/m}^2\text{s}$ . . . . .	70
7.9	Evolution of the mass flow rate using first the surge tank and then a sine wave function. . . . .	71
7.10	Evolution of the pressures using first the surge tank and then a sine wave function. . . . .	71



# List of Tables

2.1	Classifications of flow instabilities [Boure et al., 1973]. . . . .	10
3.1	Results from Liu & Kakaç [1991]. . . . .	22
4.1	Accuracy of the measurement instrumentations [Ruspini, 2013; Sørum, 2014]. . . . .	40
7.1	Heat applied from each heater during the different heat profiles. The total heat fluxes for all cases were $q'' = 35 \text{ kWm}^2$ . . . . .	65



# Nomenclature

## Abbreviations and Acronyms

DWO	Density Wave Oscillation
ID	Inner Diameter
LabVIEW	Laboratory Virtual Instrument Engineering Workbench
NTNU	Norwegian University of Science and Technology
OD	Outer Diameter
PB	Pump Bypass
PDO	Pressure Drop Oscillation
REFPROP	Reference Fluid Thermodynamic and Transport Properties Database
ST	Surge Tank
THO	Thermal Oscillation

## Variables and Parameters

$\alpha$	Void Fraction	[-]
$cp$	Heat Capacity	[J/ kg K]
$D$	Diameter	[mm]
$\varepsilon$	Surface Roughness	[mm]
$f$	Friction Factor	[-]
$G$	Mass Flux	[kg/sm <sup>2</sup> ]
$H$	Specific Enthalpy	[J]
$k$	Thermal Conductivity	[W/mK]
$K_i$	Inlet Restriction	[-]
$K_o/K_e$	Outlet Restriction	[-]
$I$	Current	[A]
$\mu$	Dynamic Viscosity	[kg/ms]

$P$	Pressure	[Pa]
$\Delta P$	Differential Pressure	[-]
$P_W$	Power	[W]
$q''$	Heat Flux	[W/m <sup>2</sup> ]
$R$	Radius	[m]
$\rho$	Density	[kg/m <sup>3</sup> ]
$T$	Temperature	[°C]
$\Delta T$	Differential Temperature	[-]
$U$	Voltage	[V]
$X_m$	Vapour mass fraction	[-]
$X_{th}$	Thermodynamic Quality	[-]
$\Delta z$	Length (of test section)	[m]

## Subscripts

$()_{ext}$	External System
$()_F$	Fluid
$()_i$	Inner
$()_{in}$	Inlet of test section
$()_{int}$	Internal System
$()_l$	Liquid
$()_o$	Outer
$()_{out}$	Outlet of test section
$()_{sat}$	Saturation
$()_{sub}$	Subcooling
$()_v$	Vapour
$()_w$	Wall
$()_{wi}$	Inner Wall
$()_{wo}$	Outer Wall

## Non-dimensional Numbers

Nu	Nusselt Number
Pr	Prandtl Number
Re	Reynolds Number

# Chapter 1

## Introduction

### 1.1 Background and Motivation

An increasing energy demand around the world requires more efficient energy solutions. The ability to reuse energy through convective heat transfer is just one of many solutions that are in use today. For flow boiling and condensation in two-phase flows, the heat transfer rate is greatly enhanced due to an increase in the heat transfer coefficient [Maulbetsch & Griffith, 1965]. Considering the constant search for energy efficient solutions in the industry, the use of two-phase flow in convective heat transfer systems is employed in equipment such as heat exchangers, nuclear reactors, steam generators, refrigeration systems, boiling water reactors and other systems involving boiling heat transfer. In addition to the positive aspects of using two-phase flows, thermo-hydraulic instabilities are likely to occur during certain operating conditions. Mechanical vibrations can be initiated from sustained flow instabilities and can cause control problems and may eventually induce fatigue of the equipment. Extensive instabilities can further disturb the heat transfer and may result in a burnout of the heat transfer surface. The problems occurring in heat exchange systems forces the systems to be operated with less efficient operational parameters. Thus, knowledge about how to restrict the instabilities while still operating at the maximum efficiency point would be valuable for the industry.

The Pressure Drop Oscillations (PDOs) are one of the types of instabilities prone to occur in two-phase flows during boiling heat transfer. A PDO occurs in systems with a large internal compressible volume, either located upstream from or within the test section. PDOs are characterized by long periods that produce big mass flow excursions accompanied by high amplitude interfering signals. The large mass flow excursions results in significant variations of the local wall temperature and may induce burnout.

The research field of two-phase flow instabilities was pioneered in the 1960s. Since then both numerical and experimental investigations concerning PDOs and other

instabilities have been carried out by various researchers. The results present a variety of distinct PDOs with great variations in parameters such as period, amplitude and the interfering oscillations. However, real understanding of the parameters affecting the characteristics of PDOs is still missing. Further studies are still needed in order to get a thorough understanding of the PDO phenomenon and how the external parameters and the heat applied to the system affects the characteristics.

## 1.2 Objectives

The objective of this thesis is to experimentally investigate PDO instabilities in two-phase flow. In particular how the external system and heat flux influence the characteristics of the PDOs will be given special consideration. The main objectives can be summarized by the four following points:

- A literature review is to be performed with focus on the physical phenomena involved during PDO occurrence, its main characteristics (such as frequency and amplitude) and how they are affected by different operating parameters such as system pressure, heat flux, mass flux and inlet temperature.
- Experiments are to be performed in the Two-Phase Flow Instabilities rig at the EPT lab, setting the appropriate conditions for the occurrence of PDOs.
- Validate the experimental facility and instrumentation for single-phase flow.
- Experimentally study the effect of heat flux, inlet and outlet restriction, compressible volume and pump bypass on PDO occurrence and their physical characteristics.

## 1.3 Scope

The experimental work has been carried out at the *Two-Phase Flow Instability Facility* located at the Varmeteknisk, EPT laboratorium at NTNU. The facility is specifically designed to study instabilities occurring in two-phase flow. By the use of R134a refrigerant in a single, horizontal channel measuring 2035 mm in length and with an internal diameter of 5 mm the experiments concerning PDOs have been carried out. For heating purpose, five electrodes systematically distributed along the length of the channel were used. In order to onset the PDOs, a compressible volume located inside an upstream surge tank has been implemented. The purpose of the surge tank was to mimic a compressible volume that naturally may occur in a heat exchange system. The effect of configurations such as inlet and outlet restrictions, compressible volume, pump bypass and the heat flux applied have been investigated using a sub-cooled inlet flow.



## 1.4 Organization of This Thesis

The theory concerning two-phase flow instabilities with main focus on PDOs will be presented in Chapter 2. This is followed by a literature review concerning experimental research performed on PDOs and other oscillations in Chapter 3. The different parameters and characteristics affecting the PDOs will be examined, giving a theoretical understanding of the phenomenon.

Further, the experimental rig used during the experiments will be presented in Chapter 4 together with methods, accuracy and computational tools needed for evaluation of the results.

Before the outcome of the experimental results are presented, Chapter 5 gives the validation and characterization of the system. Further on, the results from the experimental work will be presented. This work is divided into two chapters, Chapter 6, which concerns the effect of the external system and Chapter 7, which focuses on the effect of the heat flux on the PDOs. In addition, a discussion concerning the interfering signals, DWOs, are given. The results will be presented along with a discussion closure at the end of each chapter.

Finally, suggestions for future work concerning PDO instabilities in two-phase flow will be presented together with a closing conclusion.

During the work of this thesis, one scientific article has been produced and is already submitted to the Chemical Engineering Science journal. The manuscript can be found in Appendix A.



# Chapter 2

## Two-phase Flow Instabilities

The objective of this chapter is to present the fundamentals of two-phase flow before a more narrow discussion concerning the instabilities occurring in such boiling flows will be given.

### 2.1 Two-phase Flow

A two-phase flow is defined by a flow consisting of two different phases of the same or multiple components. In this thesis, two-phase flow will refer to a liquid and vapour mixture of the same component. As seen in Figure 2.1 a boiling two phase flow that enters a horizontal tube as liquid and exit as vapour transits through different flow patterns. In a vertical pipe the flow pattern will be symmetric, but due to buoyancy forces the flow patterns in a horizontal tube will appear asymmetrical. The flow enters as *single-phase liquid* before the heat onsets *bubbly flow* at the right temperature for its local pressure. With increasing heat the flow further develops via *plug flow* and *slug flow* before more coherent flows, *wavy flow* and *annular flow*, appear. In the end, only vapour exists and the walls of the pipe will dry out, starting with the upper wall first. Small droplets of liquid will still be present, entrained in the gas core [Collier & Thome, 1994].

#### 2.1.1 Parameters

In order to understand the mechanisms of two-phase flow, the parameters for flow quality and void fraction are needed.

The *vapour mass fraction* of a two-phase flow,  $X_m$ , can be defined as:

$$X_m = \frac{\dot{m}_v}{\dot{m}_v + \dot{m}_l} \quad (2.1)$$

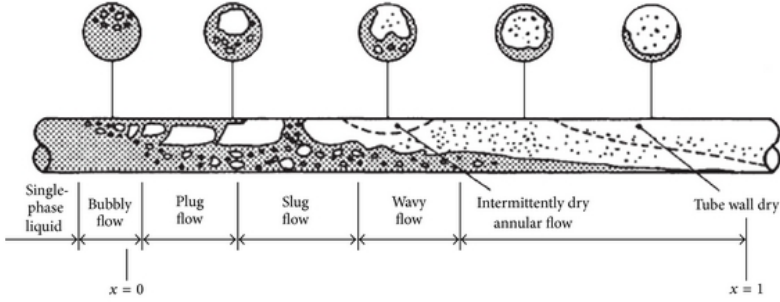


**Figure 2.1:** Flow pattern in two-phase flow in a horizontal pipe during evaporation [Collier & Thome, 1994].

where  $\dot{m}_v$  is the mass flow rate for vapour and  $\dot{m}_l$  the mass flow rate for liquid [Chiapero, 2013]. For  $X_m=0$ , no vapour is present in the system. When  $0 \leq X_m \leq 1$ , vapour and two-phase flow is present. The vapour mass fraction is often referred to as *vapour quality*.

The *thermodynamic quality*,  $X_{th}$  is given as:

$$X_{th} = \frac{H - H_l}{H_v - H_l} \quad (2.2)$$

where  $H$  is the specific enthalpy of the fluid,  $H_l$  is the specific enthalpy for saturated liquid and  $H_v$  is the specific enthalpy for saturated vapour. The values for  $X_m$  corresponding to the phase of the flow is also applicable here. In addition,  $X_{th} \geq 1$  would signify superheated vapour while  $X_{th} \leq 0$  implies only liquid. At thermodynamic equilibrium,  $X_m = X_{th}$ . In this thesis, thermodynamic equilibrium is assumed to be present. For the thermodynamic quality based on the heat applied to the system, please refer to Equation 4.3.

The *void fraction* is another parameter used for two-phase flows that informs about what fraction of the channel volume that is composed of gas or liquid. It can be defined in four different ways, depending on the measurements methods; the zero dimensional local void fraction, the one dimensional chordal void fraction, the two dimensional cross-sectional void fraction and the three dimensional volumetric void fraction. The *cross-sectional void fraction* which will be used in this thesis,  $\alpha_{c-s}$ , is given by:

$$\alpha_{c-s} = \frac{A_v}{A_l + A_v} \quad (2.3)$$

where  $A_v$  is the part of the cross-sectional area of the pipe which consists of vapour while the  $A_l$  is the cross-sectional part consisting of liquid.

## 2.2 Pressure Drop Characteristic Curve

In order to understand the instabilities that occur in two-phase flows the pressure drop characteristic curve, which visualizes the transition of the flow regimes according to the pressure drop and mass flux, is widely used. An example of the pressure drop characteristic curve, often referred to as the «N-curve» of a system due to its shape, is shown in Figure 2.2 for some given parameters. The negative slope that develops is given by the condition:

$$\frac{\partial \Delta P}{\partial G} < 0 \quad (2.4)$$

where  $G$  is the mass flux and  $\Delta P$ , the pressure drop, is a function of the mass flux and the vapour mass fraction. As seen in Figure 2.2, the negative slope occurs when both vapour and liquid are present in the system and thus the vapour quality of the outlet lies within the two-phase region,  $0 < X_m < 1$ .

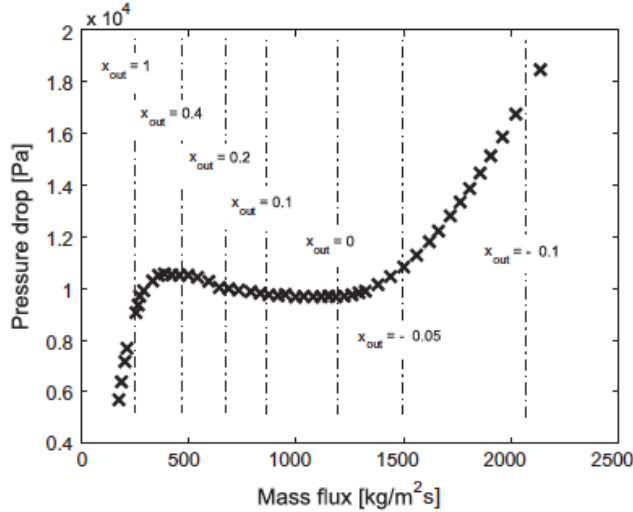
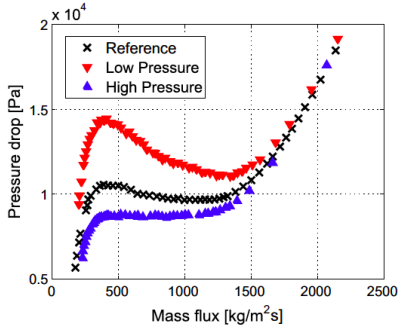
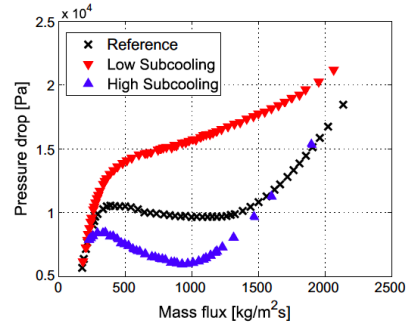


**Figure 2.2:** An example of the pressure drop characteristic curve for some given parameters ( $P_i=8.5$  bar,  $T_{sub}=30$  °C,  $q''=32$  kW/m<sup>2</sup>) [Chiapero et al., 2013].

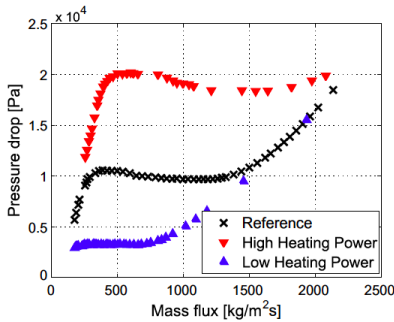
Chiapero et al. [2013] performed experiments using two-phase flow under varying operating conditions and validated the effect the different conditions had on the pressure drop characteristic curve, see Figure 2.3. They concluded that the working



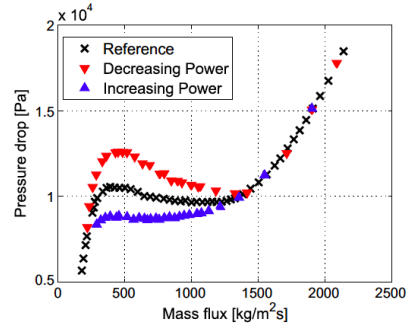
(a) Changing inlet pressure: 6.5 bar, 8.5 bar and 10.5 bar.



(b) Changing inlet subcooling: 20 °C, 30 °C and 40 °C .



(c) Changing heating powers: 48 kW/m<sup>2</sup>, 32 kW/m<sup>2</sup> and 16 kW/m<sup>2</sup>.



(d) Increasing and decreasing step wise heat flux profiles.

**Figure 2.3:** Operating reference values:  $T_{sub} = 30$  °C,  $q'' = 32$  kW/m<sup>2</sup> and  $P_{in} = 8.5$  bar. Results from Chiapero et al. [2013].

pressure in the facility had strong influence on the behaviour of the negative slope in the pressure drop characteristic curves and that increased pressures lead to a less steeper negative slope. The temperature of the inlet flow also appeared to have a great impact, with decreasing temperature forging an increase in the negative slope. As for the effect of the heat applied, it did not have any great influence on the slope when the distribution was uniform. However when the heat applied was alternated along the axial direction of the test section it had a large influence on the shape of the pressure drop characteristic curve.

Since every system behaves in different manners and its parameters affect the two-phase flow instabilities, it is essential to know how the appearance of the pressure drop characteristic curve for a given system and operational parameters looks like.

## 2.3 Flow Instabilities

In regards to two-phase flow instabilities it is usual to segregate between static and dynamic instabilities. Boure et al. [1973] defines static instability as a change from the original state of the flow disabling it from achieving another steady state in the proximity of the original one. It can lead to either a steady-state condition for the flow, different from the original one, or to a periodic behaviour of the flow. For a dynamic instability on the other hand, the inertia and feedback from the system play a major role in the evolving of the flow. For the static instabilities, the flow behaviour can be predicted by steady-state laws, but for the dynamic instabilities, due to the feedback and inertia from the system, this is not sufficient [Boure et al., 1973]. Among the most usual and frequently studied static instabilities is the *Ledinegg instability* while for the dynamic instabilities the *Density Wave Oscillation* (DWO), *Thermal Oscillation* (THO) and PDO are the most common. The Ledinegg instability, DWO and THO will briefly be described in the following sections while the PDO will be more thoroughly discussed in Chapter 2.4. The instabilities and their respective main mechanisms and characteristics are given in Table 2.1.

### 2.3.1 Ledinegg Instabilities

The static Ledinegg instability was first described by Ledinegg [1938] and the instability is named after his findings. The instability basically involves a rapid decrease in flow rate to a lower value [Ledinegg, 1938], making the system vulnerable to burn out. The best way to understand the Ledinegg instability is to look at the pressure drop characteristic curve showing the supply curve for the internal system (test section). Figure 2.4 illustrates two different supply curves for the system. In order for the instability to occur the slope of the supply curve for the internal system needs to be steeper than the supply curve of the external system. For the case of supply curve A, in the event of a decrease of flow rate from point 1 the pressure drop provided by the external system would be higher than that for the test section and the system would force itself back to the starting point and no oscillations would be present. For the case of supply curve B, being less steep than the negative slope of the N-curve, it is not possible to operate at point 1. A small decrease in flow rate would require a higher pressure drop in the internal system than the external system can deliver and the flow would decrease from point 1 to point 2. For a small increase in the flow rate on the other hand, an excursion from point 1 to point 3 would occur [Chiapero, 2013; Kakac & Bon, 2008].

Class	Type	Mechanism	Characteristics
Static Instabilities, Fundamental.	Ledinegg Instability	First order criterion, see Equation (2.5).	Flow undergoes sudden, large amplitude excursion to a new, stable operation condition.
Dynamic Instabilities, Fundamental.	Density Wave Oscillations	Delay and feedback effects in relationship between flow rate, density and pressure drop.	Low frequency (1 Hz) related to transit time of a continuity wave.
Dynamic Instabilities, Compound.	Thermal Oscillations	Interaction of variable heat transfer coefficient with flow dynamics.	Occurs in film boiling.
Dynamic instabilities, Compound instability as secondary phenomena.	Pressure Drop Oscillations	Flow excursion initiates dynamic interaction between channel and compressible volume.	Very low frequency periodic process (0.1 Hz).

**Table 2.1:** Classifications of flow instabilities [Boure et al., 1973].



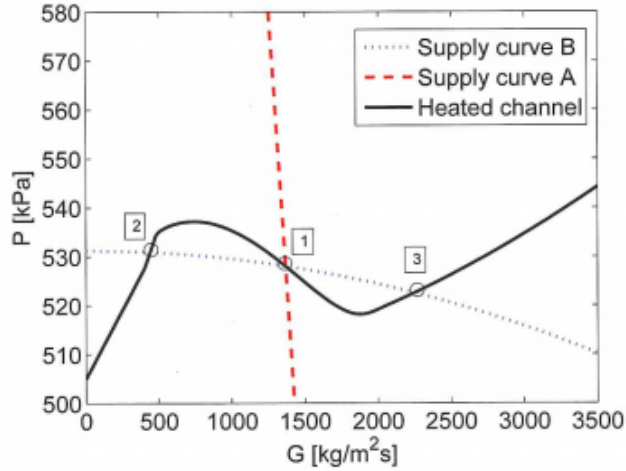


**Figure 2.4:** Different supply curves for the static pipe behaviour [Chiapero, 2013].

The criterion for Ledinegg instability to occur can be summarized by the *First-order instability criterion* [Boure et al., 1973]:

$$\frac{\partial \Delta P}{\partial G} \Big|_{int} \leq \frac{\partial \Delta P}{\partial G} \Big|_{ext} \quad (2.5)$$

It is essential to be aware that in different literature, the term Ledinegg instability may refer to the unstable region rather than the flow excursion. In this thesis, it will refer to the flow excursion.

### 2.3.2 Density Wave Oscillations

The high frequencies, purely dynamic, oscillations known as DWOs are the most frequently studied oscillatory phenomenon. It involves large oscillations in the inlet and outlet flow inducing oscillations in the fluid density. The frequency of the oscillations is assumed to be between 1.5 and 2 times the time the fluid uses to travel through the heated test section [Ruspini, 2013; Boure et al., 1973]. The main mechanisms initiating and pursuing the DWOs are delays in the propagation of disturbances and the feedback processes interfering with the inlet boundary conditions of the test section [Chiapero, 2013]. A more thorough explanation can be given by looking at Figure 2.5. The pressures at the inlet reservoir and exit restriction, respectively  $P_l$  and  $P_e$ , and the rate of vapour generation is kept constant. Assuming a sudden, small pressure drop in the exit restrictions for the heated section,  $P_e$ . The pressure here is kept constant so a small drop in value will immediately induce a

negative change in the inlet pressure,  $P_o$ . This will further lead to a small increase in the inlet flow velocity and the fluid will be of higher density. The increased velocity will also make the pressure in the test section rise. After the approximate time a particle needs to transit the test section it will force  $P_e$  to rise. Since  $P_e$  is still being constant it again induces a change, this time an increase, for  $P_o$ . This will then cause a decrease in the inlet flow velocity and a decrease in the fluid density. The lower flow will again force a pressure drop at the exit of the test section and the cycle repeats itself [Kakac & Bon, 2008]. According to Fukuda & Kobori [1979] the density wave instabilities can be divided into three different types based on the mechanisms initiating it: DWO due to gravity, DWO due to friction and DWO due to momentum.

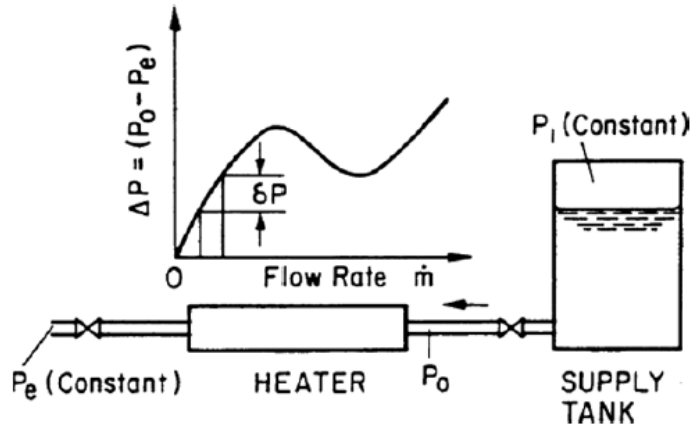


**Figure 2.5:** A simple system for DWO occurrence [Kakac & Bon, 2008].

The operational area of DWO according to the pressure drop characteristic curve is shown in Figure 2.8. As the figures shows, the DWO takes place at a high value of vapour mass fraction and thus high quality of the outlet flow.

### 2.3.3 Thermal Oscillations

THO is a dynamic instability usually referred to as a temperature fluctuation in a solid due to fluid interaction with a heated wall [Kakac & Bon, 2008]. The phenomenon was first described by Stenning & Veziroglu [1965]. As for the case of a closed loop facility, the oscillations appear in the temperature of the heated pipe wall. Most of the studies describing THOs are actually PDOs where the main focus have been on the temperature of the outlet pipe [Chiapero, 2013]. The mechanisms of PDOs are laid out in the following section.

## 2.4 Pressure Drop Oscillations

PDOs differs from the previously mentioned dynamic instabilities by its classification as a *compound dynamic instability*. This means that the dynamic instability is triggered by a static instability. According to Padki et al. [1992] when the system reaches a super-critical *Hopf bifurcation* point, where an appearance (or disappearance) of a limit cycle due to a change in the system from a stable point occurs, the PDOs are triggered. Another aspect separating it from the other instabilities is the need for a compressible volume, either upstream or within the test section, in order for the oscillations to occur [Boure et al., 1973]. In addition, it needs to operate in the negative slope region of the pressure drop characteristic curve and have an external characteristic curve steeper than the internal curve. This means it is unavailable for Ledinegg instabilities. The big flow excursion produced by PDOs results in large variations of the wall temperature in the test section, known as THOs. As for the THOs, PDOs was first described by Stenning & Veziroglu [1965] whom named the oscillation based on boiling flow pressure drop characteristics being the cause of the instabilities.

The mechanisms during PDOs can be described by using a simple system for generation of PDOs and the pressure drop characteristic curve, see Figures 2.6 and 2.7. The volume flows measured before the surge tank and before the test section are given as  $Q_1$  and  $Q_2$  respectively. The characteristic curve for the external system is steeper than the curve for the internal system and intersects in the two-phase flow area, where  $Q_1 = Q_2$ , placing it in the operational area of PDOs. The surge tank located upstream of the test section (boiling channel) allows  $Q_1$  and  $Q_2$  to differ and contains a given compressible volume,  $V_G$ . If the liquid level in the surge tank,  $V_L$ , increases, a decompression of  $V_G$  will happen inside the tank and the fluid flow  $Q_1$  will be increasingly larger than  $Q_2$ . Assume now a small positive change in the inlet pressure,  $P_1$ . This will increase  $Q_1$  relative to  $Q_2$ . Further, an increase of  $Q_1$  will lead to a decompression of  $V_G$  and even higher  $P_1$ . As seen in Figure 2.7, this development from  $C$  will continue until the state of  $D$  is reached. In order to then achieve an even higher value for  $P_1$ , a flow excursion develops from the two-phase flow to the single-phase liquid state and the point  $A$ . The compressible volume will next decompress and force the liquid out of the tank, making  $Q_2$  larger than  $Q_1$ , until it reaches the point of  $B$ . The system will then again undergo a flow excursion, this time from single-phase liquid to two-phase liquid, increasing the vapour quality until the state of  $C$  is reached and the cycle of  $C - D - A - B - C$  repeats itself [Ruspini et al., 2014; Chiapero, 2013].

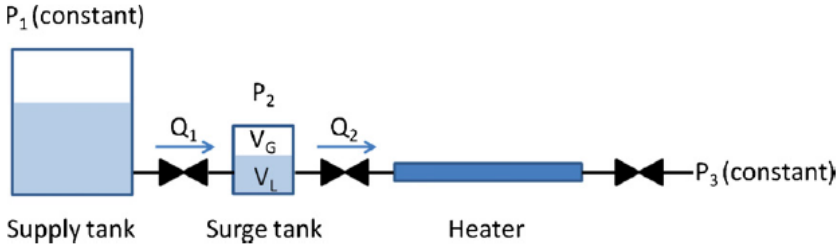


Figure 2.6: Set up for the Surge Tank [Chiapero et al., 2012].

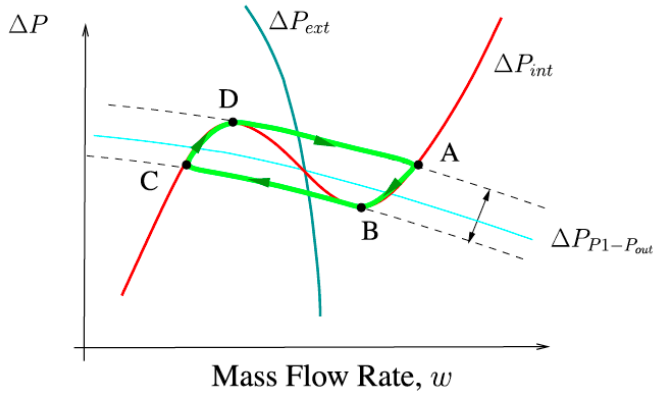


Figure 2.7: External and internal characteristics curves [Ruspini et al., 2014].

### 2.4.1 Main Characteristics

The PDOs are characterized by relatively large amplitudes and low frequencies and are often accompanied by interfering, high frequency signals. According to Grasman [2011] the long oscillation periods of PDOs are characterized by relaxation oscillations related to *van der Pol* oscillations, also known as limit cycles, and the period of the oscillations are usually larger than the time a fluid particle uses to pass through the test section.

It is a common comprehension that the interfering signals actually are DWOs interacting with PDOs [Ruspini, 2013; Maulbetsch & Griffith, 1965; Dogan et al., 1983; Liu & Kakaç, 1991; Menten et al., 1983; Yüncü et al., 1991; Padki et al., 1991; Ding et al., 1995]. The different operational areas for DWOs and PDOs in the pressure characteristic curve can be seen in Figure 2.8. It shows that there is a need for a higher vapour quality for the occurrence of DWOs than for the PDOs instabilities.

A well-known method to avoid PDOs occurring in the system is to make the slope of the internal characteristics, the pressure drop characteristic curve, consistently positive. This can for example be done by adding a restriction at the inlet of the heated channel.

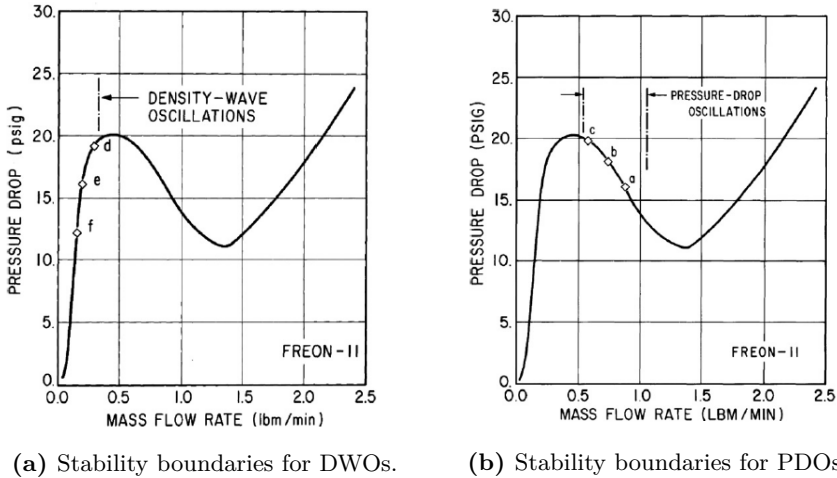


**Figure 2.8:** Stability boundaries for DWOs and PDOs according to the pressure drop characteristic curve [Kakac & Bon, 2008].



# Chapter **3**

## Previous Work

In this chapter, a literature review regarding two-phase flow instabilities with primary emphasis on pressure drop oscillations is presented. The main focus is concentrated on previous experimental work concerning the effect of the external system, the compressible volume and effects of the heat flux applied.

### 3.1 Two-Phase Flow Instabilities

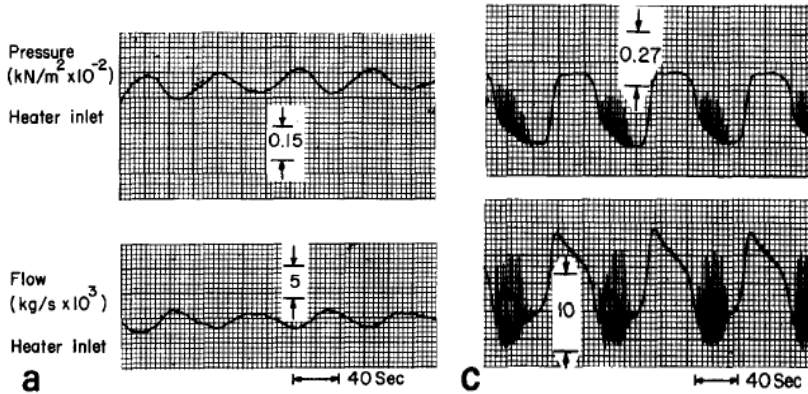
One of the earliest research done in the field of two-phase flow was performed by Lorenz [1909]. For the field of two-phase flow instabilities, the pioneering work was done by Ledinegg [1938] in the 1930's. He described the static Ledinegg instability and it was not until 30 years later, in the 1960's that additional instabilities were discovered mainly due to the increasing use of high density industrial boilers and boiling water reactors [Sørum, 2014]. Since the 1970's several literature reviews concerning two-phase flow instabilities have been published [Boure et al., 1973; Tadrist, 2007; Prasad et al., 2007; Kakac & Bon, 2008; Liang et al., 2010; Ruspini et al., 2014]. A literature review with focus on PDOs are done by Chiapero et al. [2012].

### 3.2 Pressure Drop Oscillations

As stated in Chapter 2.4 the PDOs were first described as a distinctive phenomenon by Stenning & Veziroglu [1965] during the 1960's. The characterization of DWO, THO and PDO were results of experimental work in a forced convective boiling system using Freon-11 as test fluid. They concluded that the PDOs occurred in the negative region of the pressure drop curve and therefore within the stable zones for DWOs and THOs. This theory was later confirmed by Maulbetsch & Griffith [1965]. The numerical model they developed in order to describe the physics of PDOs with an upstream compressible volume is still used today and is in good agreement with experimental data [Chiapero et al., 2012]. The only hypothesis that needs to

be taken into account is that the period of the oscillations are much larger than the travelling time of a particle in the test section. Maulbetsch & Griffith [1965] performed both analytical and experimental work analyzing PDOs. The PDOs were not named at this point, but were referred to as «compressible volume oscillations». They pointed out that the PDOs only occurred in the negative slope of the pressure drop characteristic curve.

Dogan et al. [1983] developed a numerical model in order to predict both steady state, DWOs and PDOs in two-phase flows. In order to validate the results, experiments using a single channel with forced-convection and an electrical heating up-flow system were carried out. For the experimental part, DWOs and PDOs were observed in addition to PDOs superimposed by DWOs, shown in Figure 3.1. Both the pure PDOs and PDOs superimposed with DWOs occurred in the negative slope of the pressure drop characteristic curve. The experimental results agreed well with the numerical model with respect to the period of the oscillations, but undershot for the value of the amplitudes.



(a) PDOs with parameters of  $P_W=400$  W,  $T_{in}=9$  °C and  $\dot{m}=7.6 \times 10^{-3}$  kg/s. (b) PDOs with superimposed DWOs using parameters of  $P_W=500$  W,  $T_{in}=-1$  °C and  $\dot{m}=6.8 \times 10^{-3}$  kg/s.

**Figure 3.1:** Experimental results from Dogan et al. [1983].

### 3.2.1 Effect of the External System and Heat Flux

Various researchers have examined the effect of upstream throttling of the system in order to achieve more stable conditions. Daleas & Bergles [1965] performed experimental work concerning flow oscillations altering the subcooled critical heat flux and also studied the effect an upstream compressible volume had on two-phase flow oscillations. They concluded that while using a large upstream compressible volume the only way to avoid oscillations in the flow was to operate at the right



side of the minimum in the pressure drop characteristic curve, in the liquid region. Further, they concluded that as the velocity in the system or the size of the test section tube was increased, the effect of the compressible volume was reduced. They also pointed out that a throttling of the inlet, e.g. an inlet valve, of the heated test section would prove efficient to stabilize the system and that an equivalent compressible volume could be provided by entrained or trapped gas in the system.

Maulbetsch & Griffith [1965] stated that when the compressible volume is situated outside the heated test section, the instabilities can be eliminated by a sufficient throttling between the heated test section and the external compressible volume. For a very long test section,  $L/D > 150$ , the compressible volume inside the test section itself, due to vapour generation, can be enough to onset the oscillations. No external throttling would in that case have any effect. While using a single tube system for a known amount of compressible volume and system characteristics, both the pressure drop characteristic curve, for initiation of oscillations, and the frequency of the oscillation could be calculated. The appearance of DWOs during the oscillations onset by the compressible volume was also discussed, stating that in flows with high vapour quality, the DWOs were likely to occur. The high frequency, interfering signals were also discussed by Ozawa et al. [1979]. They concluded that the signals depended only on the experimental conditions of the system and were not an essential feature of the PDOs.

The effect of different heating surfaces on two-phase flow instabilities in vertical channels have been experimentally evaluated by Menten et al. [1983]. By using six vertical heating test sections with different internal surface configurations they tested the effect the surface configurations had on the PDOs and the superimposed DWOs. For the DWOs, the period of the signals did not change throughout the different pipes, while for the PDOs there was a great difference. The authors suggested a relation to the wave propagation lags and feedback effects produced by the PDOs. According to Chiapero et al. [2012] the thermal capacity, and thereby the heat transfer coefficient, of the different six pipes would play a major role. The main idea behind this suggestion is that an alternation of the thermal capacity of the different pipes plays a minor role for the DWOs than for the PDOs.

For the exit restrictions, an experimental and numerical study performed by Yüncü et al. [1991] investigated the effect of the exit orifice diameter, heat flux and mass flux on the stable and unstable operational regions for DWOs and PDOs. For the PDOs it was concluded that the periods and amplitudes increased with decreasing exit orifice diameter or an increase in the heat flux. This was explained as an increase in the pressure in the surge tank due to the decreasing orifice diameter or increased heat flux, leading to further compression of the compressible volume in the surge tank. At increasing heat input and a fixed orifice diameter, the stability of the system

decreased for both PDOs and DWOs.

Experiments regarding THOs and PDOs superimposed by DWOs were carried out by Padki et al. [1991]. Two sets of experiments were done, one with constant inlet temperature while varying heat inputs and one with constant heat input and varying inlet temperatures. In addition to the experiments, a drift-flux model was used for numerical investigation. They concluded that both an increasing heat input and increasing inlet temperature led to an increase in periods and amplitudes for the oscillations. In addition, when the mass flow rate decreased an increase in the periods and amplitudes was observed. For the phases of the oscillations, the temperature and pressure oscillations seemed to be in phase, with a slight lag of the maximum of the pressure oscillations. The oscillations of the mass flow rate seemed to be  $180^\circ$  out of phase compared to the temperature and pressure. For the numerical drift-flux model, both the steady state and oscillations agreed well with the experimental results. The PDOs superimposed by DWOs can be seen in Figure 3.2.

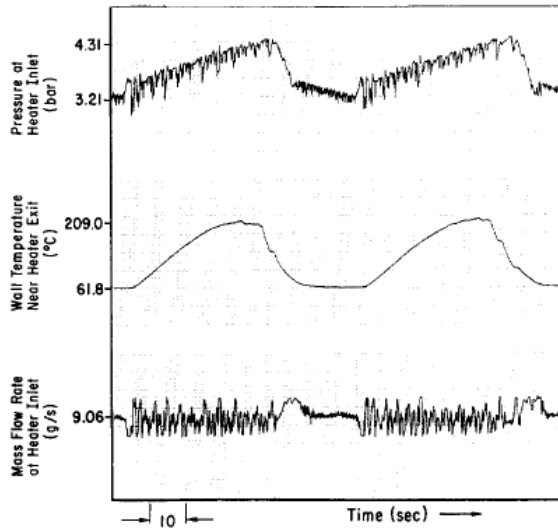


**Figure 3.2:** PDOs superimposed by DWOs shown for the pressure, wall temperature and mass flow rate during operational conditions of  $T_{in}=10^\circ\text{C}$ ,  $P_W=800\text{ W}$ ,  $G=0.05\text{ g/sec}$  [Padki et al., 1991].

Liu & Kakaç [1991] performed extensive experiments in order to investigate the effects of heat flux, subcooling of the inlet flow, mass flow rate and the upstream compressible volume on PDOs, DWOs and THOs. Three different series of experiments were performed: alternating heat flux while maintaining inlet subcooling, alternating subcooling while keeping the heat flux constant and different surge tank volumes. For the two first cases, the mass flow rate was varied. The final investigations were done

using different surge tank volumes while keeping the other parameters constant. They reported pressure drop type oscillations starting at the minimum of the pressure drop characteristic curve, at the onset of boiling. When the flow rate decreased, PDOs superimposed by DWOs occurred. The reported that PDOs were also accompanied by THOs. At the single-phase vapour region, only DWOs occurred. The phenomenon of PDOs superimposed by DWOs was described using the limit cycle, where the DWOs onsets in the vapour region of the pressure drop characteristic curve, see Figure 3.3. The results of their experiments are summarized in Table 3.1.

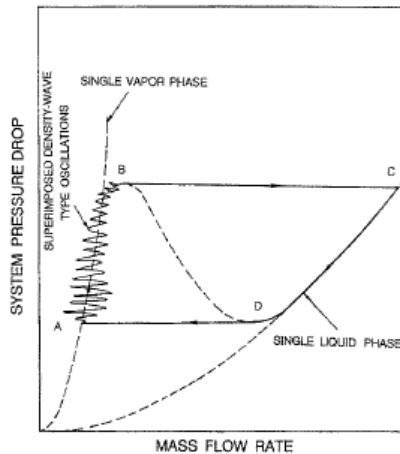


**Figure 3.3:** Drawing of the limit cycle for PDOs with the superimposed DWOs [Liu & Kakaç, 1991].

Further analysis of two-phase flow instabilities were performed by Ding et al. [1995] evaluating the characteristics of instabilities in a horizontal channel compared to a earlier works done in vertical channels. One of the main findings was that the oscillation region in a horizontal channel, with respect to the pressure drop characteristic curve, is located further to the right, at higher mass flow rates, than for a vertical channel. For experimental work in the horizontal channel, a graphical representation of the oscillations boundaries showed that both PDOs superimposed by DWOs, and pure DWOs occurred in the negative region of the pressure drop characteristic curve. This is in contradiction to other studies, stating that the pure DWOs occurs in the single-phase vapour region of the curve [Liu & Kakaç, 1991; Yüncü et al., 1991; Kakac & Bon, 2008]. The result may be explained by the distribution of the fluid in the test section. Since the fluid in almost the entire system was vapour phase, except a thin film of fluid covering the bottom of the pipe, the pressure drop characteristic curve they presented may not have been accurate according to the onset of the vapour region. By using a higher mass flow rate, a more accurate distribution of the phases of the fluid would probably have been present. For the experiments concerning PDOs,

Parameter	Change	THO		PDO with DWO			
		Amplitude	Period	Amplitudes		Periods	
				PDO	DWO	PDO	DWO
Mass Flow Rate	Decrease (20.92 – 7.31 g/s)	Increases	Increases	Increases	Decreases	Increases	Increases
Heat Applied	Increases (400 – 800 W)	Increases	Increases	Increases	Increases	Increases	Decreases
Inlet Subcooling	Increases (–10 – 23 °C)	Decreases	Decreases	Decreases	Decreases	Decreases	Consistent
Surge Tank Volume	Decreases	Decreases				Decreases	

**Table 3.1:** Results from Lin & Kakaç [1991].

it was shown that as the flow rate decreased, the amplitudes and periods decreased while they increased as the inlet subcooling increased. For the increased heat input, the amplitudes increased while the periods decreased.

A study considering the influence of the placement of the upstream compressible volume was conducted by Guo et al. [2001] utilizing a helically coiled tube. One of the compressible volumes was located in front of the test section and one located further upstream in the system, in front of the pre-heater. The different PDOs observed were referred to as *1<sup>st</sup> PDO* and *2<sup>nd</sup> PDO* as results of the compressible volume located before the pre-heater and at the inlet of the test section respectively. The experimental results are shown in Figure 3.4 and 3.5. As seen in the figures, great differences in the appearance of PDOs are likely to appear when using distinct placement of the compressible volume. The period, shapes and the amplitudes of the signals varied. In addition, the boundaries of occurrence, with respect to the pressure drop characteristic curve were dissimilar. The *1<sup>st</sup> PDO* occurred during higher vapour quality than the *2<sup>nd</sup> PDO* which occurred in the minimum of the curve, in the boiling onset region. When it came to the compressible volume needed to obtain and maintain the oscillations, the *1<sup>st</sup> PDO* required 2-4 times the volume than the *2<sup>nd</sup> PDO*. This means that a compressible volume located further upstream of the heated test section can efficiently reduce the PDO instability. In addition to the compressible volume, experiments regarding non-uniform heat flux were performed using two different heating regions in the test section. For the *2<sup>nd</sup> PDO* the non-uniform heat flux did not have any significant effect, while for the *1<sup>st</sup> PDO* it decreased the initial boundaries for occurrence. Guo et al. [2001] stated that the PDOs could be suppressed by using a uniform heat flux, and if that was not achievable, the bulk of the heat flux should be applied in the low vapour quality region.

By using helically coiled tubes a further experimental study by Guo et al. [2002] investigated the dependency THOs, PDOs and DWOs had on the main system parameters such as the compressible volume, heat flux, inlet temperature, pressure and the mass flow rate. They concluded that the system became more stable as the pressure and inlet subcooling increased and as the compressible volume and heat flux decreased.

Çomaklı et al. [2002] performed experiments investigating the effect of the channel length, inlet temperatures and mass flow rate utilizing a test section pipe of 11.2 mm inner diameter and 3.5 m in length. The length of the channel proved to have an important effect on two-phase flow instabilities by increasing the stability in the system as the length decreases. They concluded that the periods and amplitudes of the PDOs decreased as the flow rate decreased and increased with decreasing inlet temperature. Based on these findings, they stated that the stability boundaries for

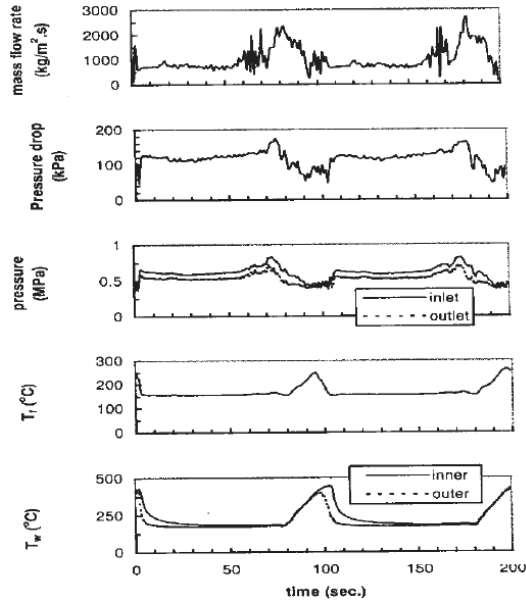


**Figure 3.4:** 1<sup>st</sup> PDO when the compressible volume was located before the pre-heater [Guo et al., 2001].

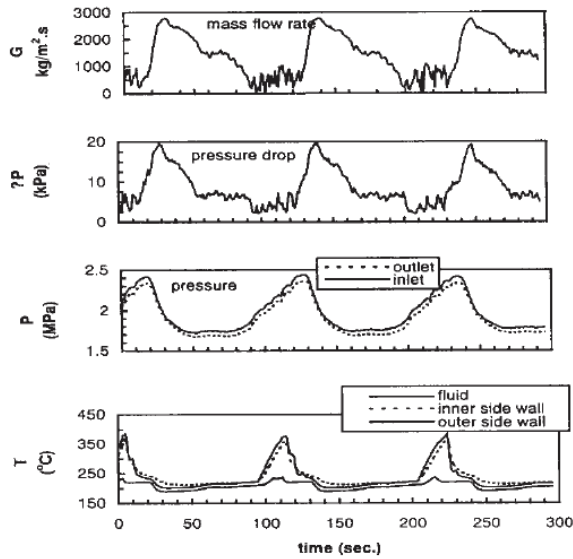


**Figure 3.5:** 2<sup>nd</sup> PDO when the compressible volume was located at the inlet of the test section [Guo et al., 2001].

PDOs are a function of the inlet temperature and the mass flow rate.

### 3.2.2 Experimental Work Done at the Two-Phase Flow Instabilities Facility at NTNU

Following the design and construction of the Two-Phase Flow Instabilities Facility at NTNU distinct studies have been conducted with regards to PDOs. Chiapero [2013] performed a numerical investigation of PDOs for both single and parallel channels. For the case of parallel channels, an experimental investigation was also carried out utilizing the two-phase flow facility. The experiments presented two different cases of heat applied to the channels, equal and distinct heating. The results showed that no PDOs for both channels were following the typical limit cycle that is usually present for a single channel, even though both channels had almost the same pressure drop characteristic curve during steady state. One of the channels usually followed the limiting cycle while the other oscillated in the superheated vapour region, see Figure 3.6. This may actually be a more relevant result for real life applications since the parallel pipes encountered in e.g. heat exchangers rarely have the exact same behaviour and constant inlet mass flow [Chiapero et al., 2014b].

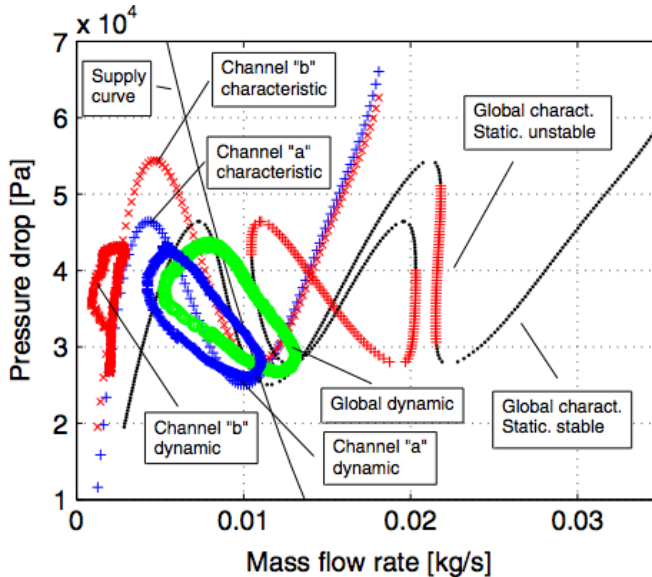


**Figure 3.6:** The limiting cycles for the two parallel channels during equal heating [Chiapero et al., 2014b].

Numerical and experimental investigations of two-phase flow instabilities were also carried out by Ruspini [2013]. For the case of PDOs, a numerical investigation of parameters such as placement and the effect of distinct compressible volumes

using a dynamic model was performed. By using a dynamic model, instead of the well-used steady-state model, he made the model able to predict the transitions of the oscillations from stable to unstable behaviour. The effect of the two different locations for the compressible volume was tested, one placed at the inlet of the test section and one at the outlet. While the one placed at the inlet induced PDOs, the one at the outlet did not induce any PDOs and actually made the system more stable in the sense of PDOs and DWOs. For the effect of the compressible volume of the surge tank placed upstream of the test section, the existence of a critical volume limit was confirmed. For volume less than this critical limit, the system evolved in a stable manner, while for greater volumes the system was predicted to be unstable and PDOs may therefore occur. With regards to the length from the compressible volume to the entrance of the test section, a longer distance stabilized the system, while a shorter distance destabilized the system and increased the amplitudes of the signals. This is in compliance with the experimental work of Guo et al. [2001]. It was stated that these results was due to a transition between PDOs and DWOs.

The phenomenon of DWOs and PDOs were studied experimentally by the use of the Two-Phase Flow Instability Facility by Ruspini [2013]. He concluded that the PDOs could not be considered a pure phenomenon, regardless of the compressible volume in the surge tank, because they interacted via energy exchange with DWOs. For the DWO mode, the presence of a compressible volume upstream of the test section was proven to have a destabilising effect. The values used for the experimental studies concerning the PDO-DWO interaction were  $P_{out} \approx 8.3$  bar,  $T_{in} \approx -13$  °C,  $Q \approx 1380$  W,  $G_{in} \approx 0 - 1500$  kg/m<sup>2</sup>s, a volume in the surge tank of 9 litres and an orifice outlet. For the experimental result, see Figure 3.7 for the evolution of mass flow, Figure 3.8 for the limit cycle and Figure 3.9 for an example of PDOs superimposed by DWOs (slightly different parameters used).

For an example of the DWOs occurring in the system, an experimental result by Ruspini [2013] is shown in Figure 3.10

### 3.3 Other Studies

Besides studies focusing on PDOs and other known oscillations, some researchers have studied and defined new types of oscillations. These findings are noteworthy as they may explain some of the distinct results obtained in different studies. An interesting experimental study concerning a new type of two-phase oscillations, *boiling onset oscillations*, in a vertical, single channel was performed by Wang et al. [1996]. The new type of oscillations occurred at the minimum of the pressure drop characteristic curve, at the onset of boiling. Figure 3.11 show where the boiling onset oscillations are likely to occur in the pressure drop curve, marked with the area *A*. When comparing the periods for the oscillations versus the ones for PDOs in the same system, the



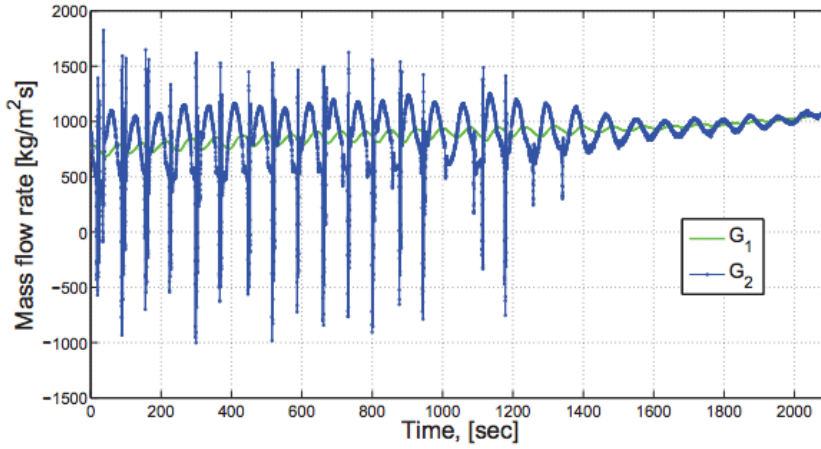


**Figure 3.7:** Evolution of PDOs superimposed by DWOs while the mass flow rate is increased [Ruspini, 2013].

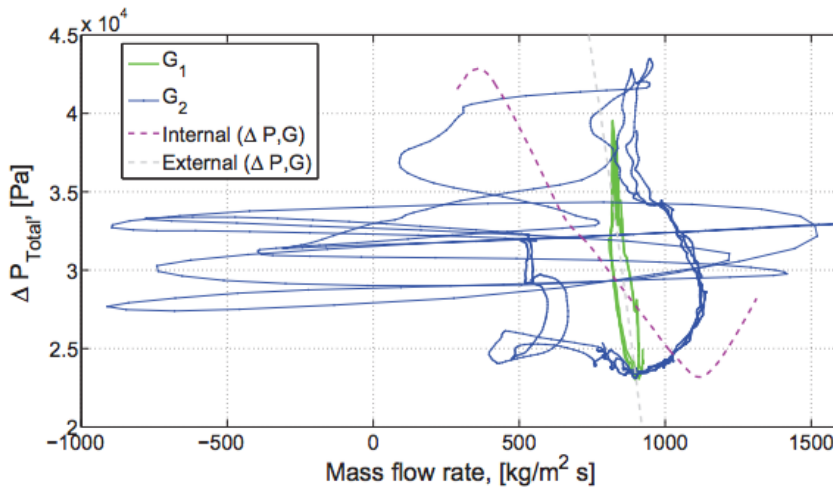


**Figure 3.8:** The limit cycle of PDOs superimposed by DWOs over the pressure drop characteristic curve [Ruspini, 2013].

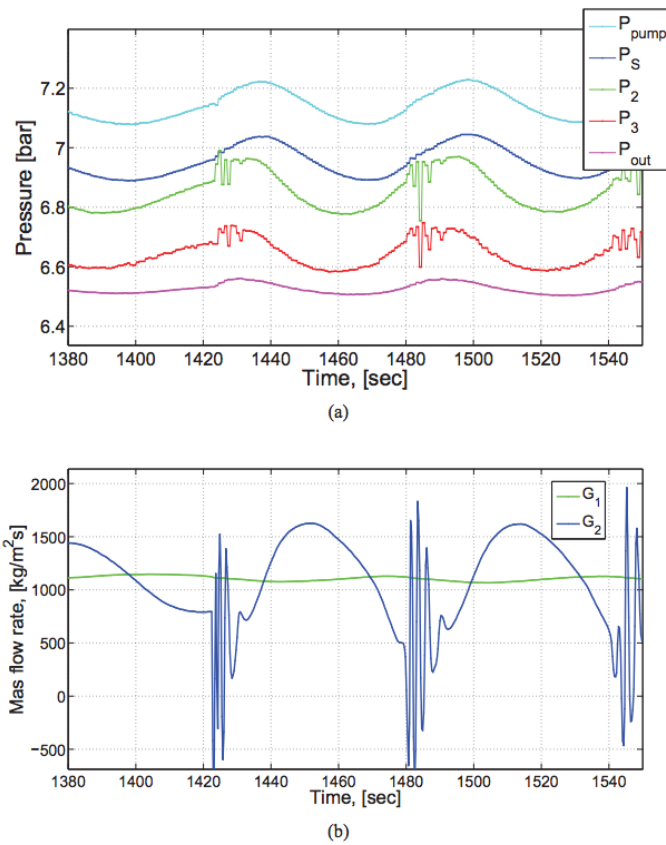


**Figure 3.9:** The PDOs superimposed by DWOs as they occur in pressure and mass flow oscillations [Ruspini, 2013].

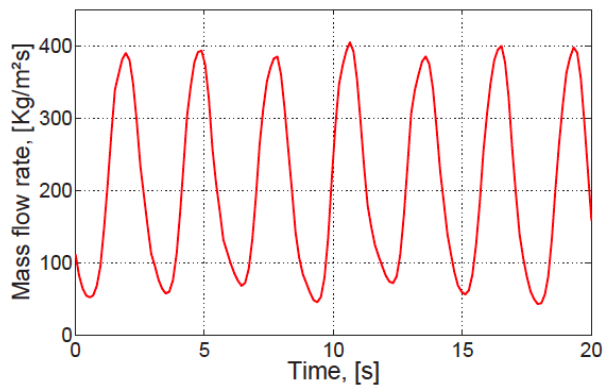


**Figure 3.10:** An example of the DWOs occurring in the system with conditions of  $P_{in}=8.4$  bar,  $T_{in}=17$  °C and  $P_W=870$  W [Ruspini, 2013].

boiling onset oscillations, as seen in Figure 3.12, had 3-5 times larger periods (60-120 seconds) than the PDOs (20 second). It was shown that the inlet subcooling had a big influence on the appearance of the onset boiling oscillations. As the subcooling was reduced, the onset boiling oscillations decreased and disappeared. Since the area of occurrence is quite narrow, the operational conditions were hard to set and maintain.

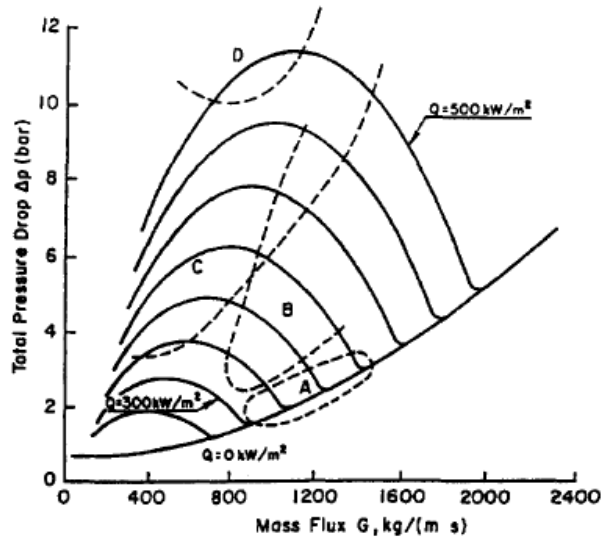


**Figure 3.11:** Pressure drop characteristic curves for distinct heat fluxes showing the different instabilities regions. The boiling onset oscillations occurred in region A, the PDOs in region B and the DWOs in region C. The parameters used were:  $P_{in}=38$  bar and  $T_{sub}=90$  °C [Wang et al., 1996].

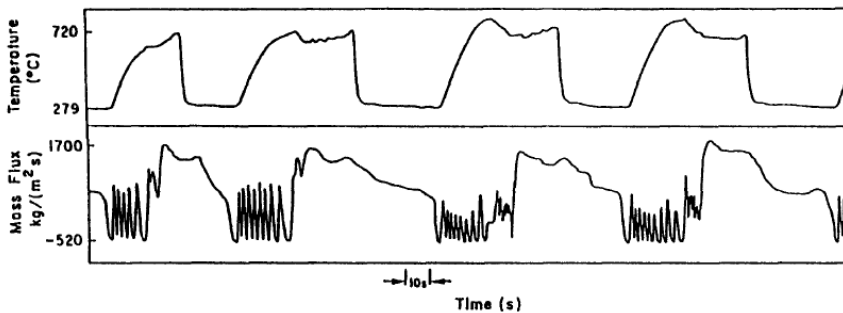


**Figure 3.12:** The temperature and mass flux oscillations developing during boiling onset oscillations using parameters of  $P_{in}=50$  bar,  $G=1124$  kg/m<sup>2</sup>s,  $q''=337$  kw/m<sup>2</sup> and  $T_{sub}=60$  °C [Wang et al., 1996].

While using parallel boiling channels, a phenomenon named  $2^{nd}$  DWO was studied by Xiao et al. [1993]. The  $2^{nd}$  DWO occurred at low vapour quality,  $X_{th} < 0.1$ , and onset right after the minimum of the pressure drop characteristic curve. The onset area was not unlike the one for boiling onset oscillations and they did sometimes coexist. But the different types of oscillations varied greatly in their appearance. The periods of the  $2^{nd}$  DWOs were about 6-12 seconds and the oscillations of the inlet flow rate and pressure drop were in phase. In addition, the flow rates in both channels were also in phase. By the use of a larger compressible volume, the amplitudes of the oscillations increased. For the wall heat flux, as the heat applied increased the  $2^{nd}$  DWO got smaller until it eventually disappeared. After the disappearance of  $2^{nd}$  DWOs, PDOs sometimes occurred and sometimes they also coexisted.

During the recent years, studies concerning two-phase flow instabilities in micro-channels have been carried out. Wang et al. [2008] performed experiments using parallel micro-channels with three different connections altering the inlet and outlet of the flow. The connection that restricted the inlet but not the outlet proved to be the most efficient in the work of damping the oscillations. In contrast to the instabilities occurring in macro-channels, as discussed in Section 3.2.1, the use of micro-channels makes it possible to operate in the negative section of the pressure drop characteristic curve since the fluctuations occurring in micro-channels are not as hazard as the ones observed for macro-channels. However, due to an increased risk of large-scale burnout in micro-channels, a shifting to far up the negative curve is not advised.

### 3.4 Summary

A wide range of different experiments, using distinct experimental setups, sizes of test sections, working fluids, operational parameters and distinct external systems have been carried out by various researchers. The results achieved from researchers from the 1960's and up to today show both similarities and dissimilarities. Different experimental setups seem to have a great influence on the resulting oscillations. The following similarities are found in the majority of the works:

- The PDOs usually occurs in the negative slope of the pressure drop characteristic curve.
- The PDOs are often accompanied by superimposed DWOs.
- A throttling of the inlet of the test section could be a way to reduce the oscillations.
- For the PDOs, an increase of heat flux or mass flow rate increases both the periods and amplitudes while an increase in subcooling decreases the signals.

- Different compressible volumes and their placement in the system have influence on the oscillations. Greater volumes seem to produce larger oscillations.

Even though there is a lot of research performed on PDOs, the contrasting results and uncertainties regarding some of the parameters requires more research. Especially when it comes to the amount of compressible volume, constraints in the system, non-uniform heat fluxes and the PDO-DWO interaction there are still more work to be conducted.



# Chapter 4

## Two-phase Flow Instabilities Facility

In this chapter the Two-Phase Flow Instabilities Facility will be outlined. The different components, measurements instrumentation and the software interface will be described. The key features and limitations of the facility will be highlighted before an outline of the operational procedures and a brief risk assessment for the facility is presented.

The Two-Phase Flow Instabilities Facility is a result of the PhD works of Ezequiel Manavela Chiapero [Chiapero, 2013] and Leonardo Carlos Ruspino [Ruspini, 2013] and is located at the Varmeteknisk lab, EPT, NTNU. The facility is designed for running experiments on two-phase flow instabilities such as for example DWOs and PDOs in both single- and multiple horizontal channels. This thesis will focus on single, horizontal channel experiments. For more information regarding the multiple channels part, please refer to Ruspini [2013].

### 4.1 Components

The working fluid for the facility is chosen to be *R134a* refrigerant based on its low boiling point, low latent vaporisation heat, non-flammable characteristics and because it is uncomplicated to operate [Ruspini, 2013]. Another benefit of using R134a is that it is more environmentally friendly than other refrigerants. All together the benefits reduces the complexity of the rig and improves its safety [Sørum, 2014]. The system is considered as a closed loop system. The flow circulation of R134a starts from the main tank where it, by the help of the pump, is forced out into the system. Before it enters the test section, it passes the surge tank that provides the necessary compressible volume for PDOs to occur. After the test section a short section of the pipe is transparent allowing for visual observation of the flow. In order to control the inlet flow of the test section a valve is installed that can restrict the flow. At the outlet, a choice of exit route between an adiabatic and an orifice section can be made. Before being retrieved to the main tank, the fluid passes through a

heat exchanger that serves as a condenser and controls the pressure in the system. A second heat exchanger is placed after the pump and serves as a preheater to the flow conditions at the inlet of the test section. A sketch of the whole test facility and its components is shown in Figure 4.1 and a picture of the facility at the lab is shown in Figure 4.2. The test section for a single channel, the surge tank, the heat exchangers and the pump will in the following sections be described in further detail.

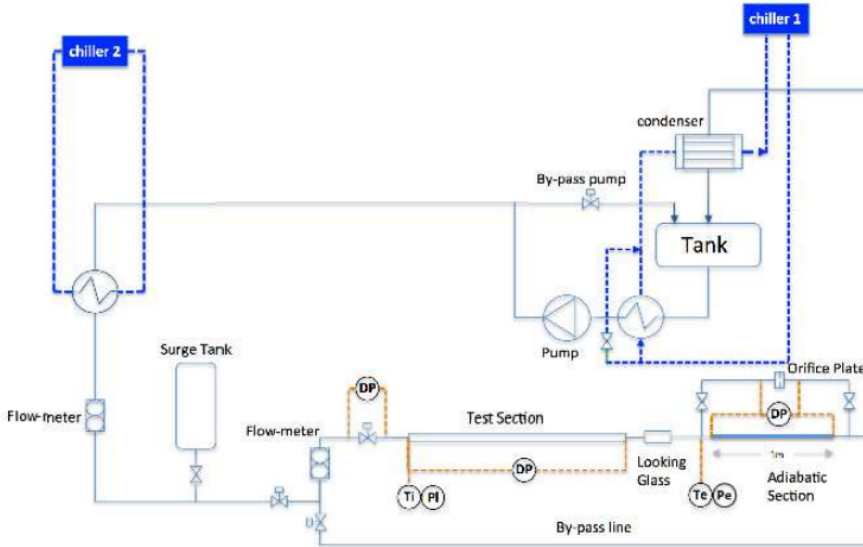


**Figure 4.1:** Sketch of the facility.

#### 4.1.1 Test Section

The test section consists of a 2035 mm long horizontal pipe with an inner diameter (ID) of 5 mm and outer diameter (OD) of 8 mm. The material used for the pipe is stainless steel, a material with a high heat transfer coefficient and good durability. Five heaters are equally distributed in five independent sections along the length of the pipe. This gives the opportunity to control the amount of heat applied to the system at the different locations and thereby controlling the heat profile. For more information about the heat flux applied see Section 4.2.1. The pipe is well insulated and the heat loss to the environment would therefore be limited. According to Ruspini [2013] the heat loss in the test section will never exceed 8%. As shown in Figure 4.3, along the test section thermocouples are measuring the temperature of the pipe walls. In addition, two thermocouples are located inside the pipe in the middle of the flow.





**Figure 4.2:** Picture of the facility at the lab [Chiapero, 2013].

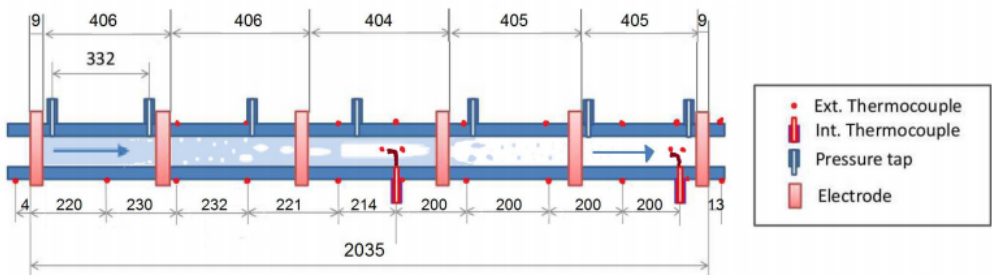


**Figure 4.3:** Set up for the heaters in the test section, dimensions given in mm. Adopted from [Ruspini, 2013; Sørnum, 2014].

### 4.1.2 Surge Tank

In order to achieve PDOs in the system, a sufficient volume of compressible gas upstream of the heated test section is needed, here located in the surge tank. To connect the surge tank to the main flow loop a valve is placed at the outlet of the tank. When no testing of PDOs are performed this valve is closed isolating the surge tank from the rest of the system. An example of the integration of the surge tank in the main loop is given in Figure 2.6. The surge tank is further connected to a nitrogen gas bottle where it is possible to adjust the compressible volume in the surge tank. The tank is approximated to have a volume of  $0.0095 \text{ m}^3$  giving it the ability to work within a variety of compressible volumes upstream of the test section.

### 4.1.3 Heat Exchangers

The two heat exchangers, Chiller 1 and Chiller 2, are placed respectively before the main tank and before the surge tank and are used to set the parameters for the flow. The condenser, Chiller 1, is a shell and tube heat exchanger and is used to control the pressure in the system by controlling the temperature in the condenser where the fluid is at saturation conditions ( $P_{condenser}=P_{system}$ ). The preconditioner, Chiller 2, a plate-and-fin heat exchanger, on the other hand regulate the value of the subcooling (temperature) for the flow of R134a entering the test section. The heat exchangers settings are operated from the software interface, see Section 4.5.

### 4.1.4 Pump

The flow of refrigerant is controlled by the pump, a magnetically coupled gear pump, by changing the voltage of the DC motor using the software interface. In addition to the flow going into the main loop, a pump bypass is placed in parallel to the main pipe leading from the pump. The bypass forces some of the flow to recirculate instead of going into the main loop, allowing for a large variety of different flow rates to be used. A valve situated above the pump control the amount of liquid to be recirculated. The more flow that recirculates in the bypass, the more unstable the flow in the system becomes, allowing for instabilities such as DWOs to easier occur. The pump bypass may also serves as a safety configuration if there is any blockage elsewhere in the system [Sørum, 2014].

## 4.2 Operational Limits

The facility is designed for a specific range of parameters for which the different instabilities are expected to appear within and are given as follow by Ruspini [2013]:

- Flow Rate,  $G$ : 5 - 2000  $\text{kg}/\text{m}^2\text{s}$

- Power Input,  $P_W$ : 0 - 2.5 kW
- Inlet Temperature,  $T_{in}$ : -20 - 40 °C
- Subcooling,  $\Delta T$ : 0 - 50 °C
- Pressure in System,  $P$ : 4 - 15 bar

### 4.2.1 Heat Flux

The heat flux in the test section is applied by five electrodes distributed equally along five sections, each measuring 0.4 m in length, of the test section, see Figure 4.3. The electrodes use Joule effect with low voltage and high current rectified sine waves in order to electrically apply heat flux to the pipe and thereby the refrigerant [Chiapero et al., 2013]. As mentioned before, it is assumed that approximately all heat applied is transferred to the fluid.

The total power applied to the test section is given by

$$P_W = \int I(t)U(t)dt \quad (4.1)$$

where  $I(t)$  [A] is the instant current and  $U(t)$  [V] is the instant voltage. The product of the instant current and voltage is integrated over time in order to achieve the total power,  $P_W$  [W], applied to the system [Chiapero et al., 2013].

The net heat flux is then given by the power applied divided by the area over which it is applied:

$$q'' = \frac{P_W}{\pi D_i \Delta z} \quad (4.2)$$

where the heat flux  $q''$  is given in [W/m<sup>2</sup>].  $D_i$  refers to the inner diameter [m] and  $\Delta z$  refers to the length of the test section for which the heat is applied [m]. For accuracy of the heat applied, see Section 4.4.1.

### 4.2.2 Vapour Quality

The thermodynamic vapour quality is given as follow:

$$X_{th}(z) = \frac{\int_{z_0}^z q'' \pi D_i dz - G A c_p T_{sub}}{G A H_{lv}} \quad (4.3)$$

where  $z$  resembles a point along the length of the test section and  $X_{th}(z)$  the vapour quality at said point.  $q''$  [ $\text{W}/\text{m}^2$ ] is the heat flux as given in Equation (4.2),  $G$  [ $\text{kg}/\text{m}^2\text{s}$ ] is the mass flux,  $A$  [ $\text{m}^2$ ] is the cross-sectional area of the pipe,  $T_{sub}$  [K] is the subcooling of the fluid entering the test section,  $cp_l$  [ $\text{J}/\text{kg K}$ ] is the heat capacity of the fluid in its liquid state and  $H_{lv}$  is the enthalpy of the vaporization [Chiapero et al., 2013].

As stated in subsection 2.1.1, when thermodynamic equilibrium exists, the vapour mass fraction (vapour quality),  $X_m$ , from Equation (2.1) and the thermodynamic vapour quality, now given by  $X_{th}(z)$ , are equal.

### 4.3 Loss Coefficients

While the test section has an ID of 5 mm the inlet valve and the orifice exit have an ID of 12.7 mm. When the inlet valve is fully opened its loss coefficient is  $K_i=400$ , though during the presentation of the results of the experiments later in Chapter 6 and 7, a legend of  $K_i=0$  will be used. This is done for clarification and the insignificant small real value. For the adiabatic exit section,  $K_o=0$  (or  $K_e$ ) will be applied. This is the part used for measuring pressure drop and is also frequently used in the PDO experiments, see Chapter 6 and 7. The orifice section has a minor loss coefficient of  $K_e=540$ , which will be used as its legend.

### 4.4 Measurements

Along the circuit of the facility different measurements instrumentations for different parameters are utilized. The variables are logged with National Instruments NI RIO data acquisition system. In the following the measurements of pressure, flow and temperature will be described.

**Pressure** For measuring pressure in the loop *differential pressure transducers*, DP-cells, are used for differential pressure and *absolute pressure transducers* are used for the absolute pressure. A total of seven pressure taps are installed in the test section alone in order to measure the differential pressure drop over the section. The pressure taps are then connected to two differential pressure transducers by a network of valves allowing for a variety of measurements points. The absolute pressure transducers used for measuring the absolute pressure in the main loop are located at the inlet and outlet of the test section, outlet of the surge tank, inside the main tank and after the pump.

**Flow** In order to measure the flow, one *coriolis flow meter* is placed after the pump and one after the surge tank, at the inlet of the test section.

**Temperature** The temperature is measured by thermocouples at six different locations in the main loop: In the main tank, before and after the pump, after the preconditioner and before and after the test section. For the test section, as can be seen in Figure 4.3 and 4.4, a total of 24 thermocouples are measuring the temperature along the test section at ten different locations. All ten locations have one thermocouple present, located at the outside bottom wall of the test section. Eight of the locations have an extra thermocouple at the top side and two of the locations also have thermocouples at the sides of the wall in addition to two temperature measurements done inside the pipe, in the centre of the flow.

Equilibrium properties of the fluid, e.g.  $T_{sub}$  and  $\rho$ , were calculated using the software REFPROP (NIST Reference Fluid Thermodynamic and Transport Properties Database). For instance, the saturation temperature for the liquid,  $T_{sat}$ , can be determined based on the absolute pressure at the inlet and outlet of the tests section. All the measurements are acquired with an acquisition frequency of 10 Hz (every 0.1 second).

#### 4.4.1 Experimental Accuracy

Concerning the accuracy of the instrumentations, both values given by the supplier and in-house calibration are used. The thermocouples are of the type-T thermocouples, 0.5 mm in diameter, and are used with an accuracy of 0.1K (in-house calibration) [Chiapero, 2013; Ruspini, 2013]. The in-house calibration of the heat flux,  $q''$ , was done during stationary conditions, single-phase flow and for different temperatures and flow rates [Ruspini, 2013]. The heat applied to the test section was calibrated during an in-house calibration by Chiapero et al. [2013] against the actual thermal heat concluding with an accuracy of 3%. For the mass flow rate, an accuracy of 0.2% of the readings was given by the supplier. An accuracy of 0.04% was given by the supplier for the inlet and outlet pressure measurements, at full scale (25 bar) with absolute pressure transducers. For the total pressure drop measurements along the test section, using differential pressure transducers, an accuracy at full scale (50 kPa) of 0.075% was given by the supplier and checked by in-house calibration [Chiapero et al., 2014b].

All the accuracy differences, percentages and the specifications for the instrumentations of interest are given in Table 4.1 [Ruspini, 2013; Sørnum, 2014].

#### 4.4.2 Error Estimation

For the error estimation of the power measurement a typical error propagation to estimate the accuracy of the measurements have been used and executed by Ruspini

Name	Instrument Type	Brand	Localization	Range	Measurement Accuracy	Max. Statistical Error	Max. Error
DP1	DP-cell	Endress+Hauser	Test Section	0-1 [bar]	0.075%	1 [mbar]	1 [mbar]
DP2	DP-cell	Endress+Hauser	Outlet Valve (Orifice)	0-1 [bar]	0.075%	5 [mbar]	5 [mbar]
DP3	DP-cell	Endress+Hauser	Inlet Valve	0-1 [bar]	0.075%	2 [mbar]	2 [mbar]
DP4	DP-cell	Endress+Hauser	Test Section distributed $\Delta P$	0-30 [mbar]			
DP5	DP-cell	Endress+Hauser	Test Section distributed $\Delta P$	0-50 [mbar]			
T 1-30	Thermocouple K	Standard	Whole Loop	-50 - 100 [°C]	0.1 [°C]	0.1 [°C]	0.2 [°C]
P 1-5	Absolute Pressure	GE-UNIK 5000	Whole Loop	1-25 [bar]	0.04%	<10 [mbar]	0.1 [bar]
G 1-2	Coriolis Flow Meter	Bronkhorst Cori-Tech	Inlet Test Section	0-3 [l/min]	0.01 [l/min]	<0.01 [l/min]	0.05 [l/min]
Q 1-5	Power Supply	Home made	Test Section	0-2500 [kW]	20 [W]	20 [W]	<40 [W]

**Table 4.1:** Accuracy of the measurement instrumentations [Ruspini, 2013; Sørrum, 2014].

[2013]. For the power supply, which is an in-house made design, Ruspini performed an error estimation for the power input measurements, temperature, voltage, current and mass flow, concluding with an accuracy of the real heat of  $\varepsilon Q_{real} < 10\%$ . This value will be the one assumed in this thesis. For the other parameters, either in-house calibration or error given by the supplier have been used.

## 4.5 Software Interface - LabVIEW

The software interface was designed especially for this facility using NI LabVIEW (2011) (Laboratory Virtual Instrument Engineering Workbench). Figure 4.4 shows the user interface as it appears on the computer. The interface allows you to control and change the value of the pump, the two heat exchangers and the heat applied to the test section. In addition it gives valuable information of the conditions in the system retrieved from the different measuring instrumentation. Settings for the file acquisition can also be performed here. As seen in Figure 4.4 there are three graphs visualizing the system. The large one on the right side is for stability analysis while the other two are for the heat applied to the test section and the flow rate in the system.

## 4.6 Experimental Procedure

During operation of the Two-Phase Flow Instabilities Facility, some general procedures have to be followed:

- The configurations of single/multi-tube section, the inlet valve, pump bypass and outlet restrictions (adiabatic or orifice) have to be set.
- Main power, the pump, heat exchangers (Chiller 1 and Chiller 2) and heaters needs to be started and the computer and control interface must be switched on.
- When the pump is running, more and more heat can slowly be added to the test section while the inlet temperature decreases. In order to set the desired parameters in the system, precaution has to be taken. This is in order to avoid getting to high, or to low, temperatures in the system. The heat exchangers, Chiller 1 and Chiller 2, that respectively control the inlet pressure and inlet temperature should be adjusted slowly in order not to overshoot the parameters. Usually the different variables and settings of the systems affects each other, making the process intricate and time consuming.

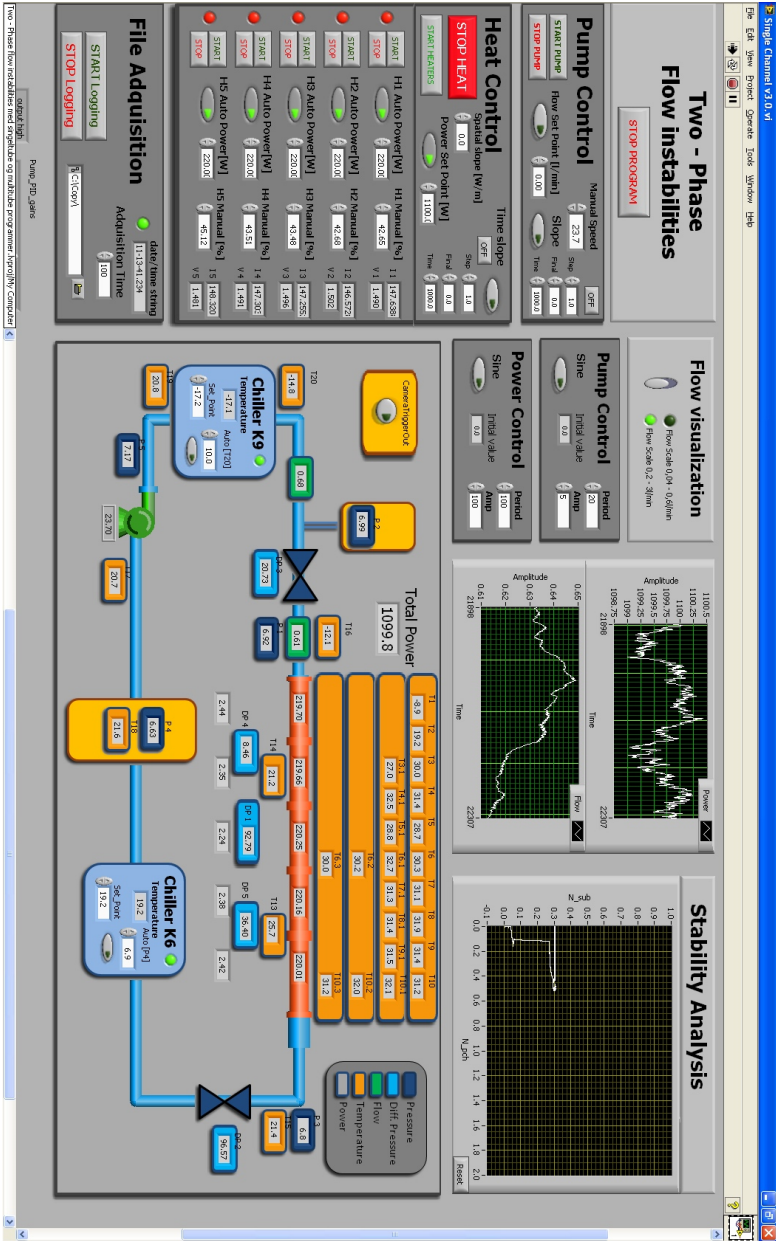


Figure 4.4: Overview of the user interface controlling the facility.



- Procedure for achieving an experimental state:
  - Adjust the wanted flow rate by increasing or decreasing the power input to the pump.
  - Set the desired heat flux for the test section by adjusting the power applied to each of the five heaters. This should be done carefully.
  - Lower the value of the preconditioner, Chiller 2, until the inlet temperature achieves the wanted subcooling.
  - The pressure in the system is controlled by the condenser, Chiller 1, and by increasing or decreasing its internal temperature the pressure for the system can be adjusted.
  - When the parameters are set and the system is stable, which can take up to 45 minutes, adjustments in some of the parameters can be made while keeping the others constant. For example reducing the mass flux while keeping the subcooling and pressure constant in order to achieve the pressure drop characteristic curve.
  - The parameters of the main system are kept constant as long as the surge tank is connected. The surge tank is connected to the main system by a valve. When opening this valve awareness of possible pressure differences between the tank and loop should be taken in order to avoid nitrogen flowing into the main system.
- When logging the result, the acquisition time has to be specified and the results are visualized and processed in MATLAB.
- The run time for the experiments vary but the system should have operated for a while and stabilized before starting the logging procedures.
- Multiple recordings of the same experiments should be taken in order to assure steady state of the parameters in the system.
- When closing down the facility precaution should again be taken in order to avoid to high or to low temperatures in the system.

## 4.7 Risk Assesment

Ruspini & Langørgen [2011] performed a thorough and complete risk assessment at the time the facility was designed and constructed. A large part of the risk assessment involves the use of lasers, but no use of lasers was needed for the work done in this thesis.

The system contains R134a under high pressure, both in standby-mode and during use, and protective eye-gear should always be worn when operating the facility. In the incident of negative temperatures at the outlet of the test section, the O-rings and gaskets could become vulnerable to breakage and a risk source for leakage of R134a. Special care should therefore be taken when operating with low, negative temperature values in the system.

# Validation and Characterization of the System

Validations of the Two-Phase Flow Instabilities Facility using known correlations for pressure drop and heat transfer during single phase flow will in this chapter be given together with characterizations of both the internal and external system. The validations and characterizations of the system provide the fundamental knowledge needed in order to perform experimental analysis on two-phase flow instabilities.

## 5.1 Validation

In order to validate the measurement methods for frictional pressure drop and the heat transfer coefficient for the facility, validations using already known correlations for pressure drop and heat transfer during single phase flow were performed. During the experimental work of the validations, the mass flux of the test section was gradually reduced while keeping the other parameters and settings constant. For each value of the mass flux, two samples of data, each taken over a period of approximately 100 seconds, were collected in order to assure stable conditions.

### 5.1.1 Single Phase Pressure Drop Validation

For the validation of the data achieved from the single-phase pressure drop, the *Colebrook* correlation was used for the friction factor,  $f$ , [Chiapero et al., 2013; Colebrook, 1939]:

$$\frac{1}{\sqrt{f}} = -2.0 \log \left( \frac{\epsilon/D_i}{3.7} + \frac{2.51}{Re_D \sqrt{f}} \right) \quad (5.1)$$

where  $\epsilon$  is the roughness of the pipe [mm] and the *Reynolds number*,  $Re_D$ , is given as  $Re_D = \frac{GD_i}{\mu}$ , where  $\mu$  is the dynamic viscosity of the fluid [kg/ms]. Equation (5.1) is valid for  $4000 < Re < 10^8$ .

The pressure drop based on the friction factor is given as [Cengel & Cimbala, 2010]:

$$\Delta P = f \frac{L}{D_i} \frac{\rho V^2}{2} = f \frac{L}{D_i} \frac{G^2}{\rho 2} \quad (5.2)$$

so that:

$$f = \frac{2D_i}{L} \frac{\Delta P \rho}{G^2} \quad (5.3)$$

The length and inner diameter of the test section are constant, the value for the density  $\rho$  was found by using the absolute pressure and fluid temperature in NIST REFPROP and the mass flux was attained from the flow meter at the test section inlet. The friction factor was determined with an error of about 5% and as seen from the graph in Figure 5.1 the results from the facility is found to be within 10% of the predicted value when using a roughness of  $\epsilon = 15 \times 10^{-3}$  mm.

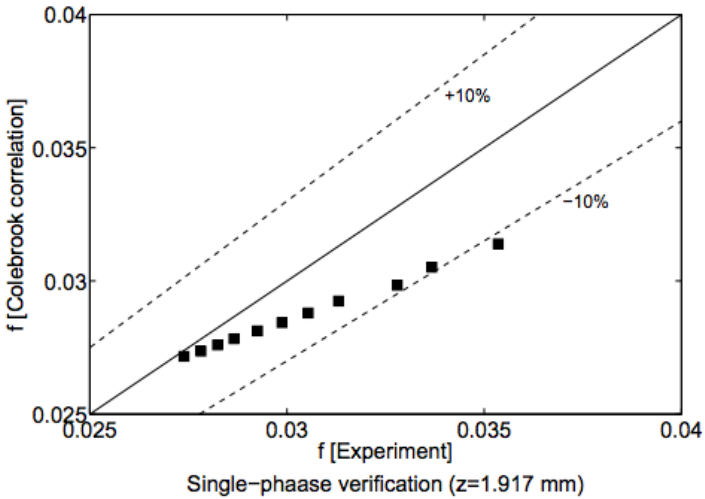


**Figure 5.1:** Measured single phase pressure drop compared to theoretical value.

### 5.1.2 Single Phase Heat Transfer Validation

For the validation of the heat transfer data achieved in single-phase, the *Petukhov-Kirilov* correlation, was used:

$$Nu_D = \frac{hD_i}{k} = \frac{(f/8)Re_D Pr}{1.07 + 12.7(f/8)^{1/2}(Pr^{2/3} - 1)} \quad (5.4)$$

where  $f$  is given by:

$$f = \frac{2D_i \rho \Delta P}{L G^2} = (0.79 \ln Re_D - 1.64)^{-2} \quad (5.5)$$

and  $h$  is the local heat transfer coefficient given by:

$$h = \frac{q''}{\Delta T} = \frac{q''}{T_{wi} - T_F} \quad (5.6)$$

The *Prandtl Number*,  $Pr$  is given by  $Pr = \frac{c_p \mu}{k}$  where  $c_p$  is the specific heat [J/kg K] and  $k$  is the thermal conductivity [W/m K] of the fluid. The  $T_{wi}$  and  $T_F$  corresponds to the temperature of the inner wall and the temperature of the fluid respectively. The temperature of the inner wall is calculated from the temperature of the outer wall measured by the thermocouples,  $T_{wo}$ , the thermal conductivity of the wall,  $k_w$ , the inner and outer radius of the pipe,  $R_i$  and  $R_o$  [m], the electrical power applied,  $P_w$ , and the length of the test section,  $\Delta z$ , by the following equation for a hollow cylinder [Chiapero et al., 2014a]:

$$T_{wi} = T_{wo} + \frac{P_w}{4\pi \Delta z} - \frac{P_w}{2\pi k_w \Delta z} \frac{R_o^2}{(R_o^2 - R_i^2)} \ln\left(\frac{R_o}{R_i}\right) \quad (5.7)$$

The absolute pressure and fluid temperature is then inserted into REFPROP in order to get the fluid properties needed. The local heat transfer coefficient is achieved from measurements of the wall temperatures located 1917 mm downstream the test section where 4 thermocouples surrounds the pipe. The experimental  $Nu_D$  could then be calculated from the measured heat flux,  $q''$ , and the difference of the fluid temperature and the inner wall temperature, see Equations (5.6) and (5.4). The results, shown in Figure 5.2, shows good correlation for the achieved data, located within 10% of the theoretical value.

## 5.2 System Characterization

Different experimental facilities and experimental conditions have distinctive pressure drop characteristic curves. Therefore it is necessary to perform a characterization of the internal and external system, which gives valuable information about the operational areas of the different oscillatory behaviours, before conducting experiments concerning instabilities.

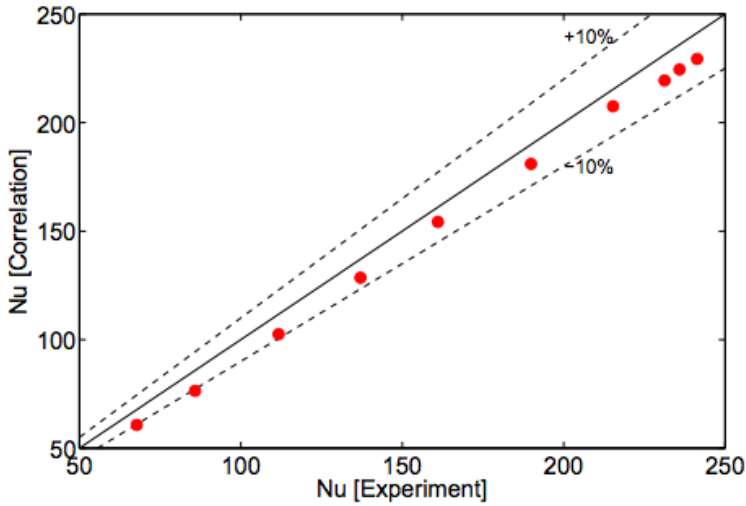


**Figure 5.2:** Single phase heat transfer achieved compared to the theoretical value.

### 5.2.1 Internal System

The pressure drop characteristic curve for the heated test section,  $\Delta P_{TS}$ , and for the complete system,  $\Delta P_{system}$ , are shown in Figure 5.3 and 5.4 respectively. The pressure drop characteristic curves, the «N-shape curves», was obtained by keeping the conditions at the inlet of the heated test section constant while stepwise reducing the mass flux. The operational parameters for the inlet are shown in the figures. The operational conditions used for this characterization were a closed pump bypass, an open inlet restriction and an adiabatic exit.

### 5.2.2 External System

For the characterization of the external system the response of the pump to changes in the pressure drop in the system has been examined. The results for the pump bypass, which were closed and opened three turns, are shown in Figure 5.5.  $\Delta P_{pump}$  defines the pressure drop along the system (corresponding to  $\Delta P_{system}$ ). The curves were obtained by keeping the inlet conditions constant and not applying any heat to the system. Stepwise the inlet valve was closed in order to increase the pressure drop in the system. As it can be seen from the results, the main effect of partially opening the bump bypass is a less steep negative curve. In accordance with the effect of the external system previously discussed, the steepness of the external curve needs to be larger than the internal curve in order for PDOs to occur. As a result of this, a choice of a configuration using a closed bypass pump while testing for PDOs was made.

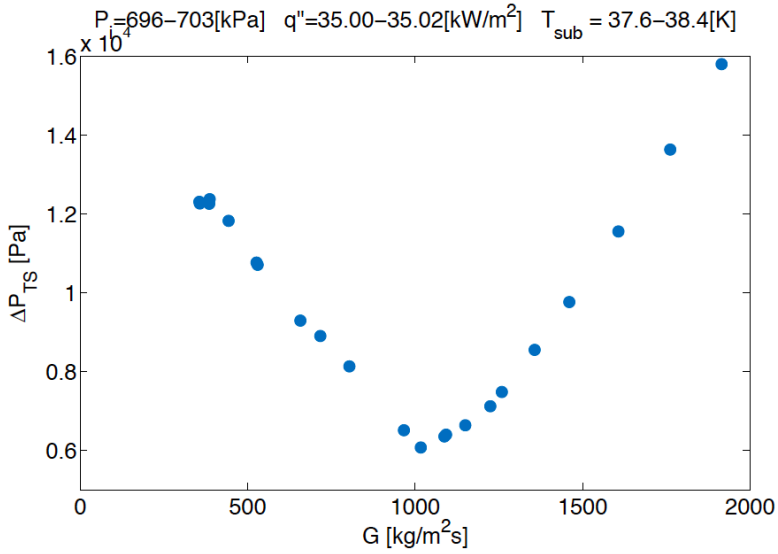


Figure 5.3: Pressure drop characteristic curve for the heated test section ( $\Delta P_{Ts}$ ).

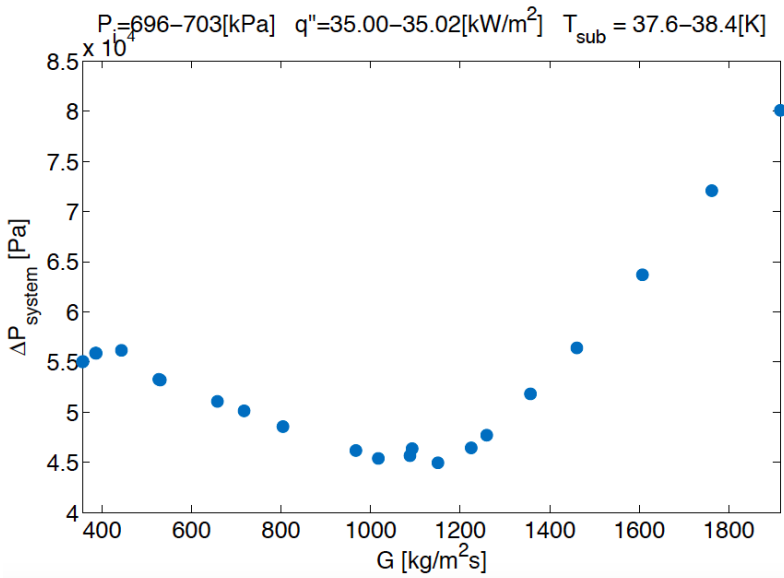
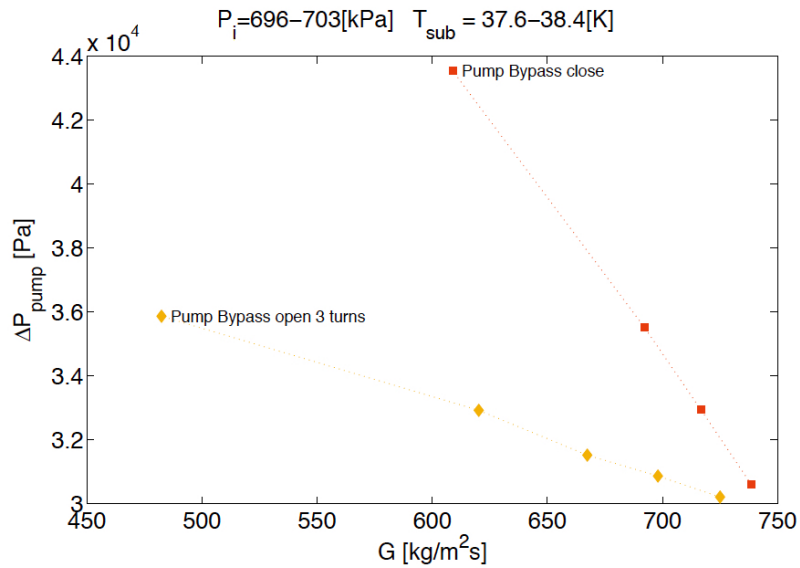


Figure 5.4: Pressure drop characteristic curve for the flow loop ( $\Delta P_{\text{system}}$ ).



**Figure 5.5:** The pump response with the pump bypass closed and opened 3 turns.

### 5.3 Summary

A validation and characterization of the system have been performed. The results show that the system lies within  $\pm 10\%$  of the theoretical value. Together with the experimental accuracy and error estimation given in Chapter 4 it gives an expectation of the accuracy of the experiments to be performed.



# Chapter 6

## Experimental Results - Effect of the External System

The Two-Phase Flow Instabilities Facility has a large range of possible settings for the external system, all of them having more or less influence on the PDOs. In this chapter the experimental results concerning the effect the external system have on the appearance and characteristics of PDOs will be presented. The main focus during the experiments have been on the effect on the PDOs due to the inlet and outlet restrictions, the pump bypass and the compressible volume stored inside the surge tank.

### 6.1 Results

In order to investigate the impact on the PDOs caused by the external system the conditions at the inlet of the heated test section, which are the pressure, subcooling, mass flux and the heat applied, were kept constant while other settings of the system were adjusted. The operational values for the constant conditions were fixed to approximately:

- Flow Rate,  $G \approx 700 \text{ kg/m}^2\text{s}$
- Power Input,  $P_W \approx 1100 \text{ kW}$
- Inlet Temperature,  $T_{in} \approx -11 \text{ }^\circ\text{C}$
- Subcooling,  $T_{sub} \approx 38 \text{ }^\circ\text{C}$
- Inlet Pressure,  $P_{in} \approx 700 \text{ kPa}$

In the beginning of the experimental work, different compressible volumes in the surge tank seemed to have great influence on the PDOs while using otherwise stable conditions. The need to control the compressible volume became clear. As a result,

a nitrogen gas tank was installed in the facility in order to regulate the compressible volume of the surge tank.

In the progress of understanding the conditions needed for PDO appearance in the system, experiments with two different values of upstream compressible volumes were performed. The results, shown in Figure 6.1 and 6.2, demonstrate two different types of PDOs. The data shown in Figure 6.1 was gathered while using a compressible volume of  $ST=2.4 \times 10^{-3} \text{ [m}^3\text{]}$ . For Figure 6.2, a larger compressible volume of  $ST=6.8 \times 10^{-3} \text{ [m}^3\text{]}$  was used. The other conditions at the inlet of the heated test section were kept constant, with no pump bypass ( $BP=0$ ), an open inlet valve ( $K_i=0$ ) and an adiabatic exit ( $K_o=0$ ). For each experimental run, after a given time of stable conditions (respectively  $\sim 60$  and  $\sim 40$  seconds) the surge tank was connected to the main system and the PDOs appeared. Both experiments lasted for longer than 500 seconds assuring stability of the oscillation. The evolution of the oscillations for mass flux, pressure and temperature are given in the figures. The mass flux corresponding to the flow meter placed after the surge tank and before the test section is visualized by the purple line, while the mass flux measured after the pump and before the surge tank is visualized by the green line. For the pressures,  $P_s$  corresponds to the pressure before the surge tank and  $P_i$  and  $P_o$  corresponds to the pressure at the inlet and outlet of the heated test section respectively. The average wall temperature and temperature of the fluid are given as  $T_{wall}$  and  $T_{fluid}$ . Both temperature measurements are located 1917 mm from the inlet of the heated test section and  $T_{wall}$  is the average value of four different wall temperatures measured at the outside of the pipe.

When comparing Figure 6.1 and 6.2, there are differences in the period of the oscillations and in the presence of interfering, high frequency signals. For the low compressible volume, Figure 6.1 shows oscillations, PDOs, with periods of  $\sim 50$  seconds, amplitudes of  $\sim 300\text{-}400 \text{ kg/m}^2\text{s}$  and no interfering, high frequency signals. For the higher compressible volume, Figure 6.2 shows longer periods of  $\sim 70$  seconds and higher amplitudes of  $\sim 400\text{-}500 \text{ kg/m}^2\text{s}$ . In addition, high frequency oscillations superimposing the long period oscillations appeared. The high frequency oscillations have periods of a few seconds, similar to the oscillatory behaviour of DWOs, and approximately the double amplitude compared to the long period oscillations. The interfering signals occurred at the low flow rates of the PDOs and disappeared as the oscillations again increased in flow rate.

The limit cycles with respect to the pressure drop characteristic curve of the two cases are shown in Figure 6.3 for the low compressible volume and Figure 6.4 for the high compressible volume. The two figures present a limit cycle for the mass flux at the inlet of the heated test section,  $G_i$ , and for the mass flux as measured after the pump and before the surge tank,  $G_p$ , considering both the pressure in

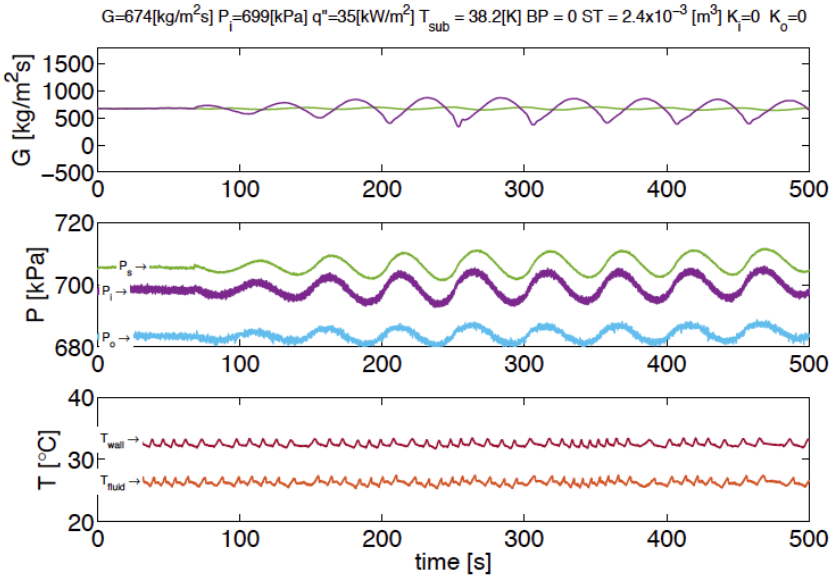


**Figure 6.1:** PDO with no interfering, high frequency components.

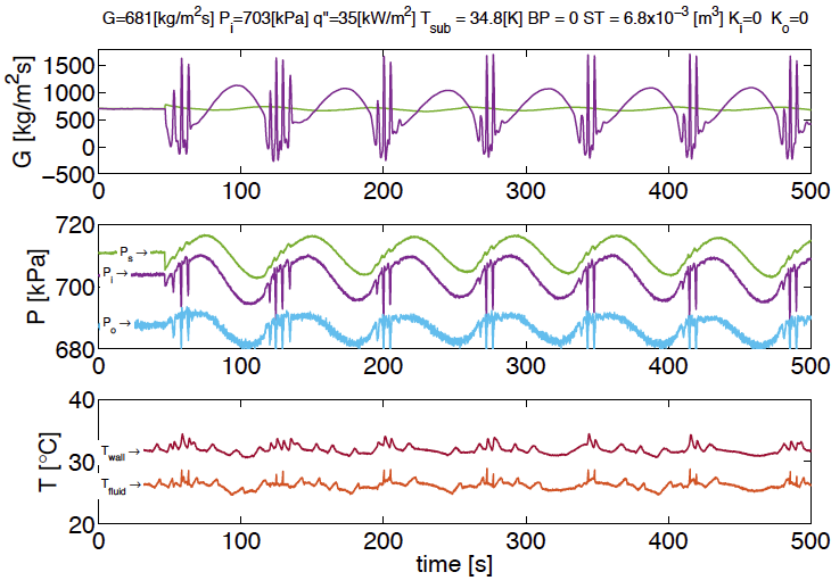


**Figure 6.2:** PDO with interfering, high frequency components.

the test section,  $\Delta P_{TS}$ , and the pressure in the system,  $\Delta P_{Loop}$ . In addition,  $ST$  indicates the surge tank volume and  $BP$  the number of rounds opened for the pump bypass. From Figure 6.4 it can be seen that the interfering, high frequency oscillations onset in a high vapour quality area,  $X_m \simeq 0.4$ . In this area the mass flux is approximately  $500 \text{ kg/m}^2\text{s}$  and the differential pressures are  $\Delta P_{TS}=1.3 \times 10^4 \text{ Pa}$  and  $\Delta P_{system}=6.0 \times 10^4 \text{ Pa}$  respectively.

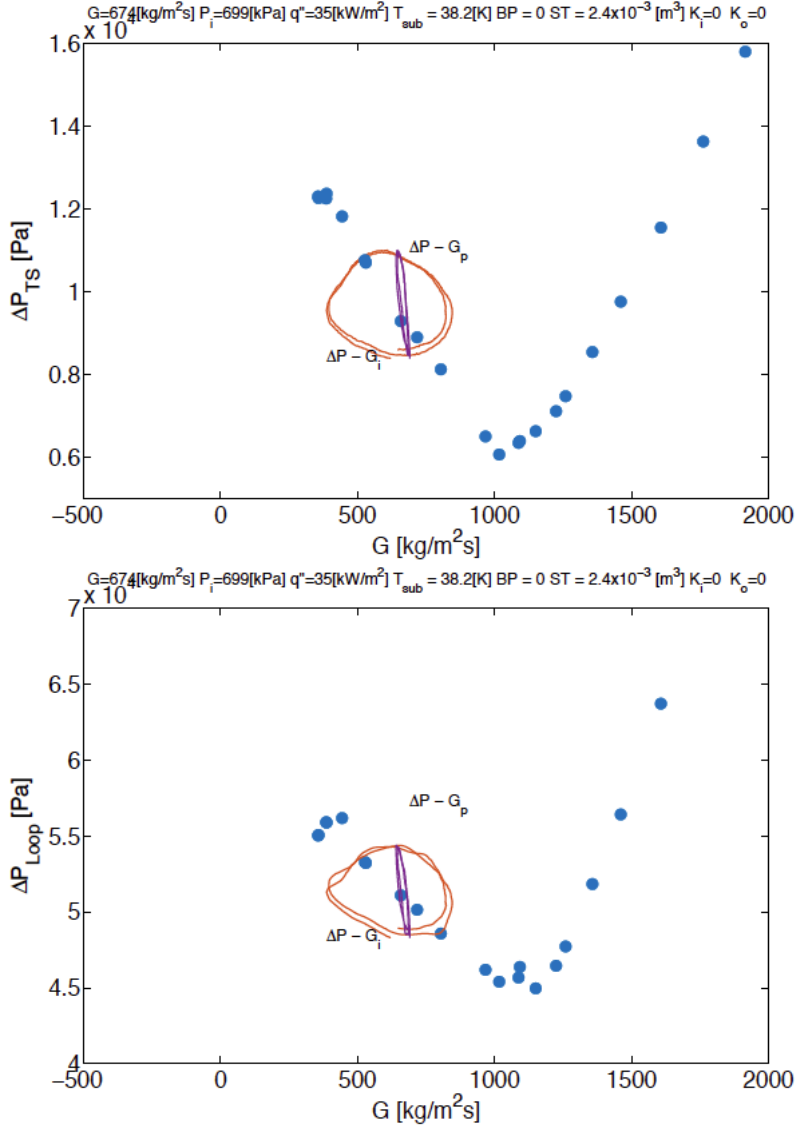
### 6.1.1 Effect of Inlet Restriction

Figure 6.5 demonstrates the effect on the PDOs by restricting the inlet valve and thereby increasing its loss coefficient,  $K_i$ . For this experiment, a compressible volume of  $3.4 \times 10^{-3} \text{ m}^3$  was used. The interfering, high frequency oscillations are barely noticeable, making it a natural development from the mass flux oscillations seen in Figure 6.1 to Figure 6.2. Figure 6.5 shows that with an increase in loss coefficient for the inlet valve, restricting the flow going into the test section, the system stabilizes. This is logical since a stabilization of the system will reduce the negative slope of the pressure drop characteristic curve, making it less vulnerable for instabilities. The results are in accordance with the conclusion of Maulbetsch & Griffith [1965] stating that the instabilities could be eliminated by a throttling between the compressible volume and the test section.

### 6.1.2 Effect of Outlet Restriction

The effect on the PDOs by altering the outlet using either an adiabatic or an orifice channel is shown in Figure 6.6 for both a low surge tank volume ( $3.4 \times 10^{-3} \text{ m}^3$ ) and for a high surge tank volume ( $6.8 \times 10^{-3} \text{ m}^3$ ). While the orifice channel restricts the flow, the adiabatic channel has no orifice and no restriction. As can be seen in the figure, the orifice exit suppressed the oscillations, reducing both its period and amplitude. In addition, the interfering, high frequency oscillations disappeared and the signals were more irregular. For the case with a low surge tank volume and an orifice exit, the signal decreased and stabilized. The effect of the surge tank, increasing the signals when using a higher compressible volume, corresponds to the previously mentioned results shown in Figure 6.1 and 6.2.

Since the main tank, located downstream of the test section, contains a large compressible volume, a decoupling of the upstream system using an orifice plate may help stabilize the system. The orifice plate in the exit channel could also reduce the steepness of the negative slope in the pressure drop characteristic curve for the external system by restraining the flow, reducing the system's vulnerability to instabilities. An earlier study concerning DWOs performed by Sørnum [2014] utilizing the same facility states that the orifice exit configuration increases the magnitude of the DWO signals and thereby making the system more unstable. Since the interfering,



**Figure 6.3:** The limit cycle for the PDOs with no high frequency components while using a low compressible volume.

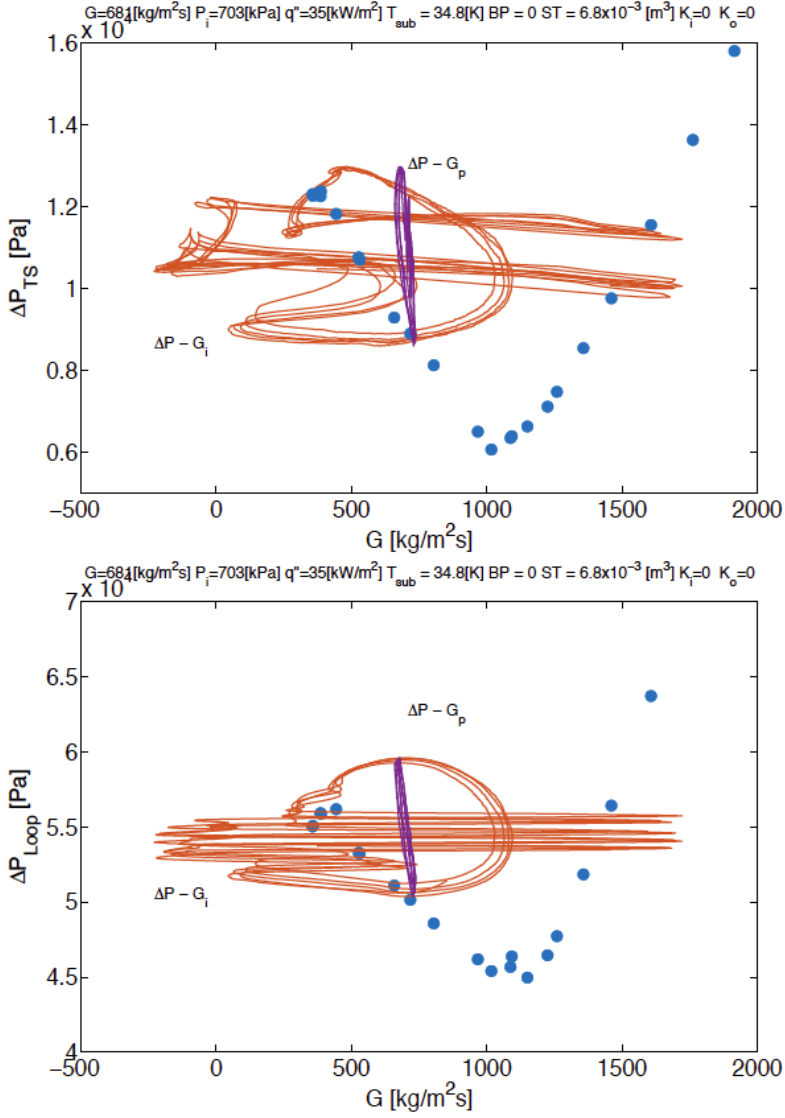


**Figure 6.4:** The limit cycle for the PDOs with high frequency components while using a high compressible volume.

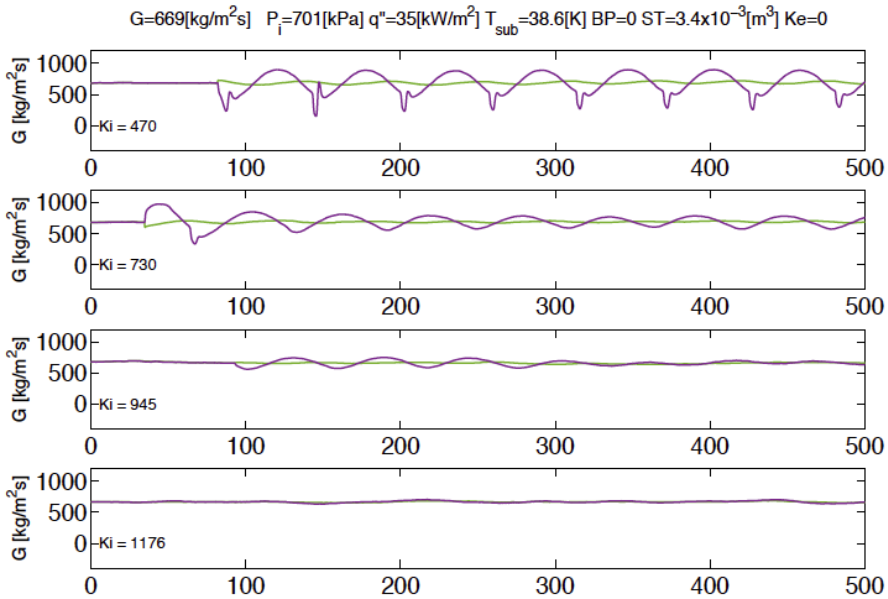
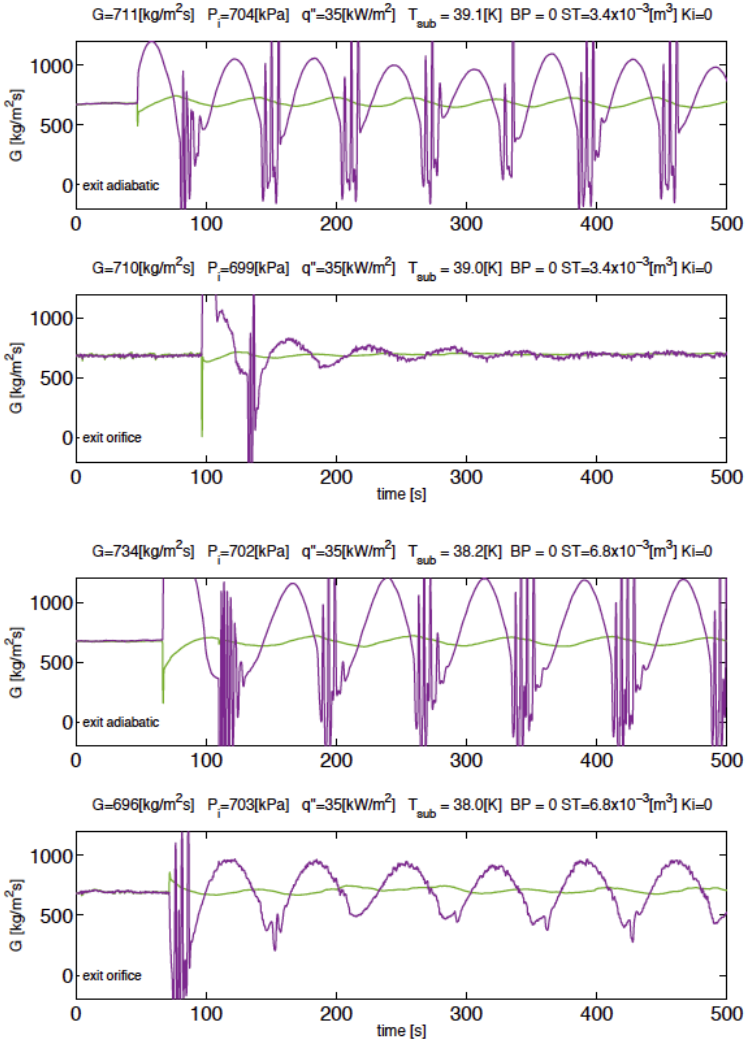


**Figure 6.5:** Effect of increasing the inlet restriction on the PDOs where green corresponds to the mass flux before the surge tank and purple to the mass flux at the inlet of the test section.

high frequency signals are commonly accepted as DWOs, the results presented here does not comply with the ones from Sørnum [2014].

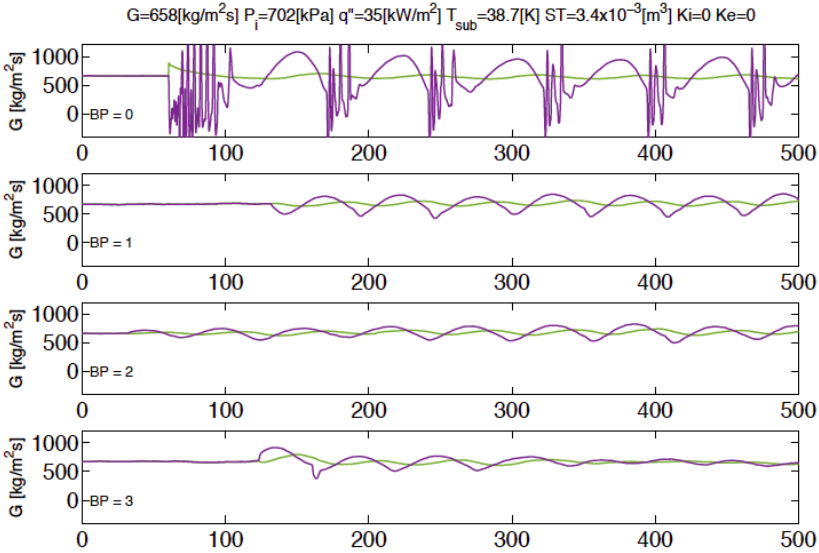
### 6.1.3 Effect of the Pump Bypass

Figure 6.7 displays the effect of the pump bypass on the PDOs during otherwise stable conditions and a fixed compressible volume in the surge tank ( $3.4 \times 10^{-3} \text{ m}^3$ ). The experiments were performed with the pump bypass closed and then stepwise opened one, two and three turns, increasing the amount of water to be recirculated and the necessary pump speed so as to maintain the same flow rate through the test section. It is not possible to quantify the amount of liquid being recirculated at the different opening conditions of the pump bypass, but the effect on the PDOs are still apparent. The second graph in Figure 6.7 shows the development of the flow during PDOs using one turn opened pump bypass. It is clear from comparing it to the one with a closed pump bypass that an opening in the pump bypass reduces both the period and amplitudes of the PDOs in addition to efficiently eliminate the interfering, high frequency oscillations. As can be seen from the last graph in the figure, when the opening of the pump bypass is large enough, it can suppress the PDOs almost entirely.



**Figure 6.6:** Effect of the outlet restrictions, adiabatic or orifice, on the PDOs while using low ( $3.4 \times 10^{-3}$  m<sup>3</sup>) and high ( $6.8 \times 10^{-3}$  m<sup>3</sup>) compressible volumes where green corresponds to the mass flux before the surge tank and purple to the mass flux at the inlet of the test section.





**Figure 6.7:** The effect of opening the pump bypass BP 0, 1, 2 and 3 turns on the PDOs where green corresponds to the mass flux before the surge tank and purple to the mass flux at the inlet of the test section.

The pump bypass seems to be able to adjust the stability of the system. By opening the pump bypass it helps absorb the PDOs making the system more stable, while a closed pump bypass makes the system more unstable and sensitive to instabilities.

#### 6.1.4 Effect of the Compressible Volume

Figure 6.8 and 6.9 shows the effect of different compressible volumes, ST, in the surge tank during closed and opened three turns pump bypass respectively. In both cases, a reduction in the compressible volume leads to smaller amplitudes and periods for the PDOs at the same time as the interfering, high frequency signals are reduced in both quantity and amplitude. The same trend as observed for the changing pump bypass configurations in Figure 6.7, with a suppressing of both the PDOs and the interfering signals, can be observed here for the closed and opened three turns pump bypass. At very low compressible volumes the PDOs are still present for the closed pump bypass case even though these are reduced in magnitude and with no interfering signals. The developing progress of the PDOs can be seen with the pump bypass opened three turns at a higher compressible volume. At the low compressible volume and pump bypass opened three turns the PDOs are not established.

From these results, both an opening of the pump bypass and a decrease in the compressible volume seem to reduce both the PDOs and the interfering signals, while

an increase in the compressible volume and a closed pump bypass seems to increase both the PDOs and the interfering signals. It was not feasible to obtain an even smaller compressible volume for testing due to the risk of getting nitrogen gas into the main system.

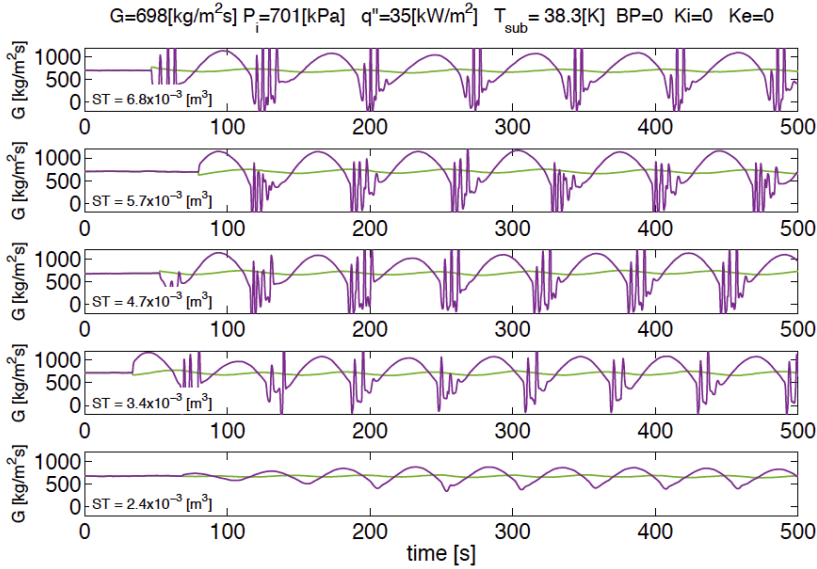


**Figure 6.8:** Effect of different compressible volumes on PDOs with the pump bypass valve closed where green corresponds to the mass flux before the surge tank and purple to the mass flux at the inlet of the test section.

## 6.2 Discussion

It has been shown experimentally that alterations of the external system can greatly affect the PDOs, even when the inlet conditions to the test section remain the same. The experimental results show that in order to restrict the PDOs several measures can be taken:

- Both a restriction of the inlet and the outlet of the test section reduces the magnitude of the PDOs efficiently.
- A lower, upstream compressible volume reduces the PDOs.
- An open pump bypass helps to absorb the PDOs and stabilizes the system.

The use of an exact compressible volume can be hard to realize in a real heat exchanger system. For the experiments, the volume is restrained and controlled

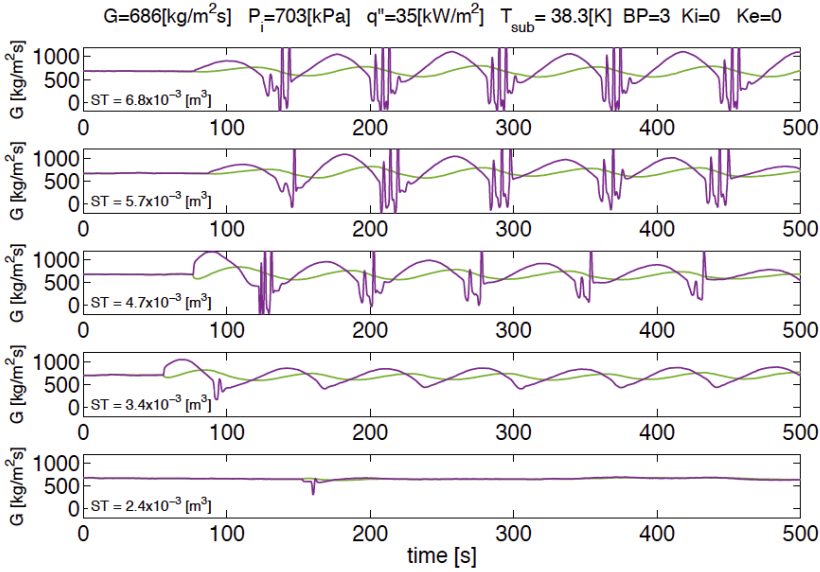


**Figure 6.9:** Effect of different compressible volumes on PDOs for pump bypass valve opened three turns where green corresponds to the mass flux before the surge tank and purple to the mass flux at the inlet of the test section.

by the use of a surge tank while in a real system the compressible volume will be within the system itself and thereby harder to control. Another issue regarding the compressible volume is discussed by Guo et al. [2001]. They pointed out that the placement of the surge tank in regards to the test section could affect the PDOs. This means that if the compressible volume is located within the test section itself, further alterations of the PDOs should be expected. As pointed out by Daleas & Bergles [1965], if the velocity or the size of the test section pipe is increased, the compressible volume will have less effect. This means that every system, using different parameters and test section sizes, requires different compressible volumes in order to onset and maintain the oscillations.

For the oscillations, it has been shown that the PDOs can appear as a single phenomenon at the right conditions as seen in Figure 6.1, and they are not necessarily accompanied by interfering, high frequency oscillations. This does not comply with the results of Ruspini [2013], stating that the PDOs can not be considered a pure phenomenon.

The oscillations of the mass flux and the pressure are out of phase of each other, as can be seen in for example Figure 6.1. This is aligned with what is seen in previous studies done by Ding et al. [1995]. For the thermal oscillations at the pipe wall, the

results presented in Figure 6.1 shows small, high frequency oscillations for both the wall and fluid temperature. Compared to the results by Padki et al. [1991] shown in Figure 3.2 their wall temperature oscillation are in phase, and at the same magnitude order, as the pressure oscillations. This may be a result of different parameters or settings for the system used, for instance have the results presented here a much lower inlet temperature and lower flow rate than the experiments by Padki et al. [1991]. It may also indicate some different sort of oscillations.

Since the external system has such a great influence on the appearance of the PDOs, detailed characterizations of each system used for PDOs are needed. Especially if the experimental results are to be used in numerical validation the parameters and settings in the system should be carefully regarded.

# Chapter 7

## Experimental Results -Effect of Heat Flux

Different magnitudes of heating and heating profiles may result in a decrease or increase of the vapour amount, and thereby the compressible volume, trapped inside the test section. In this chapter the experimental results concerning the effects of distinct heat fluxes applied to the test section on the PDOs will be presented. In addition, results from experiments regarding the PDO-DWO interaction will be discussed.

### 7.1 Results

As a reference case approximate parameters of  $q'' = 35 \text{ kW/m}^2$ ,  $T_{sub} = 39 \text{ }^\circ\text{C}$ ,  $P_{in} = 700 \text{ kPa}$  and  $G = 700 \text{ kg/m}^2\text{s}$  have been used. The external configurations were closed pump bypass, a compressible volume in the surge tank of  $3.4 \times 10^{-3} \text{ m}^3$ , a fully opened inlet valve and an adiabatic outlet. For the graphs presented in this chapter, the mass fluxes at the inlet of the test section and before the surge tank are shown in purple and green colour respectively. For the graphs representing the pressures, the purple colour represents the pressure before the surge tank and the green colour represents the pressure at the inlet of the test section.

#### 7.1.1 Effect of Heating Power

Figure 7.1 shows the effect on the PDOs of an increase and decrease in the heat flux applied to the test section. The heat flux applied,  $q''$ , was done as uniform heating along the test section. An increase for the heat flux from  $35 \text{ kW/m}^2$  to  $41 \text{ kW/m}^2$  did not have any significant effect on the oscillations, but the interfering, high frequency signals were slightly increased. A decrease in heat flux to  $31.8 \text{ kW/m}^2$  and  $30.2 \text{ kW/m}^2$  showed a development towards a more stable system. The interfering, high frequency oscillations were almost gone at  $31.8 \text{ kW/m}^2$  and disappeared completely at  $30.2 \text{ kW/m}^2$ . At the lowest heat flux value,  $30.2 \text{ kW/m}^2$ , the main PDO signals were also dampened out, with slightly larger periods and smaller amplitudes, approaching a stable condition.

An further increase in the applied heat flux is shown in Figure 7.2. The magnitude of the oscillations seems to peak around  $q''=44.6 \text{ kW/m}^2$  and a further increase of heat will lead to a decrease for the PDOs.

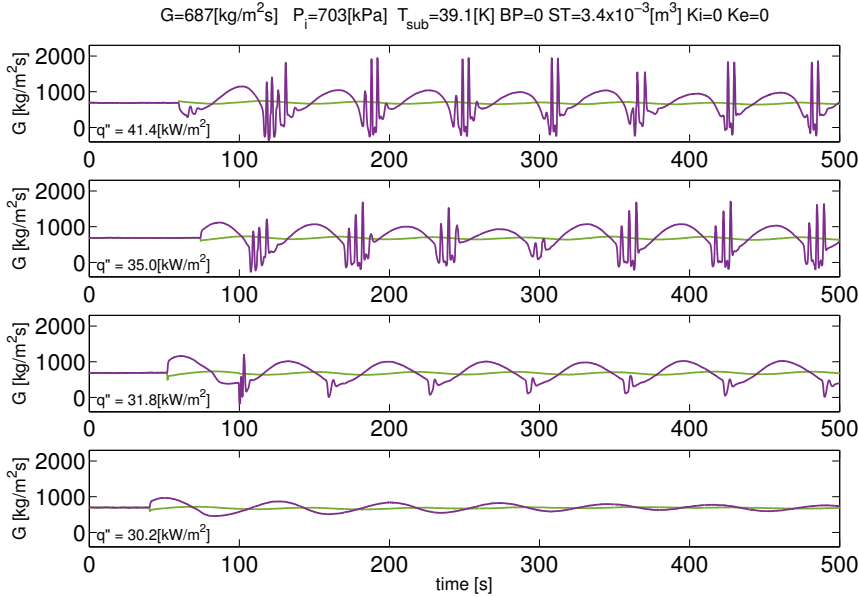


**Figure 7.1:** Effect of decreasing heat flux on the PDOs characteristics for uniform heating.

One of the most important effects of the heat flux applied to the fluid in the test section is the onset of two-phase flow. With lower heat applied this process is delayed until further along the test section. This leads to a lower vapour quality at the outlet. For the test section, lower heat applied means less vapour and smaller compressible volume both inside and downstream the test section. Since all other parameters were kept stable throughout the experiments, it can be concluded that higher heat fluxes, up to a certain limit, increase the additional compressible volume inside the test section and have a notable effect on the PDOs. At the highest heat flux value,  $q''_{\text{tot}}=50.9 \text{ kW/m}^2$ , the vapour quality was  $X_{th} \approx 0.37$ , notably higher compared to the reference case of  $X_{th} \approx 0.17$ . When referring to Figure 2.2 it can be shown that the operational point is moved further to the left in the pressure drop characteristic curve during the high heat flux and thereby outside of the boundaries of where PDOs are likely to occur.

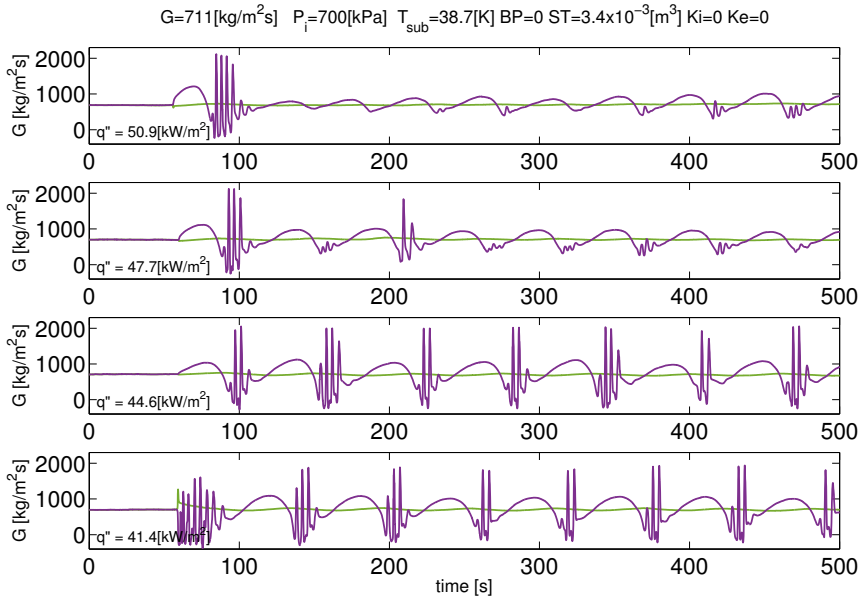


**Figure 7.2:** Effect of increasing heat flux on the PDOs characteristics for uniform heating.

### 7.1.2 Effect of Different Heating Profiles

In order to study the effect of distinct heating along the length of the test section, experiments with different heat profiles, adding up to either  $35 \text{ kWm}^2$  or  $47.7 \text{ kWm}^2$ , were performed. The heat applied by each heater during the cases shown in Figure 7.3 and 7.4, all adding up to  $35 \text{ kWm}^2$ , are given in Table 7.1.

Heat Profile	Heater 1	Heater 2	Heater 3	Heater 4	Heater 5
Uniform	220 W	220 W	220 W	220 W	220 W
Linearly increasing	100 W	160 W	220 W	280 W	340 W
Linearly decreasing	340 W	280 W	220 W	160 W	100 W
Parabolic heat	160 W	220 W	340 W	220 W	160 W
Triangle heat	148 W	238 W	328 W	238 W	148 W

**Table 7.1:** Heat applied from each heater during the different heat profiles. The total heat fluxes for all cases were  $q'' = 35 \text{ kWm}^2$ .

The theory denoting that more compressible volume inside the test section causes more instability in the system can be further confirmed by looking at Figure 7.3. The more heat applied in the start of the test section, the faster the liquid will heat up and vapour will be produced. The case of a linear increasing heat profile showed

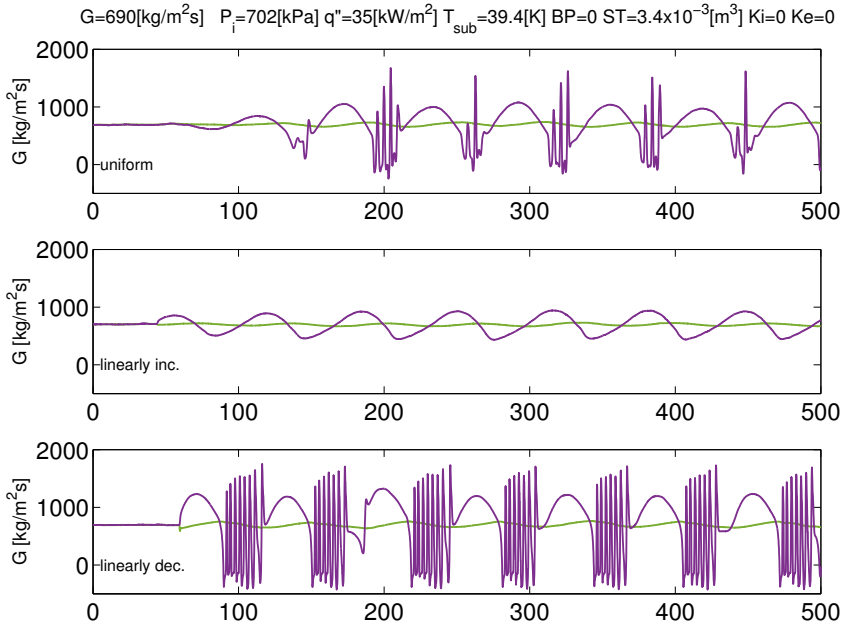


**Figure 7.3:** Effect of uniform, linearly increasing and decreasing heat profiles on PDOs for  $q''_{\text{tot}}=35 \text{ kW}/\text{m}^2$ .

a stabilization of the system, with lower amplitudes and no interfering oscillations compared to the reference case with uniform heating. The opposite was demonstrated for the linearly decreasing case, with a great share of the heat flux being applied at the beginning of the test section a greater amount of vapour was produced in the system. The periods for the three different heat profiles are approximately the same with a small increase for the uniform and linearly increasing cases. An increase in vapour quality, and thereby additional compressible volume, is still showing a trend of increasing the amplitudes and the interfering, high frequency oscillations of the PDOs.

A comparison of a parabolic and a triangle heat profile are shown in Figure 7.4. No big differences in the oscillations are present. This should be expected, as the heat profiles were not altered that much. Compared to the uniform reference case, the periods and amplitudes of the main signals are approximately the same, but the shape is somewhat altered. For the interfering, high frequency signals, the periods and amplitudes are much lower. The number of interfering signals for every period are increasing, even though they decrease in magnitude.

Experiments with the bulk of the heat applied in the start of the test section, while



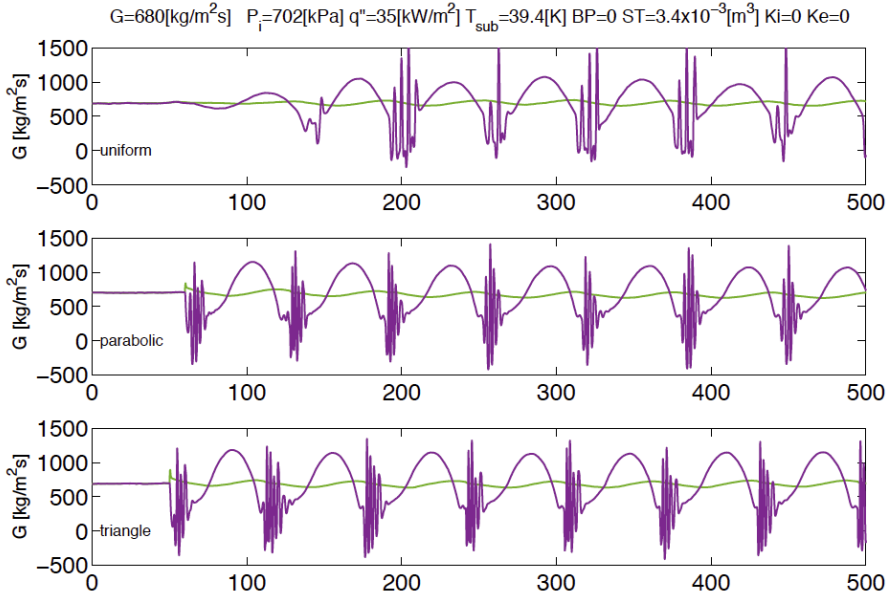


**Figure 7.4:** Effect of uniform, parabolic and triangle heat profiles on the PDOs while using  $q''_{tot}=35 \text{ kW/m}^2$ .

still using a total heat flux of  $q''_{tot}=35 \text{ kW/m}^2$  and an adiabatic outlet are presented in Figure 7.5. It can be seen that as more heat was applied in the beginning of the test section, larger quantities of interfering signals occurred while the period of the main signals decreased. This corresponds with the results for the linearly decreasing case shown in Figure 7.3.

The results from experiments with different heat profiles, a higher total heat flux of  $q''_{tot}=47.7 \text{ kW/m}^2$  and an orifice outlet are shown in Figure 7.6 for the mass flows and Figure 7.7 for the pressures. While the uniform distribution of heat seems to onset some small PDOs after the surge tank is connected to the system, the linearly increased case quickly settles back to steady state. For the linearly decreased case, applying twice as much heat at the inlet than at the outlet, short period oscillations with high amplitudes occur. These oscillations are not unlike the DWOs when it comes to the amplitude and period, but the shape of the oscillations are uneven and dissimilar to the results of Ruspini [2013], seen in Figure 3.10. The differences may be due to the different operational parameters, or that they are a distinct type of oscillations. Further investigations are therefore needed in order to determine the nature of the oscillations.

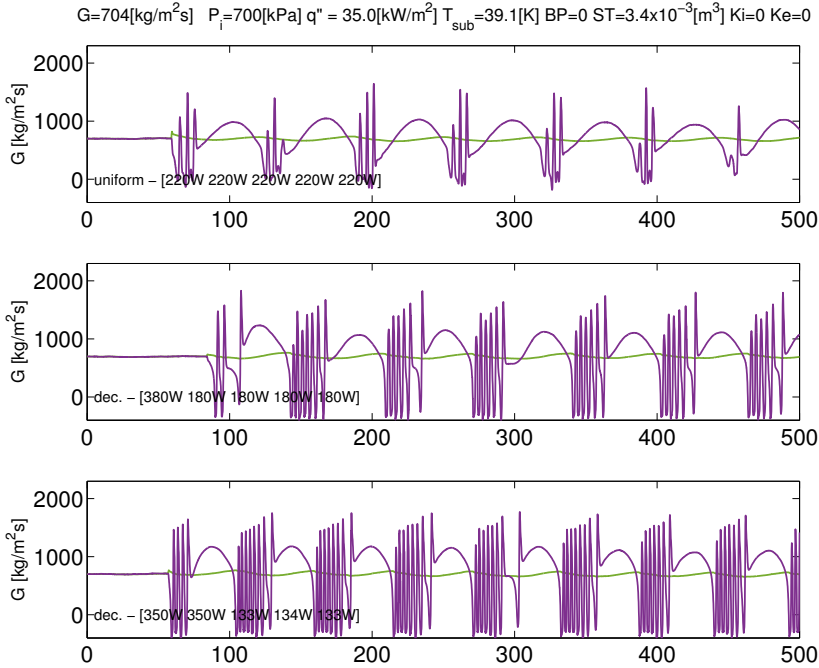


**Figure 7.5:** Mass flow rate evolution during uniform heat distribution and two cases where the bulk of the heat was applied to the first and first two heaters. All three cases were performed while using  $q''_{\text{tot}}=35 \text{ kW}/\text{m}^2$  and an adiabatic outlet.

### 7.1.3 DWO Interaction

Considering the differences between the fast interfering signals presented in this thesis and the known characteristics of DWOs, a further analysis of the phenomenon was performed. Since the DWOs are prone to occur without a compressible volume, a test case without the surge tank was conducted. Figure 7.8 shows a reference case for PDOs with interfering signals while using the surge tank. It can be seen that the fast oscillations onset in the low flow area with flow values of approximately of  $G=550 \text{ kg}/\text{m}^2\text{s}$ . This can also be seen in the limit cycles shown in Figure 6.4. For the same settings and parameters used in the system the flow rate was reduced to this approximated value while no surge tank was connected. As seen is the second graph, no oscillations occurred and the system was stable.

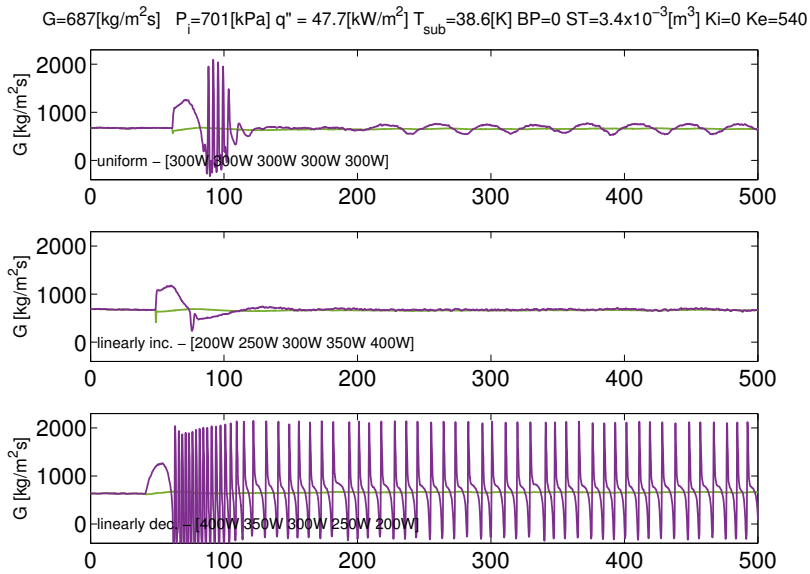


**Figure 7.6:** Mass flow rate evolution during uniform, linearly increasing and decreasing heat profiles for  $q''_{\text{tot}}=47.7 \text{ kW}/\text{m}^2$  and orifice outlet.

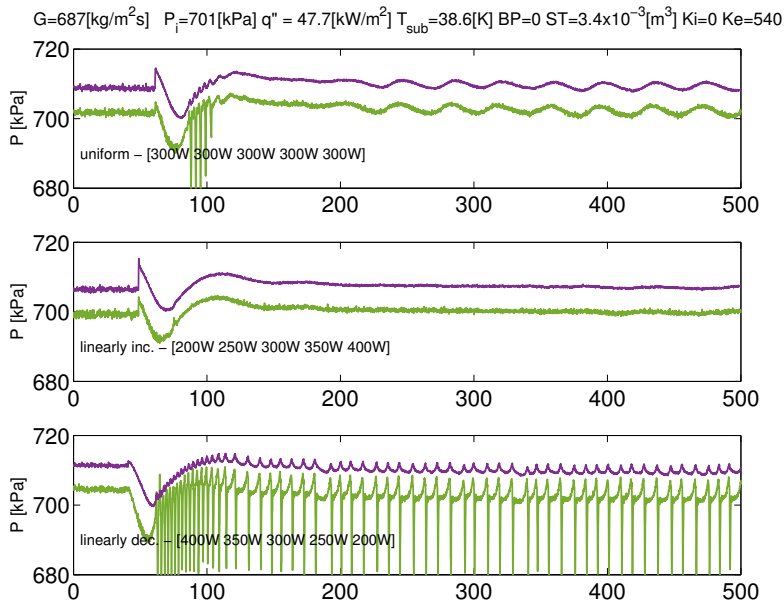


**Figure 7.7:** Pressure evolution during uniform, linearly increasing and decreasing heat profiles for  $q''_{\text{tot}}=47.7 \text{ kW}/\text{m}^2$  and an orifice outlet.

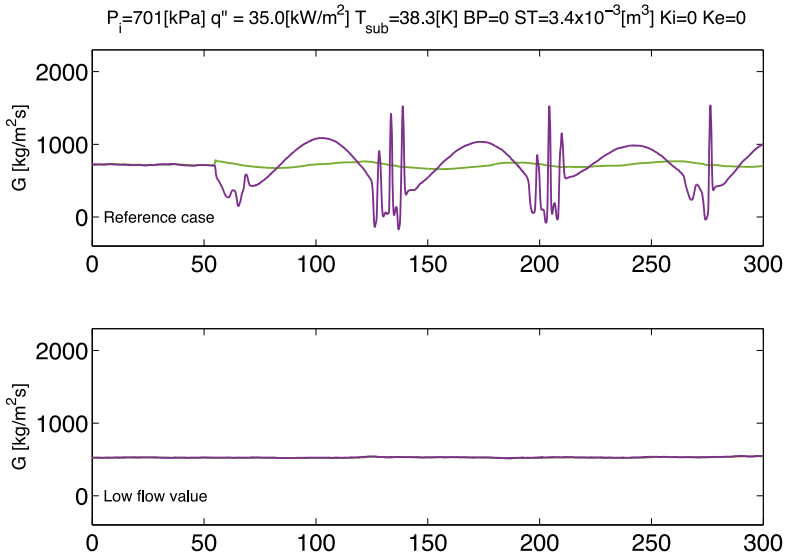


**Figure 7.8:** Reference case for the PDO evolution in mass flux compared to a low flow rate test case with  $G=550 \text{ kg/m}^2\text{s}$ .

To ensure that the fluctuations of the PDO signals do not onset the interfering oscillations, an experiment with three different cases were performed, see Figure 7.9 and 7.10. First, the system was stabilized before the surge tank was connected after  $\sim 60$  seconds. The PDOs, with interfering signals, occurred immediately. After  $\sim 500$  seconds, the surge tank was disconnected and steady state was reassumed. To test the influence of the fluctuations, a sine wave function mimicking that of the PDOs was produced by the pump and is shown from  $\sim 620$  seconds. As the figures show, no interfering signals occurred, not even at the low flow rate values.

The two cases just presented imply that the fast interfering signals are dependent of a compressible volume in order to occur. This does not comply with the known working conditions for the DWOs.

## 7.2 Discussion

Based on the experiments performed, it can be seen that the magnitude of the heat applied to the test section and the heating profiles can greatly affect the PDOs. Both an increase and decrease from the reference case for the heat flux applied showed that the oscillations could be reduced. For a decreasing heat value, the PDOs eventually faded out. For an increasing heat value, the magnitude of the signal was first increased before a reduction in magnitude appeared. An even higher heat flux

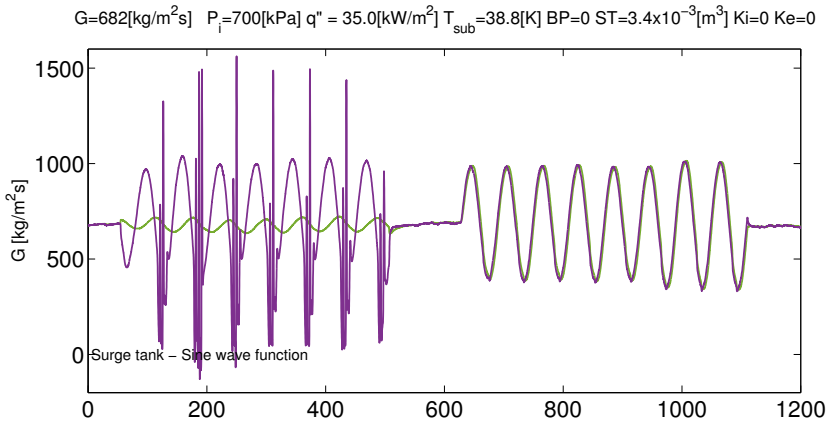


**Figure 7.9:** Evolution of the mass flow rate using first the surge tank and then a sine wave function.

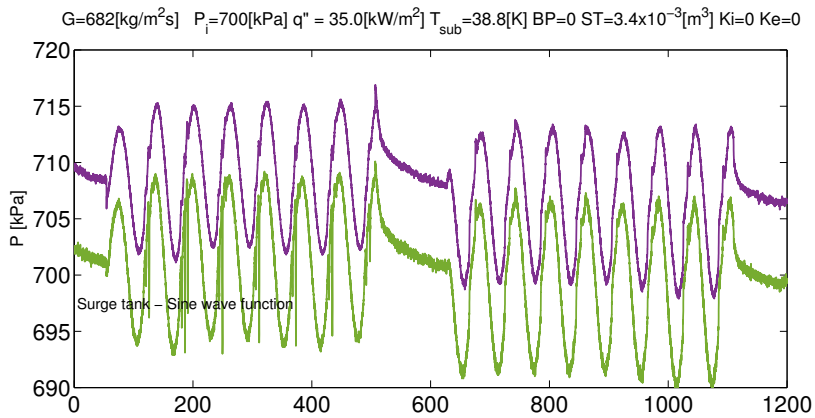


**Figure 7.10:** Evolution of the pressures using first the surge tank and then a sine wave function.

was not achievable in the system due to the risk of overheating the heaters. The increase in magnitude of the PDOs due to an increase of heat flux was also described by Padki et al. [1991] and Guo et al. [2002], but no decrease in the PDOs as the heat flux was further increased were reported. For the theory stated by Maulbetsch & Griffith [1965], proposing that a higher ratio than 150 between the length and diameter in the test section would create enough compressible volume inside the test section itself to onset the PDOs, no experimental evidence was found to support this theory during the experimental work in this thesis. It can be seen in the start-up of every experiment presented that the system is stable until the surge tank is connected, even though the ratio of the length and diameter is  $\sim 400$ .

From the different heat profiles it can be concluded that with more heat applied in the beginning of the test section, more interfering signals occurred, while the opposite was true for the case of a increasing heat profile. This may be due to generation of vapour inside the test section, and thereby an increase of the compressible volume present in the system.

To summarize the results, in order to restrict the PDOs by the use of heat flux, the following conclusions can be made:

- Reduce the heat flux. (An increase of the heat flux would also reduce the oscillations, but there are need for more research before this can be concluded).
- Obtain an increasing heating profile over the system.
- For the use of an orifice outlet, an increasing heat profile should be applied.

According to Figure 2.3c, a higher or lower heat flux would alter the pressure drop characteristic curve, making the negative curve respectively more or less steep. The minimum and maximum point of the curve also seems to relocate further to the right, at higher mass flow rates. This could mean that at higher heat fluxes, a higher mass flux is needed in order to correspond to the operational area of the PDOs. In addition, for the increasing and decreasing heat profile cases, as seen in Figure 2.3d, the shape of the pressure drop characteristic curve is altered. The results presented here visualize how the instabilities in a system can be altered by the use of different heat fluxes.

For the case of an orifice outlet, the interfering, high frequency oscillations occurred. This may imply that the oscillations are DWOs, since an orifice outlet usually increases the magnitude of the DWOs according to Sørnum [2014]. However, the shape of the signals differs from the pure DWOs known to occur in the facility [Ruspini, 2013].

The experiment performed at a lower mass flow rate, corresponding to the instability area of the DWOs, showed no signs of DWOs. Since DWOs are not reliant on a compressible volume, the oscillations should have occurred in this area of the pressure drop characteristic curve. An even lower flow rate could possibly have been used in the experiment shown in Figure 7.8, but since the results from Figure 7.9 oscillates into lower flow rate regions, and no fast oscillations are occurring, this may not be necessary. The results suggest that the interfering signals during PDOs may not be DWOs at all. They may be a distinct type of oscillations, dependent on a compressible volume and only occurring as a function of the PDOs.





# Chapter 8

## Conclusion

Instabilities occurring in two-phase flows are unwanted phenomena that may cause destruction of heat transfer equipment through burnout, vibrations or control problems. Knowledge of the boundary conditions for where the instabilities occur is therefore important. One type of instability, the PDO, generates large period oscillations in both mass flow and pressure with interfering, high amplitude signals of shorter periods. The PDOs are dependent on a compressible volume in order to onset and are likely to occur in the negative slope of the pressure drop characteristic curve, where both liquid and vapour are present.

Through the work of this thesis, a literature review concerning the PDOs has been presented along with the theory for two-phase flow instabilities. The literature review showed that there was still a need for further investigation of the PDO phenomenon due to distinct experimental results and limitations in the studies analysed. An experimental investigation of parameters affecting PDOs was performed at the Two-phase Flow Instabilities Facility at NTNU. The experiments were performed using a single, horizontal channel of 5mm ID where refrigerant R134a was evaporated by heating the pipe by Joule effect. First, the facility was validated against known correlations for pressure drop and heat transfer during single phase flow. The results showed that the system laid within  $\pm 10\%$  of the theoretical values. A pressure drop curve for the internal system at given parameters was further presented along with a characterization of the external system. Based on this information, and after testing for different configurations (inlet valve, outlet restriction, pump bypass and the compressible volume), the appropriate conditions for the occurrence of PDOs were set.

For the experimental part, it has been shown that the occurrence, characteristics and magnitudes of the PDOs are greatly affected by both the external system and the heat flux applied. For the restriction of the test section both an inlet restriction, using a valve, and an outlet restriction, using an orifice plate, were proven efficient in reducing the PDOs. By decreasing the compressible volume of the upstream surge

tank the PDOs eventually disappeared, while for a higher compressible volume the signals increased in magnitude. For the case with an open pump bypass, allowing parts of the liquid to recirculate, the system stabilized faster regarding the PDOs compared to the case of closed pump bypass, even when the mass flux going into the test section was kept constant. This was true even for the cases with larger compressible volumes. Regarding the heat flux applied to the test section, both an increase and decrease in heat flux reduced the PDOs and with a low enough heat flux the system eventually stabilized. The different heat profiles showed that with most of the heat applied at the beginning of the test section, an increase in the PDOs occurred while the opposite was shown when most of the heat was applied at the end of the test section. One of the possible reasons for this is the increased compressible volume that occurred inside the test section when more heat was applied in the beginning of the test section.

In addition to the PDOs, the interfering, high frequency signals occurring at the low flow rates of the PDOs are commonly accepted as DWOs. Two experiments concerning this matter were performed. The first was performed with a low flow rate, at the value of where the DWOs occurred during PDOs, while the second experiment was performed by varying the pump speed in order to generate a sine wave form of the flow rate into the test section, similar to what is obtained during PDOs. It was shown that the interfering, high frequency oscillations that occurred during PDOs were dependent on a compressible volume in order to occur. This does not comply with the usual working conditions for the DWOs, and may imply that the signals are not DWOs, at least not in the practice that they are usually described.

This experimental investigation of PDOs provides new data and information on how PDOs can be affected by parts of the system outside the test section and by the test section heating profile. This new information can help to elucidate possibilities for how to restrict this type of oscillations in thermal two-phase flow systems.

# Chapter 9

## Future Work

The work in this thesis does not fully confirm with previous works concerning PDOs and the field of research could benefit from even further investigations.

For the settings of the external system, the use of a larger compressible volume in order to investigate if there exists an upper limit of compressible volume needed for the PDOs would be valuable. If the surge tank also was relocatable, investigations of compressible volumes closer to the inlet and downstream of the test section could be performed. For the outlet, distinct sizes of orifice plates could be tested in order to investigate how large the restriction at the outlet needs to be in order to decrease the PDOs sufficiently.

Regarding the heat flux applied, experiments with heaters capable of higher heat fluxes than the ones used in this thesis,  $q''_{tot}=50.9 \text{ kW/m}^2$ , should be performed. This could provide information on whether the PDOs are dampened out at relative high heat fluxes after first being reduced. For the discussion about the interfering signals being DWOs, a further study could be to set the parameters for DWO occurrence and then connect the surge tank with the compressible volume to the main system in order to examine if PDOs would appear and the DWOs would maintain.

Since heat exchange systems rarely use single channels for heat transfer, a logic development of the research would be to perform the same experiments, regarding the system settings and parameters, as performed in this thesis for PDOs in multiple, parallel channels.



# Bibliography

- Boure, J., Bergles, A., & Tong, L. S. (1973). Review of two-phase flow instability. *Nuclear Engineering and Design*, 25(2), 165–192.
- Cengel, Y. A. & Cimbala, J. M. (2010). *Fluid Mechanics: Fundamentals and Applications Second Edition in SI Units* (2 ed.). McGraw-Hill.
- Chiapero, E. M. (2013). *Two-phase Flow Instabilities and Flow Mal-distribution in Parallel Channels*. PhD thesis, NTNU.
- Chiapero, E. M., Doder, D., Fernandino, M., & Dorao, C. (2013). Experimental parametric study of the pressure drop characteristic curve in a horizontal boiling channel. *Experimental Thermal and Fluid Science*, 52, 318–327.
- Chiapero, E. M., Fernandino, M., & Dorao, C. (2012). Review on pressure drop oscillations in boiling systems. *Nuclear Engineering and Design*, 250, 436–447.
- Chiapero, E. M., Fernandino, M., & Dorao, C. (2014a). Experimental results on boiling heat transfer coefficient, frictional pressure drop and flow patterns for r134a at a saturation temperature of 34° c. *International Journal of Refrigeration*, 40, 317–327.
- Chiapero, E. M., Fernandino, M., & Dorao, C. (2014b). Experimental study of pressure drop oscillations in parallel horizontal channels. *International Journal of Heat and Fluid Flow*, 50, 126–133.
- Colebrook, C. F. (1939). Turbulent flow in pipes, with particular reference to the transition region between the smooth and rough pipe laws. *Journal of the ICE*, 11(4), 133–156.
- Collier, J. G. & Thome, J. R. (1994). *Convective boiling and condensation* (Third ed.). Oxford University Press.
- Çomaklı, Ö., Karşlı, S., & Yılmaz, M. (2002). Experimental investigation of two phase flow instabilities in a horizontal in-tube boiling system. *Energy Conversion and Management*, 43(2), 249–268.

- Daleas, R. & Bergles, A. (1965). Effects of upstream compressibility on subcooled heat flux. *In: ASME Paper No. 65-HT 67.*
- Ding, Y., Kakac, S., & Chen, X. (1995). Dynamic instabilities of boiling two-phase flow in a single horizontal channel. *Experimental Thermal and Fluid Science*, 11(4), 327–342.
- Dogan, T., Kakac, S., & Veziroglu, T. (1983). Analysis of forced-convection boiling flow instabilities in a single-channel upflow system. *International journal of heat and fluid flow*, 4(3), 145–156.
- Fukuda, K. & Kobori, T. (1979). Classification of two-phase flow instability by density wave oscillation model. *Journal of Nuclear science and Technology*, 16(2), 95–108.
- Grasman, J. (2011). Relaxation oscillations. In R. A. Meyers (Ed.), *Mathematics of Complexity and Dynamical Systems* (pp. 1475–1488). Springer New York.
- Guo, L.-J., Feng, Z.-P., & Chen, X.-J. (2001). Pressure drop oscillation of steam–water two-phase flow in a helically coiled tube. *International journal of heat and mass transfer*, 44(8), 1555–1564.
- Guo, L.-J., Feng, Z.-P., & Chen, X.-j. (2002). Transient convective heat transfer of steam–water two-phase flow in a helical tube under pressure drop type oscillations. *International journal of heat and mass transfer*, 45(3), 533–542.
- Kakac, S. & Bon, B. (2008). A review of two-phase flow dynamic instabilities in tube boiling systems. *International Journal of Heat and Mass Transfer*, 51(3), 399–433.
- Ledinegg, M. (1938). Instability of flow during natural and forced circulation. *Die Warme*, 61(8), 891–898.
- Liang, N., Shao, S., Xu, H., & Tian, C. (2010). Instability of refrigeration system—a review. *Energy conversion and management*, 51(11), 2169–2178.
- Liu, H. & Kakaç, S. (1991). An experimental investigation of thermally induced flow instabilities in a convective boiling upflow system. *Waerme-und Stoffuebertragung*, 26(6), 365–376.
- Lorenz, H. (1909). Die arbeitsweise und berechnung der druckluft-flussigkeitsheber. *Zeitschrift des Vereines deutscher Ingenieure*, 545.
- Maulbetsch, J. S. & Griffith, P. (1965). A study of system-induced instabilities in forced-convection flows with subcooled boiling. Technical report, Cambridge, Mass.: MIT Dept. of Mechanical Engineering,[1965].

- Mentes, D.-I. A., Yildirim, D.-I. O., Gürgenci, I. H., Kakaç, S., Veziro, T., et al. (1983). Effect of heat transfer augmentation on two-phase flow instabilities in a vertical boiling channel. *Wärme-und Stoffübertragung*, 17(3), 161–169.
- Ozawa, M., Nakanishi, S., Ishigai, S., Mizuta, Y., & Tarui, H. (1979). Flow instabilities in boiling channels: part 1 pressure drop oscillation. *Bulletin of JSME*, 22(170), 1113–1118.
- Padki, M., Liu, H., & Kakac, S. (1991). Two-phase flow pressure-drop type and thermal oscillations. *International journal of heat and fluid flow*, 12(3), 240–248.
- Padki, M., Palmer, K., Kakac, S., & Veziroglu, T. (1992). Bifurcation analysis of pressure-drop oscillations and the ledinegg instability. *International journal of heat and mass transfer*, 35(2), 525–532.
- Prasad, G. V. D., Pandey, M., & Kalra, M. S. (2007). Review of research on flow instabilities in natural circulation boiling systems. *Progress in Nuclear Energy*, 49(6), 429–451.
- Ruspini, L. & Langørgen, E. (2011). *Risk assessment report: Two-phase flow instabilities project*. Technical report, NTNU, SINTEF.
- Ruspini, L. C. (2013). *Experimental and numerical investigation on two-phase flow instabilities*. PhD thesis, NTNU.
- Ruspini, L. C., Marcel, C. P., & Clausse, A. (2014). Two-phase flow instabilities: A review. *International Journal of Heat and Mass Transfer*, 71, 521–548.
- Sørum, M. (2014). Experimental investigation of the impact in the heat transfer coefficient and pressure drop during boiling flow instabilities.
- Stenning, A. & Veziroglu, T. (1965). Flow oscillation modes in forced-convection boiling. *Heat Transfer and Fluid Mechanics Institute. NASA Grant NsG-424*, 301–316.
- Tadrist, L. (2007). Review on two-phase flow instabilities in narrow spaces. *International Journal of Heat and Fluid Flow*, 28(1), 54–62.
- Wang, G., Cheng, P., & Bergles, A. (2008). Effects of inlet/outlet configurations on flow boiling instability in parallel microchannels. *International Journal of Heat and Mass Transfer*, 51(9), 2267–2281.
- Wang, Q., Chen, X., Kakac, S., & Ding, Y. (1996). Boiling onset oscillation: a new type of dynamic instability in a forced-convection upflow boiling system. *International journal of heat and fluid flow*, 17(4), 418–423.

- Xiao, M., Chen, X., Zhang, M., Veziroglu, T., & Kakac, S. (1993). A multivariable linear investigation of two-phase flow instabilities in parallel boiling channels under high pressure. *International journal of multiphase flow*, 19(1), 65–77.
- Yüncü, H., Yildirim, O., & Kakac, S. (1991). Two-phase flow instabilities in a horizontal single boiling channel. *Applied Scientific Research*, 48(1), 83–104.



## Appendix

# **”Effect of external system in the characteristics of Pressure Drop Oscillations”**

The submitted manuscript for the article ”Effect of external system in the characteristics of Pressure Drop Oscillations” is here presented. The article has been submitted to the Chemical Engineering Science journal.

1           Effect of external system in the characteristics of  
2                                   Pressure Drop Oscillations

3                                   Langeland, T., Fernandino, M., Dorao, C.A.\*

4           *Department of Energy and Process Engineering, Norwegian University of Science and*  
5                                   *Technology, Norway*

---

6   **Abstract**

7   The effect of the external system on the characteristics of Pressure Drop  
8   Oscillations (PDO) are studied. A horizontal test section of 5mmI.D. with  
9   R134a as working fluid is used for the experiments. The impact of the com-  
10  pressible volume in the surge tank, the pump bypass, inlet and outlet restric-  
11  tion on the PDO are analysed. It was observed that the characteristics of  
12  the PDO are strongly controlled by the external system. In particular the  
13  compressible volume in the surge tank has a major impact on the stability  
14  of the system and the characteristics of the oscillations.

15  *Keywords:* Pressure Drop Oscillation, Two Phase Flow Oscillations,  
16  Boiling

---

17  **1. Introduction**

18       Two phase flow instabilities have been extensively studied during the past  
19  decade [1][2][3][4][5] due to its relevance to different areas such as refriger-  
20  ation systems, boiling water reactors and steam generators. The induced  
21  oscillations of the flow rate and system pressure are undesirable as they can  
22  cause mechanical vibrations, thermal fatigue, transient burn-out of the heat

---

\*e-mail: carlos.dorao@ntnu.no  
*Preprint submitted to Elsevier*

23 transfer surface, degradation of the heat transfer performance and problems  
24 of system control.

25 Pressure drop oscillations (PDOs) are a particular case of two phase flow  
26 instabilities. A PDO occurs in a system having compressible volume up-  
27 stream or within the heated section and when the system operates in the  
28 negative slope region of the N-shape curve, namely pressure drop vs. flow  
29 rate curve [1]. PDOs have a long period (of the order of several seconds)  
30 and produce big excursions of the flow resulting in large variations in the  
31 local wall temperature (thermal oscillation). PDOs exhibit a long oscillatory  
32 period which are characterised by relaxation oscillations similar to the van  
33 der Pol oscillator [6]. Furthermore, PDOs are dynamic instabilities caused  
34 by a Hopf bifurcation [7].

35 The necessary conditions for the occurrence of this type of oscillations are  
36 [7]: (i) internal characteristic curve with negative slope; (ii) external char-  
37 acteristic curve steeper than internal curve; and (iii) upstream compressible  
38 volume (e.g. surge tank) in the flow circuit. The standard way to elimi-  
39 nate pressure-drop oscillations is to make the slope of internal characteristic  
40 positive (e.g. internal throttling).

41 PDOs have been widely studied theoretically, e.g.[8][9][10][7][11], and ex-  
42 perimentally, e.g. [12][13][14], during the last decade. A detailed summary  
43 of the research done on pressure drop instabilities and remaining challenges  
44 has been recently presented by Manavela et al. [15]. It was acknowledged  
45 that the characterisation and understanding of the PDOs is essential due to  
46 its relevance in two phase system ranging from large scale industrial equip-  
47 ment to microscale cooling devices. Even though the mechanisms of PDO are

48 well understood and have been widely analysed theoretically and empirically,  
49 there are still several issues that have not been clarified so far. In particular  
50 the role of the compressible volume in the characteristics of the oscillations,  
51 and whether the compressible volume in the heated section is equivalent to  
52 the compressible volume in a surge tank located upstream or downstream of  
53 the heated section. For example, Guo et al. (2001) [16] has shown that the  
54 location of the compressible volume upstream of the test section can mod-  
55 ify the characteristics of the oscillation. Furthermore the interconnection  
56 between density wave oscillations (DWOs) and PDOs in horizontal boiling  
57 systems is not well understood, in particular how to decouple, control or  
58 suppress the oscillations.

59 Gaining a better understanding of two phase flow instabilities and in  
60 particular PDOs is becoming particular relevant in mini- and micro-channels  
61 [17], [18] as these oscillations can affect the performance of the unit severely.

62 In this work the effect of the external system on the characteristics of  
63 pressure drop oscillations will be studied for a horizontal straight tube evap-  
64 orator of 50mm ID and 2m long, using refrigerant R134a as working fluid.  
65 The effect of the level of the liquid in the surge tank, i.e. the compressible  
66 volume, the pump bypass, the inlet restriction and exit restriction on the  
67 characteristics of the PDO are investigated. The article is organised as fol-  
68 lows. Section 2 describes the characteristics of the experimental facility. In  
69 section 3 the experimental results and discussion are presented. Section 4  
70 summarises the main conclusions of this work.

## 71 2. Experimental facility

72 The experiments are performed at the Two Phase Flow Instability facil-  
73 ity at the Department of Energy and Process Engineering, NTNU, [19], [20].  
74 The facility is a closed loop consisting of a main tank, a pump, a conditioner,  
75 a surge tank, a heated test section, a visualisation glass, an adiabatic test  
76 section and a condenser. The working fluid (R134a) is circulated by a mag-  
77 netically couple gear pump. The pressure in the loop is controlled by the  
78 saturation conditions at the main storage tank. A pre-heater or conditioner  
79 adjusts the inlet temperature of the refrigerant before entering the test sec-  
80 tion. The pre-heater is a shell and tube heat exchanger with glycol in the  
81 shell side.

82 For these experiments, the flow is measured with two Coriolis mass flow  
83 meters, one located after the pump and one between the surge tank and the  
84 heated test section. Before the heated section a manually operated valve is  
85 installed, while after the heated section it is possible to select an orifice plate  
86 or an adiabatic section. The heated section is a stainless steel tube with  
87 5mm I.D. and 8mm O.D. and 2035mm long, figure 1. The tube is heated  
88 by Joule effect with a rectified sine wave and is insulated to reduce heat  
89 loss to the surroundings. In order to have control of the heating profile, the  
90 heating is done by 5 independent sections of 40cm long, figure(2). The test  
91 section is equipped with 7 pressure taps for differential pressure drop mea-  
92 surements, a number of external (wall temperature) thermocouples, and 2  
93 internal thermocouples to study heat transfer to the fluid. The pressure taps  
94 are connected to two pressure transducers by a network of valves which allows  
95 for a custom point of measurement. An additional third pressure differential

96 transducer measures the overall test section pressure drop. Ten thermocou-  
97 ples are distributed along the outside bottom wall of the test section while  
98 there are seven on the top side. In particular, position 6 (at 1117mm from  
99 the inlet) and 10 (at 1917mm from the inlet) includes thermocouples on top,  
100 bottom, both sides of the wall plus an in-flow internal thermocouple. All the  
101 variables are logged with a National Instruments NI RIO data acquisition  
102 system. The temperatures, absolute pressures, pressure differences and mass  
103 flow rates were acquired at a frequency of 10 Hz.

104 In order to control the response of the external system a bypass to  
105 the pump is operated with a valve which adjusts the flow recirculated, see  
106 figure(1). The surge tank is a tank with a capacity of  $9.5 \times 10^{-3}m^3$  with  
107 an inner diameter of 219mm. The tank is pressurised with  $N_2$  which controls  
108 the level of refrigerant in the tank. The inlet valve and the exit orifice are  
109 installed in a pipe of internal diameter of 12.7mm. Considering the mass flux  
110 in this pipe, the inlet valve fully opened has a minor loss coefficient  $K_i=400$ .  
111 In order to indicate in the figure that the valve was fully opened, the legend  
112 of  $K_i=0$  will be used instead of the real value. The exit orifice has a minor  
113 loss coefficient  $K_e=540$ . If the adiabatic section is used instead of the orifice,  
114 the legend of  $K_e=0$  will be used.

### 115 *2.1. Measurements and accuracy of measurements*

116 For the temperature measurement, type-T thermocouples with 0.5mm  
117 diameter have been used with an accuracy of 0.1K (in-house calibration).  
118 The absolute pressure at the inlet and outlet of the heated section was used  
119 for determining the saturation temperature,  $T_{sat}$ , of the fluid based on the  
120 equilibrium properties calculated with the software REFPROP.

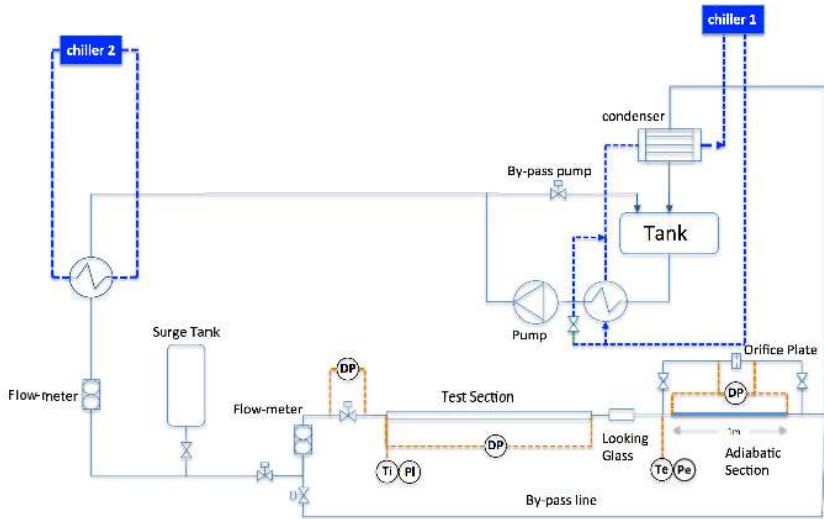


Figure 1: Sketch of the test facility.

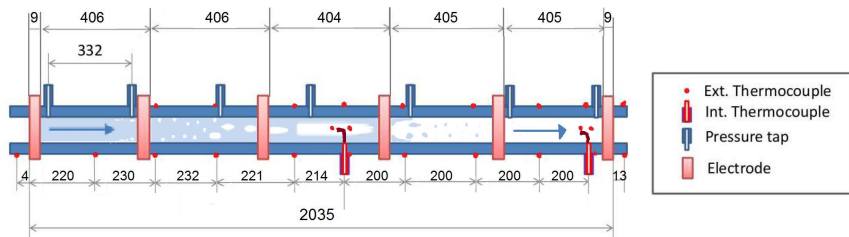


Figure 2: Sketch of the heated test section.

121 The inlet and outlet pressures are measured with absolute pressure trans-  
 122 ducers with an accuracy of 0.04% at full-scale (25bar) given by the supplier.  
 123 The two-phase total pressure drop along each test section is measured with  
 124 a differential pressure transducer with an accuracy of 0.075% at full-scale  
 125 (50kPa) given by the supplier. For the heat flux,  $q''$ , the error coming from  
 126 the propagation is the error associated with the voltage and current measure-  
 127 ments. Nevertheless, the thermal heat transfer to the fluid under stationary  
 128 conditions was calibrated against the electrical value for different temper-  
 129 atures and conditions for single-phase liquid considering the heat exchange  
 130 with the surrounding arriving to a final accuracy of 3%.

131 The vapour quality is obtained by performing a heat balance along the  
 132 test section as shown below:

$$x(z) = \frac{\int_{z_0}^z q'' \pi D_i dz - G A c_{pl} T_{sub}}{G A h_{lv}} \quad (1)$$

133 Here  $x(z)$  is the fluid quality at point  $z[m]$  along the heated section,  
 134  $G[kg/m^2s]$  is the mass flux,  $A[m^2]$  is the cross section area of the pipe,  
 135  $c_{pl}[J/kgK]$  is the liquid phase heat capacity of the fluid,  $h_{lv}[kg/m^2s]$  is the  
 136 enthalpy of vaporisation and  $T_{sub}[K]$  the inlet subcooling. A mass flow rate  
 137 accuracy of 0.2% of the reading was given by the supplier.

## 138 2.2. Single-phase validation and uncertainties

The system was tested with single-phase flows and these results were compared with known correlations. The single phase friction factor,  $f$ , was compared with the Colebrook correlation which is typically used for Reynolds



number between 4000 and  $10^8$ ,

$$\frac{1}{\sqrt{f}} = -2.0 \log \left( \frac{\epsilon/D_i}{3.7} + \frac{2.51}{Re\sqrt{f}} \right) \quad (2)$$

139 where  $\epsilon$  is the pipe wall roughness. The friction factor was determined with  
140 an error of about 5% and with a difference between the experimental and  
141 predicted one lower than 10%, see figure 3.

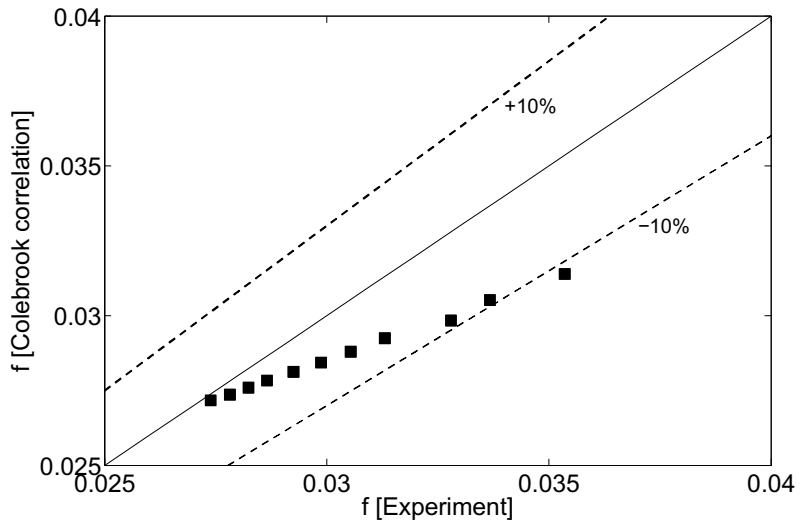
The single phase heat transfer coefficient was validated against the Petukhov–  
Kirilov correlation,

$$Nu_D = \frac{(f/8)Re_D Pr}{1.07 + 12.7(f/8)^{1/2}(Pr^{2/3} - 1)} \quad (3)$$

where the friction coefficient is obtained from

$$f = (0.79 \log Re_D - 1.64)^{-2} \quad (4)$$

142 The comparison between the experimental data and the correlation is shown  
143 in figure 3.



Single-phase verification ( $z=1.917$  mm)

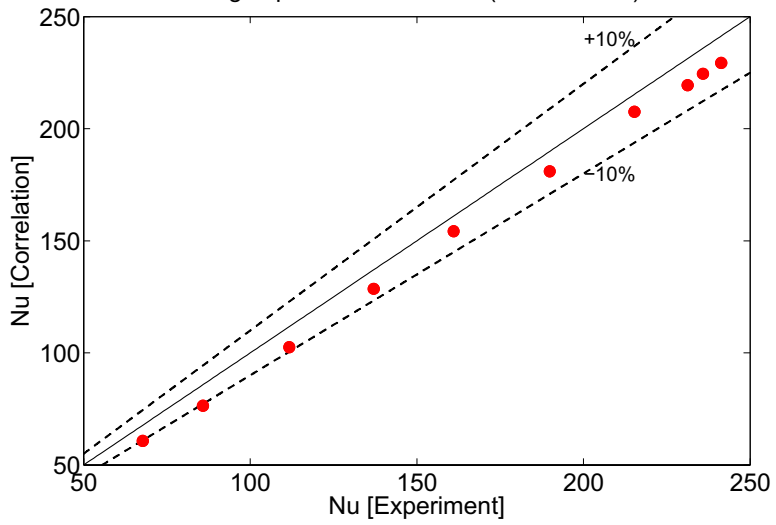


Figure 3: Single phase flow validation.

144 *2.3. Internal and external system characterisation*

145 Figure (4) shows part the N-shape curve of the heated section,  $\Delta P_{TS}$ , and  
146 of the flow loop (including the heated section),  $\Delta P_{system}$ , for the operational  
147 conditions used in this work for the case of closed pump-bypass, open inlet  
148 restriction and adiabatic exit. The effect of different operational conditions  
149 on the N-shape has been studied previously in [20]. In the present exper-  
150 iment, the N-shape curve was obtained by reducing the mass flux in steps  
151 while keeping the conditions at the inlet of the heated section fixed.

152 In order to characterise the external system, the response of the pump  
153 to an increment in the pressure drop in the flow loop is shown in figure  
154 (5). In this case  $\Delta P_{pump}$  represents the pressure drop along the flow loop,  
155 i.e. equivalent to  $\Delta P_{system}$ . In this case, the experiment was performed by  
156 maintaining the conditions at the inlet of the test section but without adding  
157 heat. In order to change the operational point, the valve corresponding to  
158 the inlet restriction was closed in steps for increasing the pressure drop of  
159 the loop. The figure includes the response of two cases corresponding to the  
160 bypass closed and partially opened. As expected, the main effect of partially  
161 opening the pump bypass is that the slope of the external system is reduced  
162 which in the limit results in an approximation of a pressure driven system.

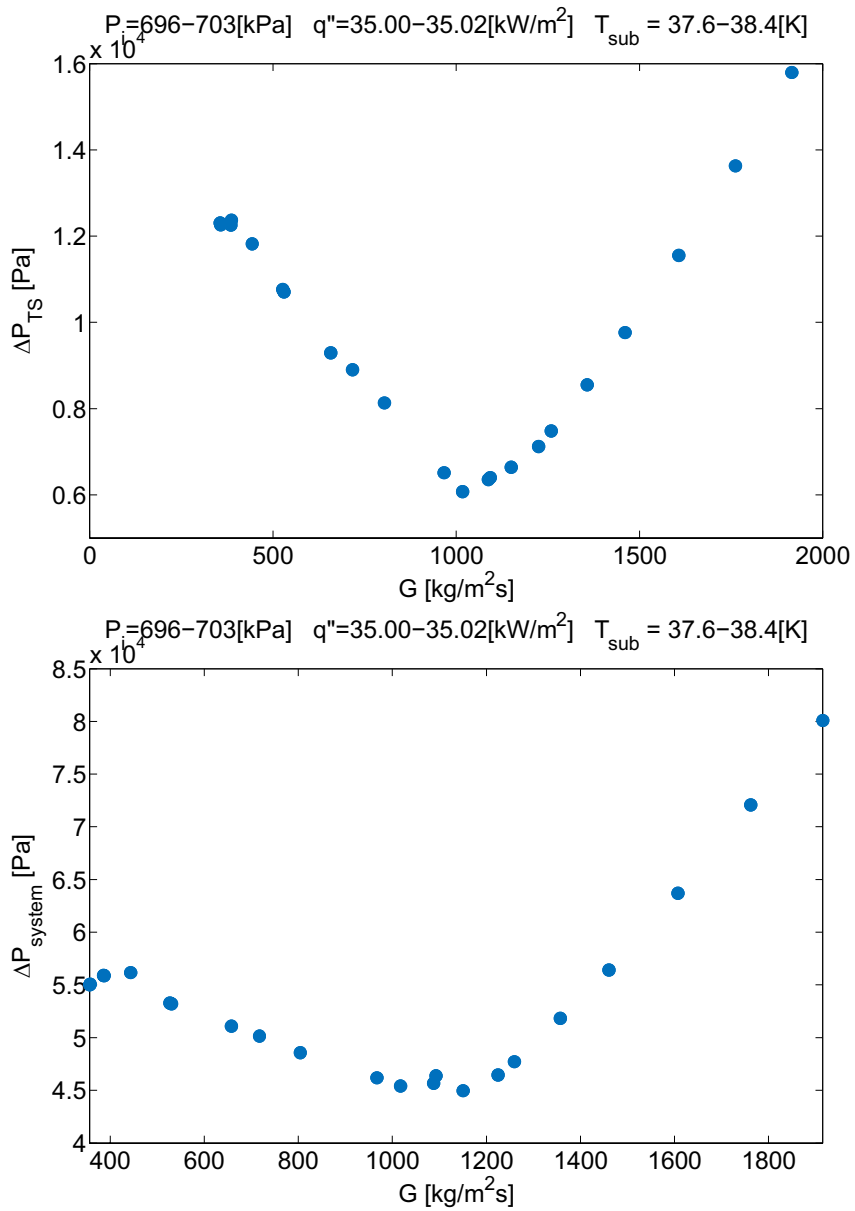


Figure 4: N-shape curve of the heated section ( $\Delta P_{TS}$ ) and the flow loop ( $\Delta P_{\text{system}}$ ).

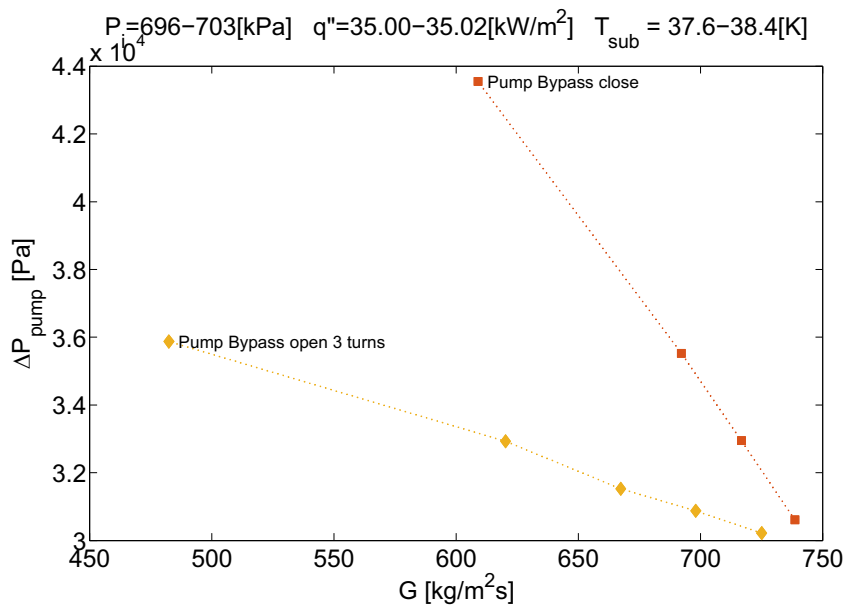


Figure 5: Pump response to with the pump bypass closed and open 3 turn.

### 163 3. Experimental Results and Discussion

164 The main goal of this work is to investigate the effect of the liquid level in  
165 the surge tank, inlet restriction, outlet restriction, and pump bypass on the  
166 characteristics of the PDOs. Preliminary work performed in the experimental  
167 facility has shown that the PDOs can present two distinct behaviours. Figure  
168 (6) and (8) show two examples of different types of PDOs. For these two  
169 cases the conditions at the inlet of the heated section are identical, but the  
170 compressible volume is different. Similar differences in the characteristics of  
171 the PDO have been observed before, for example Dogan et al. [9] observed  
172 similar differences although it was attributed to different heat fluxes.

173 Figure (6) shows an oscillation with a period of about 50s, while figure (8)  
174 presents a larger period of about 70s with a very fast oscillation of few seconds  
175 similar to a density wave oscillation. These fast oscillations superimposed  
176 over the long period oscillation have been observed in previous studies [12][9].  
177 Ozawa et al. [12] stated that the high frequency oscillations depend on the  
178 experimental conditions and they are not considered an essential feature of  
179 the PDO. Dogan et al. [9] reported that such oscillations were observed  
180 generally with high heat inputs.

181 Figure (6) and (8) show the evolution of the main variables during the  
182 PDO. The mass flow rate is shown in the flow meter placed after the pump  
183 and before the surge tank ( $G_p$ ) and the flow meter placed between the surge  
184 tank and the heated test section ( $G_i$ ). The pressure is shown before the surge  
185 tank ( $P_s$ ), at the inlet of the heated test section ( $P_i$ ) and at the outlet of the  
186 heated section ( $P_o$ ). In addition the average wall temperature ( $T_{wall}$ ) and the  
187 fluid temperature ( $T_{fluid}$ ) at 1917mm from the inlet of the heated section is

188 shown.  $T_{wall}$  is the internal wall temperature which is calculated from the  
189 4 measured outside wall temperature  $T_{w,o}$  by applying a one-dimensional,  
190 radial, steady-state heat conduction equation for a hollow cylinder with a  
191 uniform heat generation.

192 Figure (7) and (9) show the limit cycle of the mass flux at the inlet of the  
193 heated section ( $G_i$ ) and pressure in the heated test section ( $\Delta P_{TS}$ ) and the  
194 limit cycle of the mass flux after the pump ( $G_p$ ) and pressure in the heated  
195 test section. The figures include the equivalent representation but consider-  
196 ing the pressure drop along the flow loop ( $\Delta P_{Loop}$ ). Both representations are  
197 recommended for studying PDOs as the system is mainly controlled by the  
198 external system. However limited attention has been given to the characteri-  
199 sation of the flow loop and its impact on the characteristics of the oscillations.  
200 This can be particularly relevant if the experimental data might be used for  
201 code validation.

202 Ideally the PDO is approximated as a relaxation oscillation. However,  
203 this approximation is appropriate in the limit of a large compressible volume  
204 and almost negligible flow inertias and wall thermal capacity [21]. As shown  
205 in figure (6), the limit cycle in this case is closer to a sinusoidal oscillation  
206 implying that the thermal capacity of the pipe plays an important role during  
207 the oscillation [21].

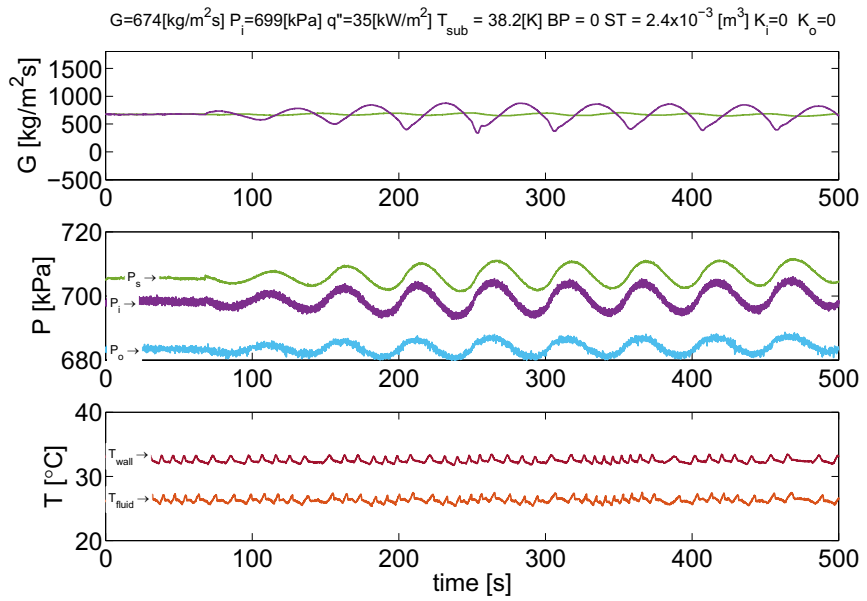


Figure 6: PDO without high frequency components.



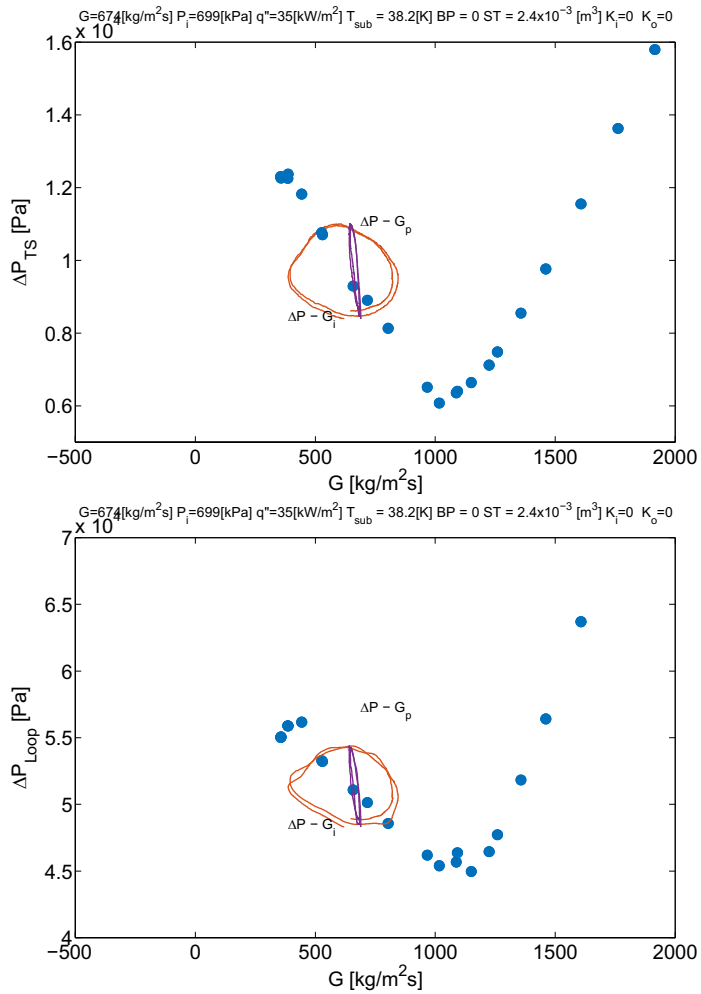


Figure 7: Limit cycle for the PDO without high frequency components.

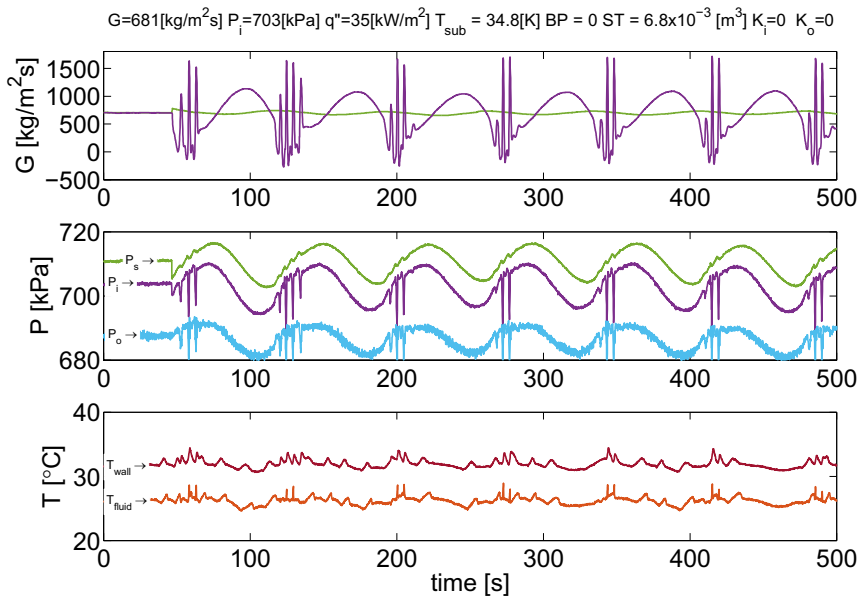


Figure 8: PDO with high frequency component.

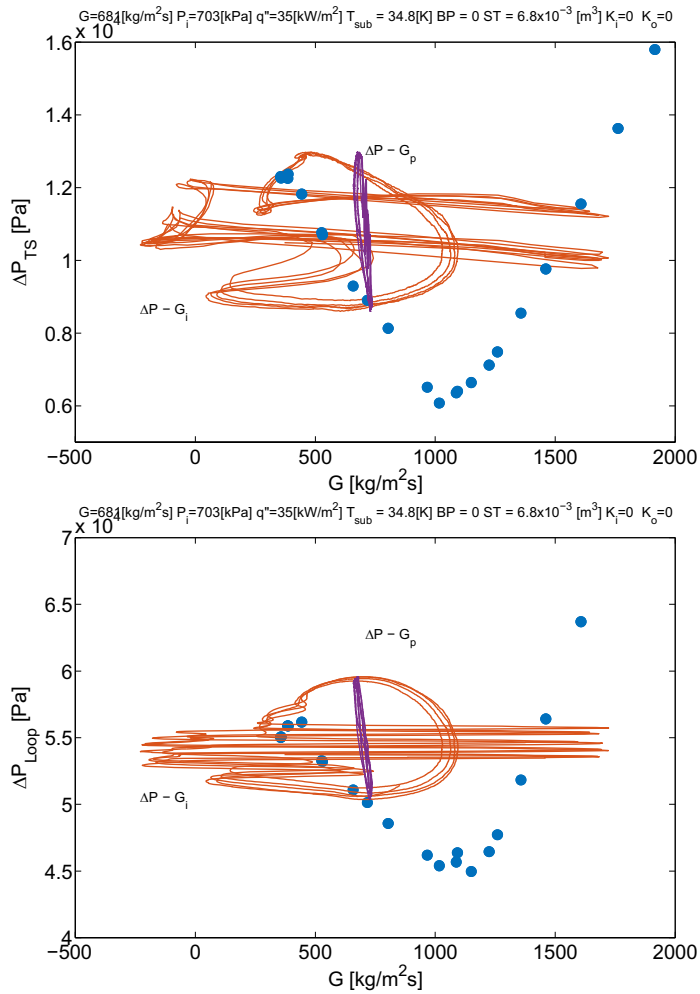


Figure 9: Limit cycle for the PDO with high frequency components.

208 *3.1. Effect of external components on the PDOs*

209 In this section the effect of the pump bypass, compressible volume in  
210 the surge tank, inlet restriction and exit restriction on the PDO will be  
211 discussed. In order to investigate the impact of the external system on the  
212 PDOs, the conditions at the inlet of the heated section were maintained  
213 fixed while different external parameters were changed. The conditions at  
214 the inlet of the heated section are fixed to  $G_i = 700[kg/m^2s]$ ,  $P_i = 700[kPa]$ ,  
215  $q'' = 35[kW/m^2]$  and  $T_{sub} = 38K$  for all the cases in this work. The values  
216 reported in the plots correspond to the average values over the presented  
217 time sequence.

218 *3.1.1. Effect of the compressible volume*

219 Figure (10) shows the effect of changing the compressible volume in the  
220 surge tank (ST). In the first case the pump bypass is closed (BP=0), while in  
221 the second case the pump bypass is opened 3 turns (BP=3). Even though it  
222 is not possible to quantify the partition of the fluid recirculated, the effect on  
223 the PDOs is noticeable. For the case of a large compressible volume (ST) the  
224 oscillations present a high frequency oscillation when the mass flux reaches  
225 the minimum value. When the compressible volume is reduced, it is possible  
226 to observe that the high frequency vanishes. For a minimum compressible  
227 volume the oscillation is damped and finally not established.

228 The main conclusion drawn from this study is that closing the pump  
229 bypass makes the system more unstable, while opening the pump bypass  
230 helps to absorb the pressure oscillations, thus making the system more stable.

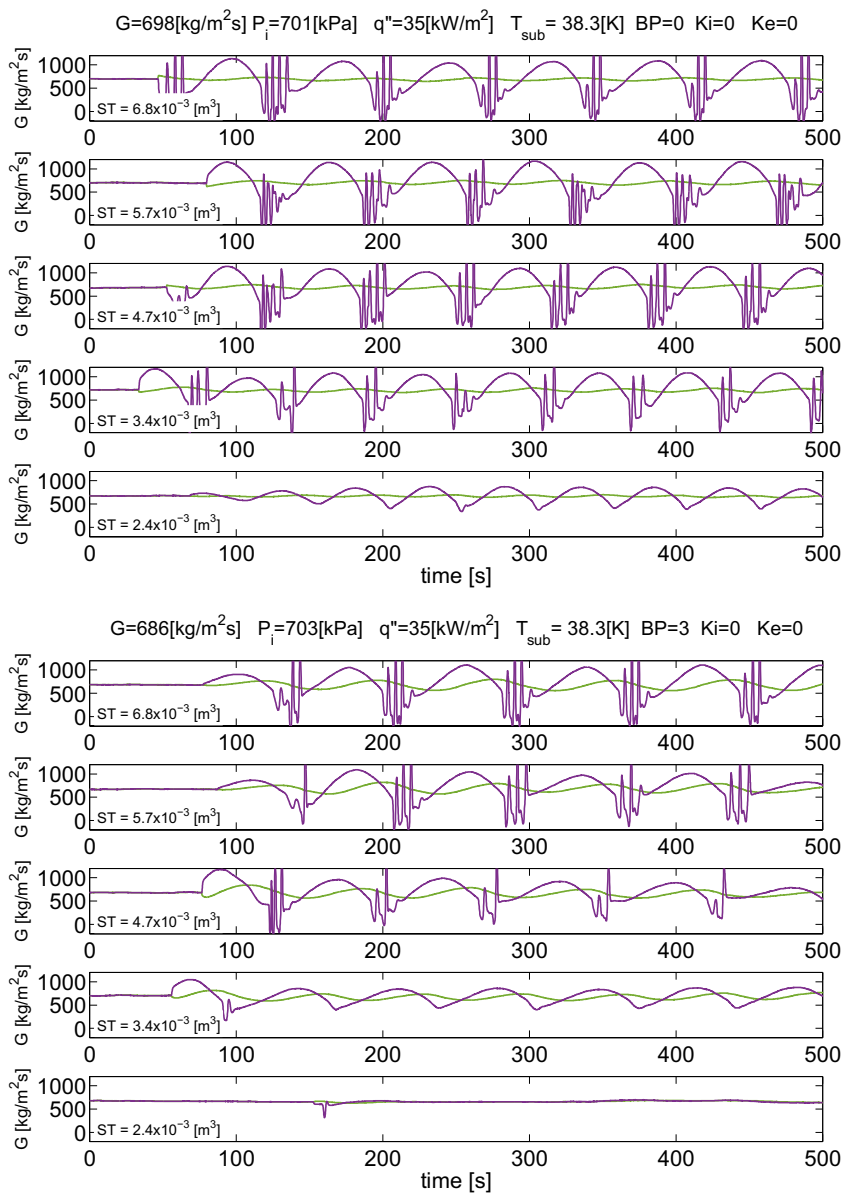


Figure 10: Effect of the liquid level (ST) in the surge tank on the PDOs.

231 3.1.2. Effect of the pump bypass

232 Figure (11) shows the effect of opening the pump bypass for a fixed com-  
233 pressible volume in the surge tank. It is clearly observed that allowing the  
234 recirculation of the flow in the pump bypass helps to absorb the pressure  
235 fluctuations downstream reducing the amplitude of the oscillations. A large  
236 aperture of the bypass can suppress the PDOs.

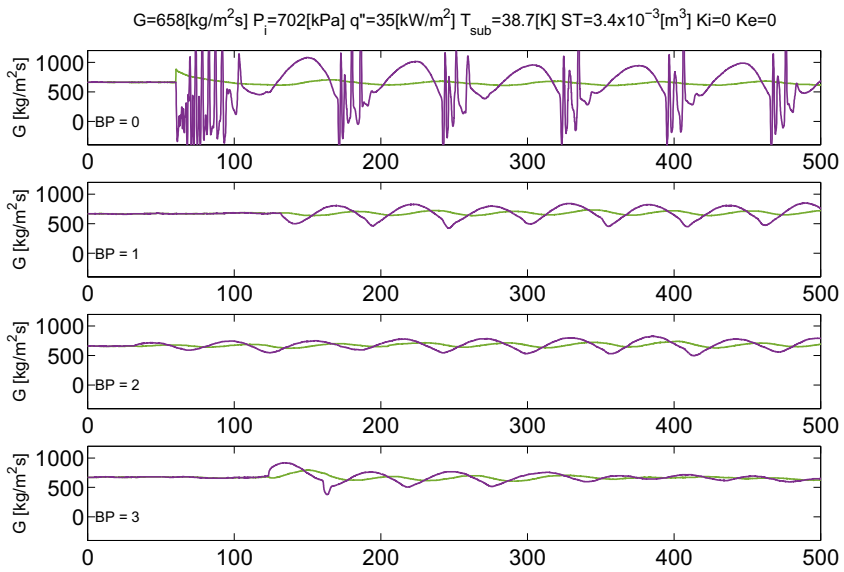


Figure 11: Effect of opening the pump bypass on the PDOs.

237 *3.1.3. Effect of the inlet restriction*

238 Figure(12) shows the effect of the inlet restriction on the PDO for a given  
 239 compressible volume. Increasing the value of the valve  $K_i$  the system is  
 240 stabilised as this reduces the negative slope of the N-shape.

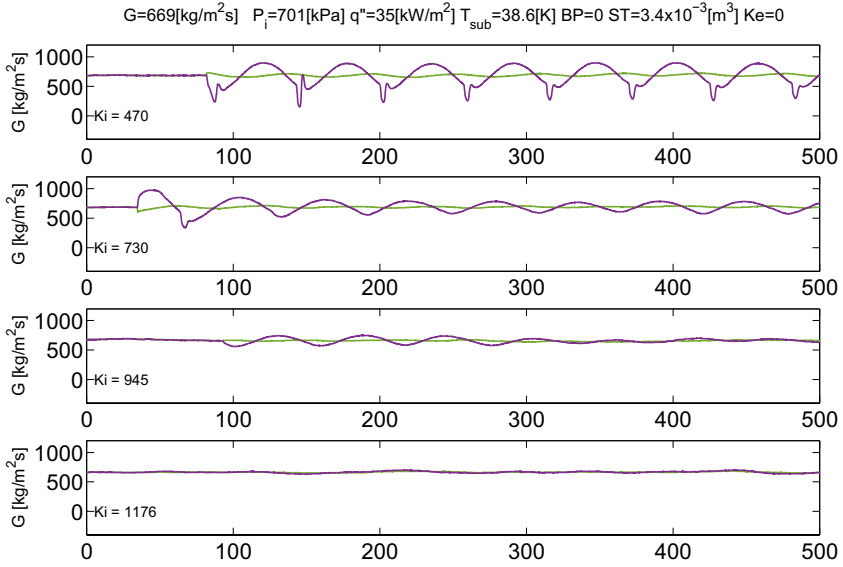


Figure 12: Effect of the inlet restriction on the PDOs

241 *3.1.4. Effect of the exit restriction*

242 Figure(13) shows the effect of the exit configuration on the PDO. The  
 243 facility can use two different exit configurations, namely adiabatic or orifice.  
 244 The figure shows that changing from the adiabatic to the orifice configuration  
 245 the PDOs can be partially stabilised or suppressed depending on the com-  
 246 pressible volume in the surge tank. In this case, the orifice restriction might

247 help to decouple the upstream system from the main tank which represents  
248 a large compressible volume, while at the same time the orifice configuration  
249 reduces the negative slope of the N-shape.

250       Summing up, the characteristics of the PDO are controlled by the system  
251 upstream and downstream of the heated section. This fact might explain the  
252 different PDOs observed in previous studies during the past decade. Each  
253 flow loop can trigger PDOs with particular characteristics depending on the  
254 components and configuration of the loop. This fact implies that the study  
255 of PDOs requires a detailed characterisation of each component in the flow  
256 loop in particular if the experiments are planned to be used in code validation.



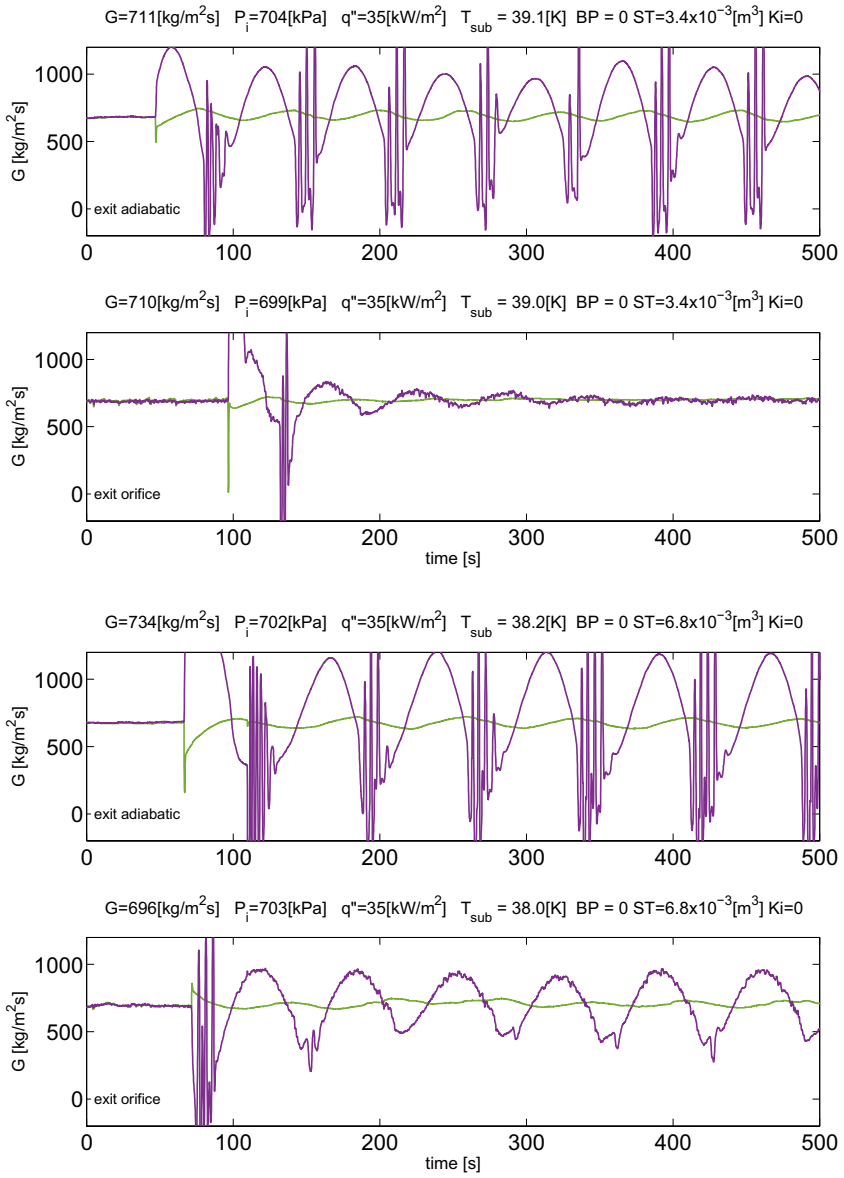


Figure 13: Effect of the exit restriction on the PDOs

## 257 4. Conclusions

258 In this work the effect of the external system on the characteristics of  
259 pressure drop oscillation was investigated. The main conclusion drawn from  
260 this study is that the components of the flow loop play a major role in setting  
261 the characteristics of the PDOs. The pump bypass can control the stabil-  
262 ity of the PDOs by changing the response of the external system. Closing  
263 the pump bypass made the system more unstable. Apparently opening the  
264 pump bypass helps to absorb the pressure oscillations helping to stabilise the  
265 system. Reducing the compressible volume in the surge tank help to stabilise  
266 the PDOs as expected. Further work is required in order to identify the min-  
267 imum compressible volume required for triggering the PDOs, although this  
268 may be difficult to quantify since the vapor in the test section itself acts as  
269 part of the available compressible volume. The inlet and outlet restrictions  
270 help to stabilise the PDOs probably by decoupling the external system from  
271 the heated section.

272 Summing up, the study of the PDOs requires a proper description of  
273 the different elements in the facility. Each flow loop can trigger PDO with  
274 particular characteristics depending on the components and configuration  
275 of the loop. This fact can explain the different PDO observed in previous  
276 studies.

## 277 5. Acknowledgements

278 Funding for this work from the Research Council of Norway under the  
279 FRINATEK project 231529 is gratefully acknowledged.

280 **6. References**

- 281 [1] J. A. Boure, A. E. Bergles, L. S. Tong, Review of Two-Phase Flow  
282 Instability, *Nuclear Engineering and Design* 25 (1973) 165–192.
- 283 [2] L. Tadrist, Review on two-phase flow instabilities in narrow spaces,  
284 *International Journal of Heat and Fluid Flow* 28 (1) (2007) 54–62.  
285 doi:10.1016/j.ijheatfluidflow.2006.06.004.
- 286 [3] G. V. Durga Prasad, M. Pandey, M. S. Kalra, Review of research on flow  
287 instabilities in natural circulation boiling systems, *Progress in Nuclear*  
288 *Energy* 49 (6) (2007) 429–451. doi:10.1016/j.pnucene.2007.06.002.
- 289 [4] S. Kakac, B. Bon, A Review of two-phase flow dynamic instabilities in  
290 tube boiling systems, *International Journal of Heat and Mass Transfer*  
291 51 (3-4) (2008) 399–433. doi:10.1016/j.ijheatmasstransfer.2007.09.026.
- 292 [5] N. Liang, S. Shao, H. Xu, C. Tian, Instability of refrigeration system A  
293 review, *Energy Conversion and Management* 51 (11) (2010) 2169–2178.  
294 doi:10.1016/j.enconman.2010.03.010.
- 295 [6] J. Grasman, *Relaxation Oscillations*, 2011. doi:10.1119/1.1991506.
- 296 [7] M. Padki, K. Palmer, S. Kakaç, T. Veziroglu, Bifurcation analy-  
297 sis of pressure-drop oscillations and the Ledinegg instability, *Inter-  
298 national Journal of Heat and Mass Transfer* 35 (2) (1992) 525–532.  
299 doi:10.1016/0017-9310(92)90287-3.

- 300 [8] A. H. U. o. M. Stenning, T. Veziroglu, Flow oscillation modes in forced-  
301 convection boiling, in: Heat Transfer and Fluid Mechanincs Institute.  
302 NASA Grant NsG-424, 1965, pp. 301–316.
- 303 [9] T. Doan, S. Kakaç, T. Veziroglu, Analysis of forced-convection boil-  
304 ing flow instabilities in a single-channel upflow system, International  
305 Journal of Heat and Fluid Flow 4 (1983) 145–156. doi:10.1016/0142-  
306 727X(83)90060-7.
- 307 [10] M. Padki, H. Liu, S. Kakac, Two-phase flow pressure-drop type and  
308 thermal oscillations, International Journal of Heat and Fluid Flow 12 (3)  
309 (1991) 240–248. doi:10.1016/0142-727X(91)90058-4.
- 310 [11] P. R. Mawasha, R. J. Gross, D. D. Quinn, Pressure-Drop Oscillations in  
311 a Horizontal Single Boiling Channel, Heat Transfer Engineering 22 (5)  
312 (2001) 26–33. doi:10.1080/01457630152496296.
- 313 [12] M. Ozawa, S. Nakanishi, S. Ishigai, Y. Mizuta, H. Tarui, Flow Instabil-  
314 ities in Boiling Channels: Part 1 Pressure Drop Oscillations, Bulletin of  
315 the JSME Vol. 22 (No. 170) (1979) 1113–1118.
- 316 [13] S. K. H, Yünco, O.T. Yildirim, Yuncu 1,, Applied Scientific Research  
317 48 (1991) 83–104.
- 318 [14] Z. P. Feng, E x p e r i m e n t a l Investigation of Forced Convective  
319 Boiling Flow Instabilities in Horizontal Helically Coiled Tubes 5 (3).
- 320 [15] E. Manavela Chiapero, M. Fernandino, C. Dorao, Review on pressure  
321 drop oscillations in boiling systems, Nuclear Engineering and Design 250  
322 (2012) 436–447. doi:10.1016/j.nucengdes.2012.04.012.

- 323 [16] L. J. Guo, Z. P. Feng, X. J. Chen, Pressure drop oscillation of steam-  
324 water two-phase flow in a helically coiled tube, *International Journal*  
325 *of Heat and Mass Transfer* 44 (2001) 1555–1564. doi:10.1016/S0017-  
326 9310(00)00211-8.
- 327 [17] S. M. Kim, I. Mudawar, Review of databases and predictive methods  
328 for heat transfer in condensing and boiling mini/micro-channel flows,  
329 *International Journal of Heat and Mass Transfer* 77 (2014) 627–652.  
330 doi:10.1016/j.ijheatmasstransfer.2014.05.036.  
331 URL <http://dx.doi.org/10.1016/j.ijheatmasstransfer.2014.04.035>
- 332 [18] H. Lee, I. Park, I. Mudawar, M. M. Hasan, Micro-channel evap-  
333 orator for space applications - 1. Experimental pressure drop and  
334 heat transfer results for different orientations in earth gravity, *Inter-*  
335 *national Journal of Heat and Mass Transfer* 77 (2014) 1213–1230.  
336 doi:10.1016/j.ijheatmasstransfer.2014.06.012.  
337 URL <http://dx.doi.org/10.1016/j.ijheatmasstransfer.2014.06.012>
- 338 [19] E. Manavela Chiapero, M. Fernandino, C. Dorao, Experimen-  
339 tal results on boiling heat transfer coefficient, frictional pressure  
340 drop and flow patterns for R134a at a saturation temperature of  
341 34 C, *International Journal of Refrigeration* 40 (2014) 317–327.  
342 doi:10.1016/j.ijrefrig.2013.11.026.
- 343 [20] E. Manavela Chiapero, D. Doder, M. Fernandino, C. Dorao, Experi-  
344 mental parametric study of the pressure drop characteristic curve in a  
345 horizontal boiling channel, *Experimental Thermal and Fluid Science* 52

346

(2014) 318–327.

347

URL <http://www.sciencedirect.com/science/article/pii/S0894177713002392>

348

[21] E. Manavela Chiapero, M. Fernandino, C. a. Dorao, On the influence

349

of heat flux updating during pressure drop oscillations - A numerical

350

analysis, *International Journal of Heat and Mass Transfer* 63 (2013)

351

31–40. doi:10.1016/j.ijheatmasstransfer.2013.03.047.

352

URL <http://dx.doi.org/10.1016/j.ijheatmasstransfer.2013.03.047>